Republic of Iraq

Ministry of Higher Education and Scientific Research

University of Babylon / College of Science

Department of Physics

Laser Irradiation Effect on the Structural, Optical and Dispersive Properties of PVA/ Methyl Orange Composite Thick Films

A Thesis

Submitted to the Physics Department, College of Science, University of Babylon in Partial Fulfillment of the Requirements for the Degree of Master of Science in Physics.

By

Sarah Maysam Tareq Ali

B.Sc. in physics 2020

Supervised

By

Asst. Prof. Dr.
Nihal Abdullah AbdulWahhab

Lecturer Dr.
Addnan Hammood Mohammed

2023 A.D. **1445 A.H.**

بسم الله الرحمن الرحيم

﴿وَلَمَّا بَلَغَ أَشُدَّهُ وَاسْتَوَىٰ آتَيْنَاهُ حُكْمًا وَعِلْمًا وَكَذَٰلِكَ نَجْزِي الْمُحْسِنِينَ﴾

صَدَقَ اللهُ العَلِيُّ العَظيم

سورة القصص الآية (١٤)

Dedication

To…

My Father

My Mother

My Brothers

My Teachers

With My love and Respect

Sarah Maysam

Acknowledgments

First of all, I want to express my undying gratitude to ALLAH, JALA JALALAH, for all that has made me who I am today.

I would like to express my deep gratitude and appreciation to my supervisors ***Asst. Prof. Dr. Nihal Abdullah Abdulwahhab*** *and* ***Lecturer Dr. Addnan Hammood Mohammed*** *for suggesting the topic of the thesis, continuous advice and their guidance throughout this work.*

Many thanks go to the deanery of the College of Sciences at the University of Babylon and the Department of Physics for offering me the opportunity to complete my thesis.

Special thanks are due to ***Dr. Ehssan Al-Bermany*** *in Department of Physics, College of Education for Pure Science, University of Babylon, for helping.*

Finally, my great thanks, love and respect go to all who help me.

Sarah

Summary

This thesis presents the effect of the semiconductor laser with 405 nm (violet) wavelength and 60mW power irradiation on the optical properties of solutions and thick films prepared by casting method of polyvinyl alcohol (PVA), methyl orange (MO) and their composites (PVA/MO). Samples were laser irradiated at different times 10, 20, 30 and 40 minutes. The optical measurements of the solutions and the dispersion properties of the films are taken and compared with measurements of non-irradiated samples.

The structural properties included XRD, FTIR examination are also studied for material powder to be able to identify them. The structural parameters are studied such as the particle size and roughness by AFM microscope.

A PVA solution is prepared with a concentration of 10 g/l and the MO concentration of 0.01 g/l, and both solutions are mixed to obtain the composite. Then, thick films are prepared with different thicknesses around 2000 and 3000 nm for PVA and MO and within 2000, 4000 and 6000 nm for PVA/MO composites. The solutions and thick films were irradiated with 405 nm violet laser of for different times.

The optical properties of solutions and thick films show a decrease in the absorbance and reflectance spectrum with an increase in the irradiation time due to bond breakage, while the transmittance increases. The energy gap (direct and indirect) increases with increasing irradiation time. Other optical constants, for example optical conductivity and dielectric constants (both real and imaginary) as well as absorbance and absorption coefficient decrease with increasing laser irradiation time.

The dispersion coefficients were investigated for thick films before and after laser irradiation, single oscillators energy, dispersion energy, direct energy gap and

average oscillator strength increases with irradiation time, while Urbach energy and oscillator wavelength decreases with increasing irradiation time.

Contents

No.	Subject	Page No.
	Chapter one	
1.1	Introduction	1
1.2	Semiconductors	1
1.3	Organic Semiconductors	2
1.4	Organic Dye	3
1.5	Poly(vinyl) Alcohol	3
1.6	Methyl Orange (MO)	5
1.7	Composite Materials	6
1.8	Literature Survey	6
1.9	Aim of the Project	8
	Chapter two	
2.1	Introduction	10
2.2	Laser Interaction with Matter	10
2.3	Uv-Visible Spectrophotometer	11
2.4	Optical Properties	12
2.4.1	Direct Transitions	13
2.4.2	Indirect Transitions	13
2.4.3	Optical Constants	15
2.5	Dispersion Energy Parameters	16
2.6	X-ray diffraction	18
2.7	Fourier-Transform Infrared Spectroscopy (FTIR)	20
2.8	Atomic Force Microscopy (AFM)	21
2.9	Photoluminescence	21
	Chapter 3	
3.1	Introductions	24
3.2	Materials	24

3.3	FTIR Measurements	**25**
3.4	X–Ray Diffraction	**25**
3.5	Preparation of samples	**26**
3.5.1	The Solutions	**26**
3.5.2	The thick Films	**27**
3.6	Laser Source	**28**
3.7	UV-Visible Absorption Spectroscopy	**29**
3.8	AFM Measurements	**30**
3.9	photoluminescence Spectrophotometer	**30**
3.10	Excel programs	**31**
	Chapter four	
4.1	Introduction	**32**
4.2	FTIR Transmittance Spectra of Powders	**32**
4.2.1	FTIR for PVA Powder	**32**
4.2.2	FTIR for Methyl Orange Powder	**33**
4.3	X-ray diffraction of Powders	**34**
4.3.1	X-ray diffraction of PVA	**34**
4.3.2	X-ray diffraction methyl orange powder	**35**
4.4	Atomic Force Microscope (AFM)	**37**
4.5	Optical properties	**41**
4.5.1	The Solutions	**41**
4.5.2	The Thick Films	**46**
4.6	Dispersive properties for Thick Films	**58**
4.7	Photoluminescence of Thick Films	**81**
	Chapter five	
5.1	Conclusions	**84**
5.2	Suggestions	**84**
5.3	Future Works	**85**
	References	

List of Figures

Figure No.	Caption	Page No.
	Chapter one	
1-1	PVA structural formula: (A) partly hydrolyzed; (B) completely hydrolyzed.	**4**
1-2	Structure of methyl orange dye.	**5**
	Chapter two	
2-1	The electric and magnetic field vectors of EM radiation	**11**
2-2	Schematic diagram of a cuvette-based UV-Vis spectroscopy system.	**12**
2-3	The optical transitions (a) permitted direct, (b) prohibited direct; (c) permitted indirect, (d) prohibited indirect	**14**
2-4	The complement of the angle of incidence is the reflection of an X-ray beam of wavelength from a certain set of atomic planes separated by equal distances d.	**19**
2-5	Transitions giving rise to absorption and fluorescence emission Spectra.	**22**
	Chapter three	
3-1	Schematic diagram of the experimental work	**24**
3-2	FTIR spectrophotometer diagram.	**25**
3-3	(a)X-ray exterior cover. (b) A Schematic diagram of XRD	**26**
3-4	The solution of methyl orange, PVA and PVA/MO composite.	**27**
3-5	Laser Irradiation system.	**29**
3-6	A diagram of atomic force microscopy.	**30**
	Chapter four	
4-1	The FTIR transmittance spectra of PVA powder.	**33**
4-2	The FTIR spectrum of MO powder.	**34**
4-3	The XRD of PVA powder.	**35**
4-4	The XRD of MO powder.	**36**
4-5	AFM for non-irradiated PVA thick film at thickness 3000 nm.	**37**
4-6	AFM for PVA thick film with thickness 3000nm irradiated for 40 min by a 405 nm violet laser.	**38**
4-7	AFM for MO thick film with thickness 3000 nm for non-irradiated sample.	**38**
4-8	AFM for MO thick film with thickness 3000 nm and time irradiated 40 min by 405 nm violet laser.	**39**

4-9	AFM for PVA/MO thick film with thickness 6000 nm for non-irradiated sample.	**39**
4-10	AFM for PVA/MO thick film with thickness 6000 nm and time irradiated 40 min by 405 nm violet laser.	**40**
4-11	(a) The PVA absorbance spectra for different laser exposure times (0, 10, 20 and 30) min. (b) The absorbance as a function of irradiating time at 405 nm wavelength.	**42**
4-12	(a) The MO absorbance spectra for different laser exposure times (0, 10, 20 and 30) min. (b) The absorbance as a function of irradiating time at 405 nm wavelength.	**42**
4-13	(a) The PVA/MO absorbance spectra for different irradiating times (0, 10, 20 and 30) min. (b) The absorbance as a function of irradiating time at 405 nm wavelength.	**43**
4-14	(a) The PVA $(\boldsymbol{\alpha h v})^{1/2}$ as a function of the photon energy for different irradiating times (0, 10, 20 and 30) min. (b) The indirect energy gap as a function of irradiating time at 405 nm wavelength.	**44**
4-15	(a) The MO $(\boldsymbol{\alpha h v})^{1/2}$ as a function of the photon energy for different irradiating times (0, 10, 20 and 30) min. (b) The indirect energy gap as a function of irradiating time at 405 nm wavelength.	**44**
4-16	(a) The PVA/MO $(\boldsymbol{\alpha h v})^{1/2}$ as a function of the photon energy for different irradiating times (0, 10, 20 and 30) min. (b) The indirect energy gap as a function of irradiating time at 405 nm wavelength.	**45**
4-17	(a) The absorbance spectra of PVA thick films with 2000 nm thickness for different irradiating times (0, 10, 20, 30 and 40) min. (b) The absorbance as a function of irradiating time at 405 nm wavelength.	**47**
4-18	(a) The absorbance spectra of PVA thick films with 3000 nm thickness for different irradiating times (0, 10, 20, 30 and 40) min. (b) The absorbance as a function of irradiating time at 405 nm wavelength.	**48**
4-19	(a) The absorbance spectra of MO thick films with 2000 nm thickness for different irradiating times (0, 10, 20, 30 and 40) min. (b) The absorbance as a function of irradiating time at 405 nm wavelength.	**48**
4-20	(a) The absorbance spectra of MO thick films with 3000 nm thickness for different irradiating times (0, 10, 20, 30 and 40) min. (b) The absorbance as a function of irradiating time at 405 nm wavelength.	**49**
4-21	(a) The absorbance spectra of PVA/MO thick films with 2000 nm thickness for different irradiating times (0, 10, 20, 30 and 40) min. (b) The absorbance as a function of irradiating time at 405 nm wavelength.	**49**
4-22	(a) The absorbance spectra of PVA/MO thick films with 4000 nm thickness different irradiating times (0, 10, 20, 30 and 40)	**50**

	min. (b) The absorbance as a function of irradiating time at 405 nm wavelength.	
4-23	(a) The absorbance spectra of PVA/MO thick films with 6000 nm thickness different irradiating times (0, 10, 20, 30 and 40) min. (b) The absorbance as a function of irradiating time at 405 nm wavelength.	**50**
4-24	(a) The PVA at thickness 2000nm $(\boldsymbol{\alpha h v})^2$ as a function of the photo energy for different irradiating times (0, 10, 20, 30 and 40) min. (b) The direct energy gap as a function of irradiating time at 405 nm wavelength.	**51**
4-25	(a) The PVA at thickness 3000nm $(\boldsymbol{\alpha h v})^2$ as a function of the photo energy for different irradiating times (0, 10, 20, 30 and 40) min. (b) The direct energy gap as a function of irradiating time at 405 nm wavelength.	**52**
4-26	(a) The MO at thickness 2000nm $(\boldsymbol{\alpha h v})^2$ as a function of the photo energy for different irradiating times (0, 10, 20, 30 and 40) min. (b) The direct energy gap as a function of irradiating time at 405 nm wavelength.	**52**
4-27	(a) The MO at thickness 3000nm $(\boldsymbol{\alpha h v})^2$ as a function of the photo energy for different irradiating times (0, 10, 20, 30 and 40) min. (b) The direct energy gap as a function of irradiating time at 405 nm wavelength.	**53**
4-28	(a) The PVA/MO at thickness 2000nm $(\boldsymbol{\alpha h v})^2$ as a function of the photo energy for different irradiating times (0, 10, 20, 30 and 40) min. (b) The direct energy gap as a function of irradiating time at 405 nm wavelength.	**53**
4-29	(a) The PVA/MO at thickness 4000nm $(\boldsymbol{\alpha h v})^2$ as a function of the photo energy for different irradiating times (0, 10, 20, 30 and 40) min. (b) The direct energy gap as a function of irradiating time at 405 nm wavelength.	**54**
4-30	(a) The PVA/MO at thickness 6000nm $(\boldsymbol{\alpha h v})^2$ as a function of the photo energy for different irradiating times (0, 10, 20, 30 and 40) min. (b) The direct energy gap as a function of irradiating time at 405 nm wavelength.	**54**
4-31	(a) $\ln \alpha$ as a function of the photon energy of PVA thick film with 2000 nm thickness. (b) Urbach energy as a function of irradiating times.	**59**
4-32	(a) $\ln \alpha$ as a function of the photon energy of PVA thick film with 3000 nm thickness. (b) Urbach energy as a function of irradiating times.	**59**
4-33	(a) $\ln \alpha$ as a function of the photon energy of MO thick film with 2000 nm thickness. (b) Urbach energy as a function of irradiating times.	**60**
4-34	(a) $\ln \alpha$ as a function of the photon energy of MO thick film with 3000 nm thickness. (b) Urbach energy as a function of irradiating times.	**60**

4-35	(a) $\ln \alpha$ as a function of and photon energy of PVA/MO thick film with 2000 nm thickness (b) Urbach energy as a function of irradiating times.	**61**
4-36	(a) $\ln \alpha$ as a function of and photon energy of PVA/MO thick film with 4000 nm thickness (b) Urbach energy as a function of irradiating times.	**61**
4-37	(a) $\ln \alpha$ as a function of and photon energy of PVA/MO thick film with 6000 nm thickness (b) Urbach energy as a function of irradiating times.	**62**
4-38	$1/(n^2-1)$ vs. Square photon energy of 2000 nm PVA thick film.	**63**
4-39	Laser irradiating time effect of 2000 nm PVA thick film on (a) The dispersion energy (b) Single oscillator energy.	**63**
4-40	$1/(n^2-1)$ vs. Square photon energy of 3000 nm PVA thick film.	**64**
4-41	Laser irradiating time effect of 3000 nm PVA thick film on (a) The dispersion energy (b) Single oscillator energy.	**64**
4-42	$1/(n^2-1)$ vs. Square photon energy of 2000 nm MO thick film.	**65**
4-43	Laser irradiating time effect of 2000 nm MO thick film on (a) The dispersion energy (b) Single oscillator energy.	**66**
4-44	$1/(n^2-1)$ vs. Square photon energy of 3000 nm MO thick film.	**66**
4-45	Laser irradiating time effect of 3000 nm MO thick film on (a) The dispersion energy (b) Single oscillator energy.	**66**
4-46	$1/(n^2-1)$ vs. Square photon energy of 2000 nm PVA/MO thick film.	**67**
4-47	Laser irradiating time effect of 2000 nm PVA/MO thick film on (a) The dispersion energy (b) Single oscillator energy.	**67**
4-48	$1/(n^2-1)$ vs. Square photon energy of 4000 nm PVA/MO thick film.	**68**
4-49	Laser irradiating time effect of 4000 nm PVA/MO thick film on (a) The dispersion energy (b) Single oscillator energy.	**68**
4-50	$1/(n^2-1)$ vs. Square photon energy of 6000 nm PVA/MO thick film.	**69**
4-51	Laser irradiating time effect of 6000 nm PVA/MO thick film on (a) The dispersion energy (b) Single oscillator energy.	**69**
4-52	The relation between $1/(n^2-1)$ and $1/\lambda^2$ for PVA thick film at thickness 2000 nm.	**71**
4-53	The PVA thick film 2000 nm (a) Average oscillator strength as a function of irradiating times. (b) Average inter band oscillator wavelength as a function of the irradiation time.	**71**
4-54	The relation between $1/(n^2-1)$ and $1/\lambda^2$ for PVA thick film at thickness 3000 nm.	**72**
4-55	The PVA thick film 3000 nm (a) Average oscillator strength as a function of irradiating times. (b) Average inter band	**72**

	oscillator wavelength as a function of the irradiation time.	
4-56	The relation between $1/(n^2-1)$ and $1/\lambda^2$ for MO thick film at thickness 2000 nm.	**73**
4-57	The MO thick film 2000 nm (a) Average oscillator strength as a function of irradiating times. (b) Average inter band oscillator wavelength as a function of the irradiation time.	**73**
4-58	The relation between $1/(n^2-1)$ and $1/\lambda^2$ for MO thick film at thickness 3000 nm.	**74**
4-59	The MO thick film 3000 nm (a) Average oscillator strength as a function of irradiating times. (b) Average inter band oscillator wavelength as a function of the irradiation time.	**74**
4-60	The relation between $1/(n^2-1)$ and $1/\lambda^2$ for PVA/MO thick film at thickness 2000 nm.	**75**
4-61	The PVA/MO thick film 2000 nm (a) Average oscillator strength as a function of irradiating times. (b) Average inter band oscillator wavelength as a function of the irradiation time.	**75**
4-62	The relation between $1/(n^2-1)$ and $1/\lambda^2$ for PVA/MO thick film at thickness 4000 nm.	**76**
4-63	The PVA/MO thick film 4000 nm (a) Average oscillator strength as a function of irradiating times. (b) Average inter band oscillator wavelength as a function of the irradiation time.	**76**
4-64	The relation between $1/(n^2-1)$ and $1/\lambda^2$ for PVA/MO thick film at thickness 6000 nm.	**77**
4-65	The PVA/MO thick film 6000 nm (a) Average oscillator strength as a function of irradiating times. (b) Average inter band oscillator wavelength as a function of the irradiation time.	**77**
4-66	Emission spectra of PVA thick film at thickness 3000 nm irradiated by 405 nm laser (a) Before irradiating (b) After 40 minute irradiation time.	**82**
4-67	Emission spectra of MO thick film at thickness 3000 nm, irradiated by 405 nm laser (a) Before irradiating (b) After 40 minute irradiation time.	**82**
4-68	Emission spectra of PVA/MO thick film at thickness 6000 nm irradiated by 405 nm laser (a) Before irradiating (b) After 40 minute irradiation time.	**83**

List of Tables

Table No	Caption	Page No.
	Chapter three	
3-1	Thickness measurments of PVA, MO and PVA/MO thickfilms	**28**
3-2	Discription of laser used.	**28**
	Chapter four	
4-1	The analysis of FTIR for PVA	**32**
4-2	XRD measurement of PVA powder	**35**
4-3	XRD measurement of MO powder	**36**
4-4	AFM measurements of PVA, MO and PVA/MO thick films before and after 405 nm laser irradiating.	**40**
4-5	The optical constants of PVA solution for different irradiating times at 280 nm wavelength.	**45**
4-6	The optical constants of MO solution for different irradiating times at 469 nm wavelength.	**46**
4-7	The optical constants of PVA/MO solution for different irradiating times at 479 nm wavelength.	**46**
4-8	The optical constants of PVA thick film with 2000 nm for different irradiating times at 350 nm wavelength.	**55**
4-9	The optical constants of PVA thick film with 3000 nm for different irradiating times at 360 nm wavelength.	**55**
4-10	The optical constants of MO thick film with 2000 nm for different irradiating times at 480 nm wavelength.	**56**
4-11	The optical constants of MO thick film with 3000 nm for different irradiating times at 490 nm wavelength.	**56**
4-12	The optical constants of PVA/ MO thick film with 2000 nm for different irradiating times at 500 nm wavelength.	**57**
4-13	The optical constants of PVA/ MO thick film with 4000 nm for different irradiating times at 520 nm wavelength.	**67**
4-14	The optical constants of PVA/ MO thick film with 6000 nm for different irradiating times at 560 nm wavelength:	**58**
4-15	The dispersion parameters of PVA with 2000 nm thickness at 348 nm wavelength:	**78**
4-16	The dispersion parameters of PVA with 3000 nm thickness at 348 nm wavelength:	**78**
4-17	The dispersion parameters of MO with 2000 nm thickness at 470 nm wavelength:	**79**
4-18	The dispersion parameters of MO with 4000 nm thickness at 470 nm wavelength:	**79**
4-19	The dispersion parameters of PVA/MO with 2000 nm thickness at 500 nm wavelength:	**80**

4-20	The dispersion parameters of PVA/MO with 4000 nm thickness at 520 nm wavelength:	**80**
4-21	The dispersion parameters of PVA/MO with 6000 nm thickness at 560 nm wavelength:	**81**
4-22	The energy gap of PVA, MO and PVA/MO thick film measured by Tauc and PL methods	**83**

List of Symbols

Symbol	Description
A	Absorbance
α	Absorption Coefficient
c	Velocity of Light in Vacuum
C	Concentration
d_{hkl}	The Inter Planar Distance
E	Dielectric Constant
$\mathbf{E_d}$	Dispersion energy
E_g	Energy Gap
E	Electric Filed
E_o	Single oscillator energy
E_u	Urbach energy
$\varepsilon_{im.}$	Imaginary Part of Dielectric Constant
ε_{Real}	Real Part of Dielectric Constant
h	Plank Constant
hv	Photon Energy
I_o	Incident Photon Intensity
I	Transmitted Photon Intensity
k	Extinction Coefficient
θ	Diffraction Angle
$\sigma_{Optical}$	Optical Conductivity
R	Reflectance
n	Refractive Index
r	Constant in Tauc Formula
S_0	Average oscillator strength

T	Transmittance
t	Thickness of Thin Film
V	The volume
v	Frequency
λ_o	Oscillator wavelength
λ	Wavelength
ρ	Resistivity
ρ_m	Material Density

List of Abbreviations	
Abbrev.	**Term**
AFM	Atomic force microscopy
C. B.	Conduction Band
FTIR	Fourier Transform Infrared
FWHM	Full Width at Half Maximum
HOMO	High Occupied Molecular Orbit
IR	Infrared Radiation
LOMO	Lowest Occupied Molecular Orbit
MO	Methyl orange
PL	Photoluminescence
PVA	Poly(vinyl) alcohol
PD	Photo Detector
UV	Ultra Violet
V. B.	Valence Band
Vis	Visible
XRD	X-Ray Diffraction

CHAPTER ONE

INTRODUCTION

1.1 Introduction

The word "polymer" comes from the Greek words "poly" (many) and "mere" (parts), and it is used to describe molecules with a high molecular mass that are made up of numerous smaller parts. Polymers, also known as macromolecules, are huge molecules with a high molecular weight that are made up of many smaller molecules, or monomers, that are bound together. The reaction between monomers to form a polymer is called polymerization[1][2].

Light amplification through stimulated emission of radiation is referred to as "laser" informally. Schawlow and Townes had initially put out the idea. A laser must have three main components: an active medium that allows light to be amplified, a pumping source that stimulates the active medium to the amplifying device, and optical feedback produced by an optical resonator[3].

Lasers have a wide range of uses, including information processing and medical procedures including ear, nose, and throat surgery as well as cutaneous and cosmetic surgery. Lasers are used in a variety of commonplace devices, including barcode scanners, optical computers, and laser printers. For military applications like distance measuring, very precise distance measurement is crucial[4].

1.2 Semiconductors

The physics of semiconductors has become one of the important topics of solid state physics in terms of applications because of its astonishing progress[5]. Semiconductors are named by this name as their capacity to carry electricity is moderate. Actually, temperature may change a conventional semiconductor's conductivity to the point that most of them appear to be insulators at low temperatures and metals at high temperatures. Impurities might also be a useful aspect. Intrinsic semiconductors are impurity-free, whereas extrinsic semiconductors are doped with impurities. Both of these characteristics are

required for the operation of microelectronic devices[6]. A semiconductor is frequently defined as a substance with an resistivity of 10^{-2}-10^{9} Ω.cm. Metals and semimetals have zero band gaps, whereas insulators have an energy gap greater than 3 eV [7].

1.3 Organic Semiconductors

The semiconductors as it may be widely classifying into two base semiconductors, both inorganic and organic. Despite the fact that inorganic semiconductors such as germanium and silicon are widely utilized in industry of electronics, organic semiconductors are projected to replace inorganic semiconductors in the near future. Organic semiconductors have received a lot of interest due to their effective application in optical and electrical devices with promising results[8].

Organic semiconductors are often composed of hydrocarbons (bonding between hydrogen and carbon atoms, occasionally with extra oxygen and nitrogen atoms depending on organic molecule structure). Organic solids are created via weak Van der Waals forces, which result in fragile bonding due to the poor overlap of electronic wave functions between nearby molecules. The intermolecular separation in organic solids is typically much greater than that in inorganic solids due to the weak bonds between organic molecules, resulting in much narrower electronic bands than in inorganic solids. As a result, the energies of the valence and conduction bands of solids can be well approximated by those of the highest occupied molecular orbitals (HOMO) and lowest unoccupied molecular orbitals (LUMO), respectively, of individual molecules[9].

The characteristics of organic semiconductors are dictated, or at least greatly influenced, by π electrons in π bonds. Because π bonds are weaker than σ bonds and π electrons are delocalized throughout a network of linked p-orbitals, it is

much simpler to add an electrons from π electrons as well as excite $\pi*$ electrons with visible light. In the molecules, the p_z-orbitals of sp^2-hybridized C-atoms create a conjugated π-electron system in both. As a result, the $\pi - \pi^*$-transitions exhibit the lowest electronic excitations of conjugated molecules, with an energy gap of 1.5 to 3 eV and absorption bands spanning from near infrared to near ultraviolet. The energy gap can be controlled by the degree of conjugation in a molecule [10].

1.4 Organic Dye

Since 1870, researchers have examined the structural features of chemical compounds as well as their colors. A chromophore is a component of an organic molecule created by a combination of electrons and atoms that gives the molecule its color. The phenomenon of unsaturation, which allows compounds to absorb hydrogen, is caused by the presence of electrons between specific pairs of atoms that are not well fixed within covalent bonds. However, the presence of these electrons in molecular orbitals, where they may bind to several atoms, does not negate the fact that, within a given wavelength range, these electrons may absorb energy from light, and the reflection or transmission of the remaining light gives the compound its visible color[11].

1.5 Poly(vinyl) Alcohol (PVA)

Organic polymers are extremely versatile materials with several uses and applications. Polymers have been utilized for a variety of purposes, including as homopolymers, homopolymer blends, copolymers, and chemically modified homo- or copolymers. Nowadays, practically all businesses employ polymeric materials in some form or another, as much as their intrinsic features are desired. As it is well known, such features are partly dependent on the chemical properties of the polymer, namely the chemical binding nature, the organic functional groups,

the manner in which these functional groups are connected, and the manner in which they are spatially distributed[12].

Poly vinyl alcohol (PVA) is an artificial polymer extensively used in the first half of the twentieth century. It may also be easily blended with a number of natural materials and has properties that make it suited for a wide range of applications. Natural fibers and additives can improve mechanical properties even more without compromising overall degradability. PVA has been used to manufacture a variety of end products in the commercial, medical, food, and industrial fields, materials that come into direct contact with food, lacquers, surgical threads, and packaging materials [13]. Transparent films with excellent tensile strength and tear resistance are created. The melting point of PVA polymer is 180 degrees Celsius with molecular weights of (26,300, 72,000, and 30,000) g/mol [14]. Structural formula for PVA shown in Figure (1-1)[15].

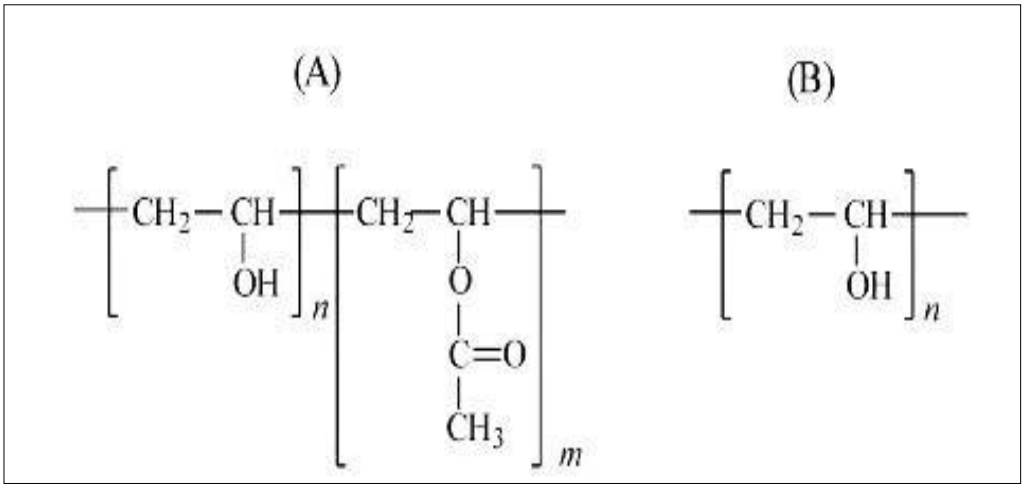

Figure (1-1): PVA structural formula: (A) partly hydrolyzed; (B) completely hydrolyzed [15].

Because there are many different examples of several polymer kinds employed as polymer hosts, it was chosen because of its remarkable features

including as Biocompatible, non-toxic, and biodegradable, excellent chemical resistance and good mechanical strength performance; easy preparation[16].

1.6 Methyl Orange (MO)

Methyl orange (MO) dye, is a synthetic organic semiconductor used as a pH indicator in many different types of food and beverages, medicines, wastewater treatment, laboratory experiments, agriculture, and healthcare are just a few examples. It is a carcinogenic and mutagenic chemical. This azo dye is extremely difficult to degrade using standard treatment procedures, resulting in pollution and health issues.[17][18]. MO is commonly used in titrations due to its obvious and noticeable color shift. Its usage in acid titrations is widespread because it exhibits a color shift at the pH of a diluted acid. It doesn't have a full spectrum of color change like a universal indication, but it has a sharper end point. When a solution come lower acidic, MO will transit from red to orange, then to yellow, and when the solution grows more acidic, the reverse occurs. In acidic situation, the whole color change happens [19]. Methyl orange dye's chemical formula:($C_{14}H_{14}N_3O_3SNa$) It is illustrated in the Figure[20]:

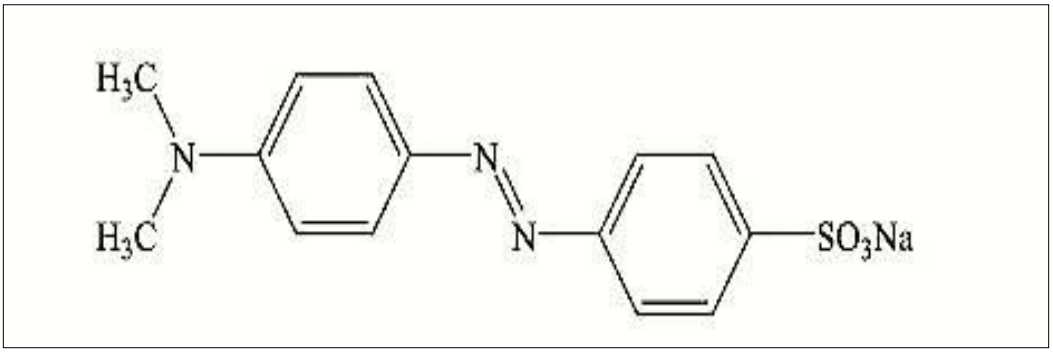

Figure (1-2): Structure of methyl orange dye [20].

1.7 Composite Materials

Composite materials have long been utilized to solve technical issues, but the development of polymer-based compounds in the 1960s drew the attention of industries. Composite materials have now become popular engineering materials and have been designed and manufactured for a variety of applications such as automotive vehicle production, materials, product, maritime and oil industries, process engineering components, aircraft parts, and consumer products. The compound's popularity is also growing as a result of greater product performance awareness and competitiveness in the worldwide lightweight ingredients industry[21].

A composite material is a combination of two or more materials, with the finished assembly possessing attributes superior to the individual parts. Composite materials are now generally referred to as reinforcing arrangements (also known as fillers) contained in a matrix. It is also possible to express the stresses that the composite experiences when subjected to load [22].

1.8 Literature Survey

In (**2011**), S.S Chiad *et al.* studied Changes in PVA:Ag Optical Parameters as a Function of Film Thickness, PVA with silver added was used to make films of different sizes. The pictures that were made were 10, 20, 30, and 40 m thick. Transmission and absorption spectra had been taken to studied how increased thickness affects optical constants like transmittance, reflectance, absorption coefficient, refractive index, extinction coefficient, and the real and imaginary parts of dielectric constant. This study showed that all of these factors affect the thickness by making it thicker[23].

In (**2014**), N.A.B. Sabah A. Salman *et al*. examined the optical characterization of red methyl doped poly (vinyl alcohol) films. The effect of (red

methyl) doping on the absorption spectra and the optical energy gap of PVA films has been studied. The optical transmission of films formed using the casting method was tested in the wavelength range (190-1100) nm. The absorbance results show that the doping has an effect on the absorption edge, causing a red shift in its values. The films exhibit indirect permitted inter band transitions that are modified by doping, and the optical energy gap has been decreased after doping [24].

In (**2014**) M. F. Hadi *et al*. studied the He-Ne laser irradiation's influence on the optical characteristics of methyl orange doped PVA films, 10 ml of MO doped PVA films, The films were prepared using the casting method and it was examined using laser irradiation at various irradiant periods. All samples' absorption and transmission spectra were determined using a UV-Visible spectrophotometer. Laser irradiation influenced the optical constants, including the refraction index, extinction coefficient, complex dielectric constants, and optical energy gap. All of them are reduced as irradiation time increased. [25].

In (**2014**) E.M. Antar examined the effect of γ -rays on the optical properties of dyed PVA films, the films are prepared using the dipping method. The spectrum behavior was explored, as well as the effects of dosage on the absorption coefficient, optical energy gap, refractive index, and extinction coefficient. It is concluded that the values of indirect band gap are lower than the corresponding values of direct band gap in films with gamma irradiation. And also the band gap (Eg) decreases with increase of gamma absorbed dose. [26].

In (**2017**) K. Haneen *et al.* examined Urbach energy (E_u) and dispersion characteristics of Co_3O_4 thin films. The Co_3O_4 films of different thicknesses were prepared using the chemical spray pyrolysis process. The films spread on heated glass at 420°C. UV-Visible spectrophotometer was utilized to measure the transmittance spectrum from 450 to 900 nm. The obtained Urbach energy rose as the film thickness grew. The outcomes are also revealed that when the film

thickness increased, the average excitation energy determined for electrical transitions (E_o), the dispersion energy (E_d), and the predicted optical gap (E_g) decreased[27].

In (**2018**) N.F. Habubi *et al.* studied the parameters of dispersion for poly(vinyl alcohol) Films doping with Fe. The PVA polymer was melted in water to make films with varying Fe concentrations using the casting method. The optical characteristics was determined by keeping a record of the transmittance spectrum in the (300-900) nm wavelength region. The Wemple-DiDomenico technique was used to compute the dispersion parameters. The energy of single oscillator of electronic transited, while the dispersion energy of the PVA-Fe films decreased as the Fe concentration increased. Urbach's energy was enhanced. The energy gap in the PVA:4% Fe film dropped from 4.08 eV to 3.52 eV[28].

In (**2020**) D. Jyoti and *et al.* studied the investigation on dispersion parameters of molybdenum oxide thin films via Wemple–DiDomenico (WDD) single oscillator model. The dispersion parameters of molybdenum oxide thin films viz: oscillator energy, dispersion energy, transition moments, static refractive index, oscillator strength, and oscillator wavelength are estimated via Wemple–DiDomenico (WDD) single oscillator model. Moreover, the optical constants viz: film density, porosity, absorption coefficient, optical band gap, Urbach energy, steepness parameter, and strength of electron–phonon interaction are also studied as a function of substrate temperature. This is to establish a correlation between optical constants and dispersion parameters[29].

In (**2021**) S. Kumari Nisha *et al.* showed that the Polyvinyl alcohol/methyl orange are flexible films as reusable pH indicator, PVA and MO are combined in a water-based solvent at 100 degrees Celsius to create the film. Every polymeric substance demonstrated excellent UV-Vis absorption in the electromagnetic

spectrum, the absorption intensity increases with the intensity of absorption increases as the amount of MO in a polymer matrix increases[30].

1.9 Aim of the Project

1) Study spectra of polymer, dye and their composite for both solution and thick films, before and after laser irradiation effect.
2) Study the ability to control the energy gap (which effects on optical, electrical and thermal properties of the material) with laser irradiating. This can be exploited to produce suitable optical filters.
3) Study effect of laser radiation on Urbach energy of the thick films.
4) Investigating the dispersion coefficients of PVA, MO and PVA/MO thick films before and after laser irradiation. In addition, study the ability to control dispersion coefficients laser irradiation.

CHAPTER TWO

THEORETICAL PART

CHAPTER THREE

EXPERIMENTAL PART

2.1 Introduction

This chapter presents a concise summary of the fundamental ideas guiding the theoretical topics relevant to the work of this thesis, from laser interaction with matter to the diagnostic methods including UV-Vis spectroscopy, dispersion properties, fluorescence, surface morphology, and structural features.

2.2 Laser Interaction with Matter

Light amplification through stimulated emission of radiation is referred to as "LASER", Schawlow and Townes made the initial suggestion[3][31]. Laser is very important because of its coherent, monochromatic, brightness and directionality that allow them to be focused at a point and induce ionization, excitation, and scattering when passed through matter, which can be used to examine the properties of some materials[32].

Laser radiation is a form of electromagnetic radiation (EM), which is represented by two electric and magnetic fields, Figure(2-1). When the wave of electromagnetic (laser beam) strikes a surface (air/solid interface) it undergoes a reflection and transmission. Some radiation is transmitted, some reflected and, some absorbed. As it passes through a new medium it is absorbed according to Beer Lambert's law[33]:

$$I = I_0 e^{-\alpha t} \quad \ldots\ldots\ldots\ldots\ldots (2-1)$$

Where α is the absorption coefficient, I_o is the incident photon intensity and I is the transmitted intensity.

The EM wave passes through a small elastically bound charged particle, as a result the particle will be set in motion by the electric force from the electric field, E. The force is small and incapable of vibrating an atomic nucleus[33].

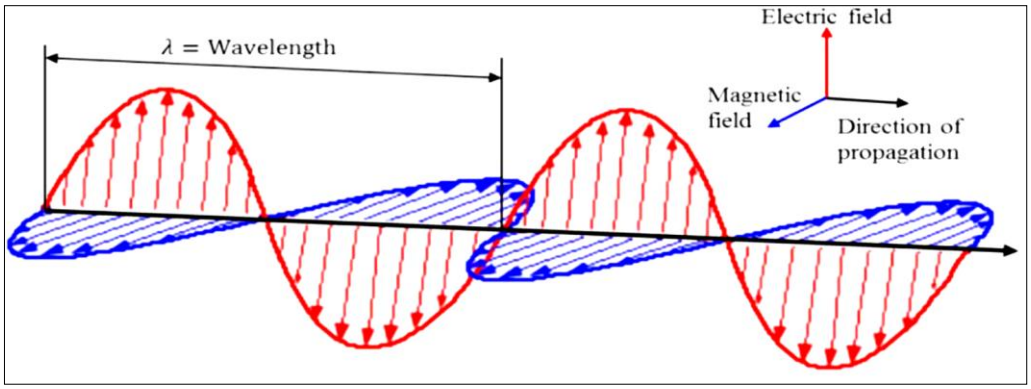

Figure(2-1): The electric and magnetic field vectors of EM radiation[34]

2.3 UV-Visible Spectrophotometer

Ultraviolet and visible radiation are only a small fraction of the electromagnetic spectrum, which also contain radio, microwave, infrared (IR), visible, ultraviolet light, X-rays, and gamma rays[35].

UV-Vis spectrophotometers included a source of light to illuminate a sample with rang from UV to visible light wavelengths (usually 190 to 900 nm). The instrument then measures the amount of light absorbed, transmitted, or reflected by the sample at each wavelength. The spectrum can be used to determine the chemical or physical characteristics of the material. In general, one can determine the concentration of a certain molecule in solution, characterize the absorbance or transmittance of a liquid or solid over a variety of wavelengths, as well as the reflectance qualities of a surface or the color of a substance[36].

A spectrophotometer's principal elements are as follows as [36]36]:

- A light source that emits a broad spectrum of electromagnetic radiation in the UV-visible range.
- The broad-band radiation is separated into wavelengths using a dispersion device.
- A sample region is a location where light travels through or reflects off a sample.

- One or more detectors are used for determining the intensity of reflected or transmitted radiation. Light is relayed through the device by other optical components such as lenses, mirrors, or fiber optics, as shown in Figure(2-2).

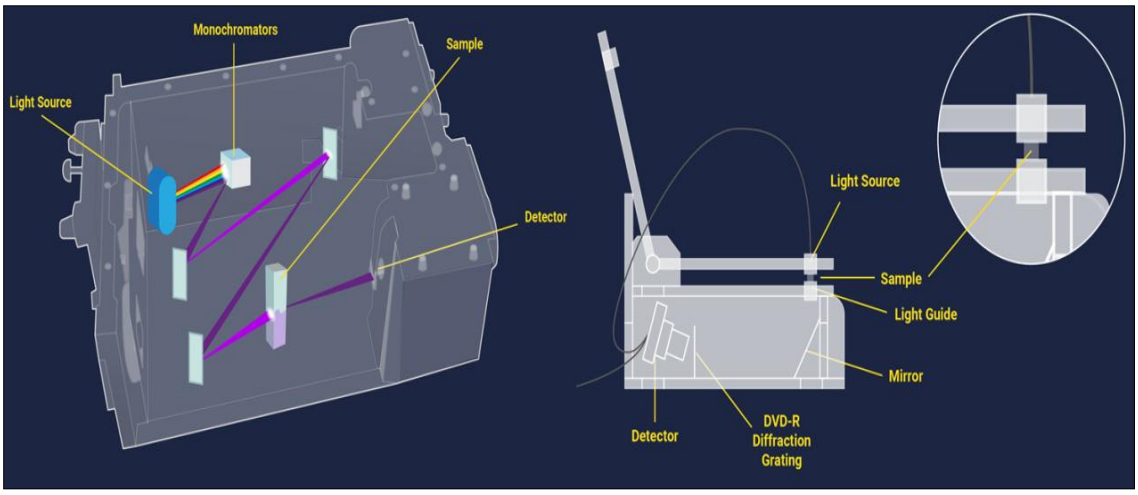

Figure(2-2): Schematic diagram of a cuvette-based UV-Vis spectroscopy system[38].

2.4 Optical Properties

The optical properties give us an expounding about the interaction between the light and materials. The optical properties of materials are those that are discovered when the electromagnetic radiation hit the material [11].

The semiconductor absorbs photons from the incident beam; the absorption is energy-dependent ($h\nu$); where h is Planck's constant and ν is the frequency of the input photons. The absorption is related with the electronic transition between the valence band (V.B.) and the conduction band (C.B.) in the material that began at the absorption edge and corresponds to smallest energy gap (Eg) between the lowest minimum of the C.B. and the greatest maximum of the V.B.[39].

The photon can interact with a valence electron, elevate the electron into the C.B., and produce an electron-hole pair if the photon energy is equal to or greater than the energy gap. The incoming photon's maximal wavelength (λ), which produces the electron-hole pair, is specified as[8]:

$$\lambda(nm) = \frac{hc}{E_g} = \frac{1240}{E_g(eV)} \dots\dots\dots\dots\dots (2-2)$$

There are two different kinds of optical transitions, direct and indirect transitions that will be explained in the following.

2.4.1 Direct Transitions

For momentum conservation, the direct transition occurs between the top of the valence band and the bottom of the conduction band (vertical transition) at the same wave vector Δk = 0. When the wave vector is equal to zero, the transition between the valence band's top and the conduction band's bottom is referred to as the allowed direct transition as seen in Figure(2-3a). The following equation describes this transition[40]:

$$\alpha h\nu = B(h\nu - E_g)^{1/2} \dots\dots\dots\dots\dots (2-3)$$

Where *B*: is inversely proportional to amorphusity.

The transition is known as a prohibited direct transition, as shown in Figure(2-2b), if it also happens between states of the same wave vector but the wave vector is not zero. It will yield to the following relationship [40]:

$$\alpha h\nu = B(h\nu - E_g)^{3/2} \dots\dots\dots\dots\dots (2-4)$$

2.4.2 Indirect Transitions

There is a significant momentum difference between the valence and conduction band transition points in an indirect transition, so the conduction band minima are not at the same k value as the valence band maxima, necessitating the assistance of a phonon to conserve momentum, thus[41]:

$$h\nu = E_g \mp E_p \dots\dots\dots\dots\dots (2-5)$$

Where Ep is the energy of an absorbed or emitted phonon.

For an allowed indirect transition, the transition takes place as seen in Figure(2-3c), from the top of the valence band to the bottom of the conduction band therefore [42].

$$\alpha h\upsilon = B(h\upsilon - E_g)^2 \ldots\ldots\ldots\ldots(2-6)$$

While, as shown in Figure(2-3d), forbidden indirect transitions take place from any location near the top of V.B. to any point other than the bottom of C.B. [42].

$$\alpha h\upsilon = B(h\upsilon - E_g)^3 \ldots\ldots\ldots\ldots(2-7)$$

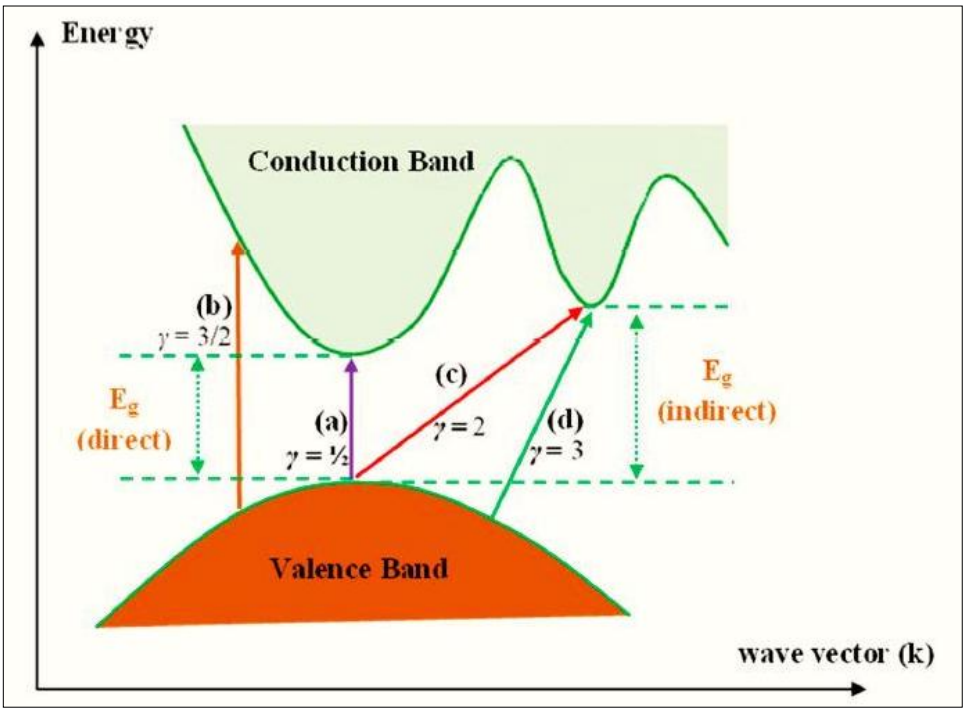

Figure(2-3): The optical transitions (a) permitted direct, (b) prohibited direct; (c) permitted indirect, (d) prohibited indirect [43]**.**

Experimentally, the level of the absorption coefficient may be used to distinguish between direct and indirect processes; α takes values between 10^4 and 10^5 cm^{-1} for direct transitions and between 10 and 10^4 cm^{-1} for indirect transitions near the absorption edge[42].

2.4.3 Optical Constants

When the electromagnetic radiation falls on the material and interacts with it, many processes happen some of the electromagnetic radiation is absorbed by the material and the other part is transmitted because it passes through the material while another part of the electromagnetic radiation is reflected from the surface of the material called the reflected part[44]. To obtain information about the internal structure of the material and the nature of its bonds, transmittance and absorption must be known, reflections of the electromagnetic radiation falling on the material. For instance, by examining the UV spectra, it is possible to identify energy bundles and the type of transitions present in the material. As for the field of practical applications in which the materials are used, the visible spectrum must be studied[45].

The absorbance (A) is defined as the ratio between the intensity of the absorbed rays through the surface of the film to the intensity of the incident rays, which is a unit-free quantity, while the ratio between the intensity of the transmitted rays to the intensity of the rays incident on the surface of the thick films called the transmittance (T). Reflectance (R) is the ratio between the intensity of the rays reflected from the surface of the thin film to the intensity of the incident rays. Through the absorbance and transmittance spectrum, the reflectivity will be calculated according to the law of energy conservation according to the following relationship[46].

$$R + T + A = 1 \dots\dots\dots\dots\dots (2-8)$$

Where the absorption is given by the following equation

$$\mathrm{A} = \log \frac{\mathrm{I}_0}{\mathrm{I}} \dots\dots\dots\dots\dots (2-9)$$

The material's absorption coefficient α is the important function of photon energy and band gap energy given by the following formula[23]:

$$\alpha = \frac{2.303\ A}{t} \dots\dots\dots\dots\dots (2-10)$$

Where t is the thickness of the sample.

The refractive index n can be calculated from the following equation[47]:

$$\mathrm{n} = \sqrt{\frac{4\mathrm{R}}{(1-\mathrm{R})^2} - k^2} + \frac{1+\mathrm{R}}{1-\mathrm{R}} \dots\dots\dots\dots\dots (2-11)$$

Where R is the reflectance that calculated by[48]:

$$R = \frac{(n-1)^2 + k^2}{(n+1)^2 + k^2} \dots\dots\dots\dots\dots (2-12)$$

Where k is the extinction coefficient that is related to the exponential decay of the light that passes through the solution which is given by[49]:

$$k = \frac{\alpha\lambda}{4\pi} \dots\dots\dots\dots\dots (2-13)$$

The dielectric constants both of real and imaginary for the solution are evaluated using the following relations [50]:

$$(n - ik)^2 = \varepsilon_r - i\varepsilon_i \dots\dots\dots\dots\dots (2-14)$$

$$\varepsilon_r = n^2 - k^2 \dots\dots\dots\dots\dots (2-15)$$

$$\varepsilon_i = 2nk \dots\dots\dots\dots\dots (2-16)$$

The optical conductivity σ_{op} depends directly on the refractive index n, c is speed of light and absorption coefficient α by the following relation[51]:

$$\sigma_{op} = \frac{\alpha nc}{4\pi} \dots\dots\dots\dots\dots (2-17)$$

2.5 Dispersion Energy Parameters

The electronic dielectric constant's dispersion is described by a new energy parameter. There are more than 50 ionic and covalent crystals with credible

refractive-index dispersion data, it is discovered that this dispersion energy obeys an incredibly straightforward empirical connection[52]. When determining a way laser irradiation may affect organic materials, the dispersion characteristics are important, Wemple – DiDomenico description is used to apply the dispersion relations. To define the dispersion energy parameters, a single oscillator description of the frequency dependent dielectric constant is employed[53]. To analyze the data of the dispersion refractive index, below the inter band absorption edge was used a single-effective-oscillator. The equation that relates the oscillator strength to the refractive index is given in the following [54] [55]:

$$n^2 - 1 = \frac{E_0\, E_d}{E_0^2 - (h\nu)^2} \dots\dots\dots\dots (2-18)$$

Where, n is the refractive index, E_0 is the energy of the single oscillator energy for electronic transition. E_d is the dispersion energy used to calculate the intensity of inter band optical transitions.

The Urbach energy is defined as the width of the confined state, this exists in the optical band gap and can be connected to the exponential tails for the density of states as indicated by the relationship [56]:

$$\alpha = \alpha_0 exp \frac{E_g}{E_U} \dots\dots\dots\dots (2-20)$$

Where (E_U) is Urbach energy while, (α_o) is a constant. Urbach energy may be calculated by plotting ($ln\alpha$) on the y-axis and photon energy ($h\nu$) on the x-axis, then the inverted slope represents the Urbach energy.

There are new parameters that appeared in the normal dispersion behavior on the materials also these values are of the same order as those obtained by DiDomenico and Wemple. This parameters is the long wavelength refractive index (n_∞), average inter band oscillator wavelength (λ_o) and the average oscillator strength (S_o) were determined using the following relationship[57]:

$$\frac{(n_\infty^2 - 1)}{(n^2 - 1)} = 1 - (\frac{\lambda_o}{\lambda})^2 \dots\dots\dots\dots\dots (2-21)$$

$$n^2 - 1 = \frac{(S_o \lambda_o^2)}{\left(1 - {}^{\lambda_o^2}/_{\lambda^2}\right)} \dots\dots\dots\dots\dots (2-22)$$

A simple association between the spectrum and (E_d) and the single-oscillator parameters (E_o) can be reaped and comparing terms in an expansion in powers. The resultant correlations can be stated succinctly in terms of spectrum moments. It is also described in the following equations [54]:

$$E_d^2 = \frac{M_{-1}^3}{M_{-3}} \dots\dots\dots\dots\dots (2-23)$$

$$E_o^2 = \frac{M_{-1}}{M_{-3}} \dots\dots\dots\dots\dots (2-24)$$

It is necessary to keep in thoughts that the momentum obtained from the optical is a crucial parameter for the usage of the material in optical applications[27].

2.6 X-ray Diffraction

X-ray diffraction is more commonly employed to determine structure than neutron or electron diffraction. The type of the radiation influences both the penetration depth of the incoming radiation into the sample and the relative intensity of the diffracted beam. Crystal atoms are placed in parallel at identical distances (d), and X-rays are reflected secularly from them according to reflection rules. The phase difference between rays reflected from successive planes is determined by the distance between the planes. When the phase difference between rays reflected from neighboring planes is an integral multiple of (2π), constructive interference occurs; otherwise, the rays dispersed by the planes interact destructively. As a result, dispersed beams appear only at certain angles of incidence, as seen in Figure(2-4)[5].

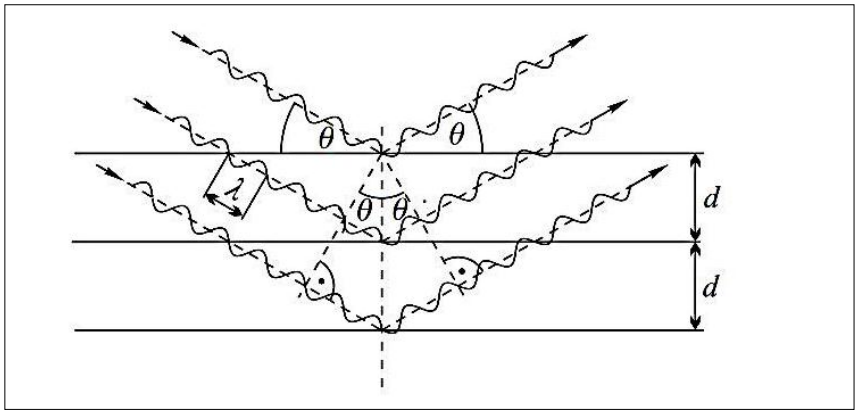

Figure(2-4): The complement of the angle of incidence is the reflection of an X-ray beam of wavelength from a certain set of atomic planes separated by equal distances d[5]**.**

The crystal planes' orientation may be changed in an unlimited number of ways. When many of them satisfy the criteria for constructive interference for a fixed incoming beam, dispersed beams can be appeared in several directions. According to the rules of reflection, the dispersed beam creates the same angle with the plane as the incident beam; hence the angle of deflection of the incident beam is (2θ). Δs = 2d sin θ is the path difference between two reflected photons from neighboring planes., as it is seen in the Figure(2-4). When the path difference (Δs) is an integral multiple of the wavelength (λ), constructive interference occurs. As a result, dispersed rays appear only when the requirement is met[58].

$$2d \sin\theta = m\lambda \ldots\ldots\ldots\ldots (2-25)$$

Where (d) is the inter planer distance, (θ) it is the diffraction angle which is met by a family of crystal planes, where (m) is an integer.

The diffraction Bragg condition. The reflected beam's intensity displays prominent peaks in the appropriate directions[59].

The investigation of grain size backs up the observed difference in crystallization in the films, the grain size of crystallite is calculated using Scherer's equation [60]:

$$\left(D = \frac{0.9\,\lambda}{\beta\,cos\theta}\right) \ldots\ldots\ldots\ldots\ldots (2-26)$$

Where 0.9 is the Scherrer constant, λ is the X-ray wavelength, β is the FWHM, and θ is the Bragg angle.

2.7 Fourier-Transform Infrared Spectroscopy (FTIR)

Infrared spectroscopy has the benefit of being virtually ubiquitous. Many compounds have high absorbance in the mid-infrared range, which is why we study spectra in this range[61]. Fourier transformation is a decoding method that converts a signal from the time domain, where it is a function of duration, to the frequency domain, where it is a function of frequency[62].

The wavenumbers include of infrared light that is divided into three regions, far-infrared (4 - 400) cm^{-1}, mid-infrared (400 - 4000) cm^{-1} and near-infrared (4000 - 14000) cm^{-1}[42]. The intensity of light is measured and plotted as a function of the location of the moveable mirror in a FTIR Spectrometer; the resulting graph is the Fourier Transform of the intensity of light as a function of wavenumber. Light is focused onto the material of interest in FTIR spectroscopy, and the intensity is measured with an infrared detector. The intensity of light reaching the detector is measured as a function of mirror position and Fourier-transformed to get a plot of intensity vs. wave number Fourier-transformed Infrared spectrum for the sample[63].

2.8 Atomic Force Microscopy (AFM)

The introduction of scanning probe microscopes, particularly the atomic force microscopy, has opened up a new path for the research of biological specimens, inspiring us to look at our samples with a fresh outlook[64].

The AFM is made up of a tiny needle on the end of a micro machined flexible cantilever that raster scans the sample's surface. The cantilever is deflected by attraction and repulsion forces as the tip gets closer to the specimen surface. This deflection is identified and processed as a function of position in the $(\mathbf{x}, \mathbf{y})$ plane to create topographical images. The AFM can work in contact mode (the tip is constantly in contact with the surface) or non-contact mode (the cantilever vibrates and variations in resonance frequency are used to create images), the cantilever travels fast in both continuous and intermittent modes (the cantilever vibrates and changes in its resonance frequency are employed to form pictures), with a strong oscillation between repulsive and attraction forces[65].

2.9 Photoluminescence

Luminescence is the emission of light from any substance that occurs when it is electrically stimulated. Luminescence is classified into two types based on the nature of the excited state: fluorescence and phosphorescence. It should be highlighted that distinguishing fluorescence from phosphorescence is not always possible[66].

Most molecules are at ambient temperature in the lowest vibrational level of the ground electronic state, and when light is absorbed, they are lifted to produce excited states. Figure(2-5) depicts molecule absorption [67].

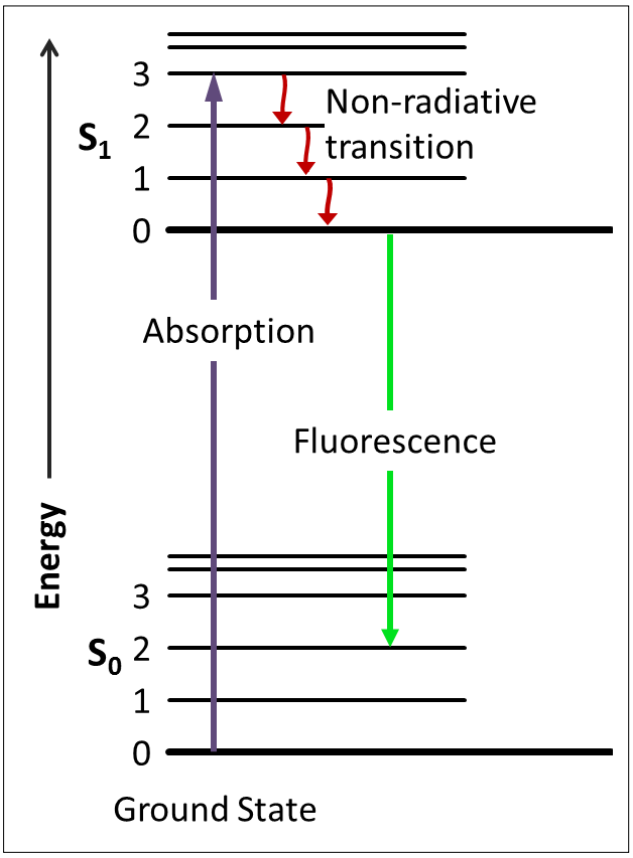

Figure(2-5): Transitions giving rise to absorption and fluorescence emission[1].

After absorbing energy and reaching one of an excited state's higher vibrational levels, the molecule quickly loses its excess vibrational energy through collision and falls to the excited state's lowest vibrational level. Additionally, almost all molecules in an electronic state higher than the second undergo internal conversion and move with the same energy from the lowest vibrational level of the upper state to a higher vibrational level of a lower excited state. From then, the molecules lose energy until they hit the lowest vibrational levels of the initial excited state. The molecule can return to any of the vibrational levels of the ground state from here, producing energy in the form of fluorescence. If this process occurs for all of the molecules that absorbed light, the quantum efficiency of the sample will be one. If any alternative path is used, the quantum efficiency will be less than one and may even be close to zero. Because fluorescence is always

emitted from the lowest vibrational level of the initial excited state, the shape of the emission spectrum remains constant regardless of the wavelength of the exciting light[67].

3.1 Introductions

This chapter describes the materials and devices used in the research. The structural properties are studied using XRD, AFM, FTIR devices. The solution preparation, the films deposition and thickness measurement techniques are also presented. There are many techniques and devices are used to characterize the samples such as spectrophotometers, fluorescence measurements, XRD, AFM and FTIR. Figure (3-1) shows the schematic diagram of the experimental work.

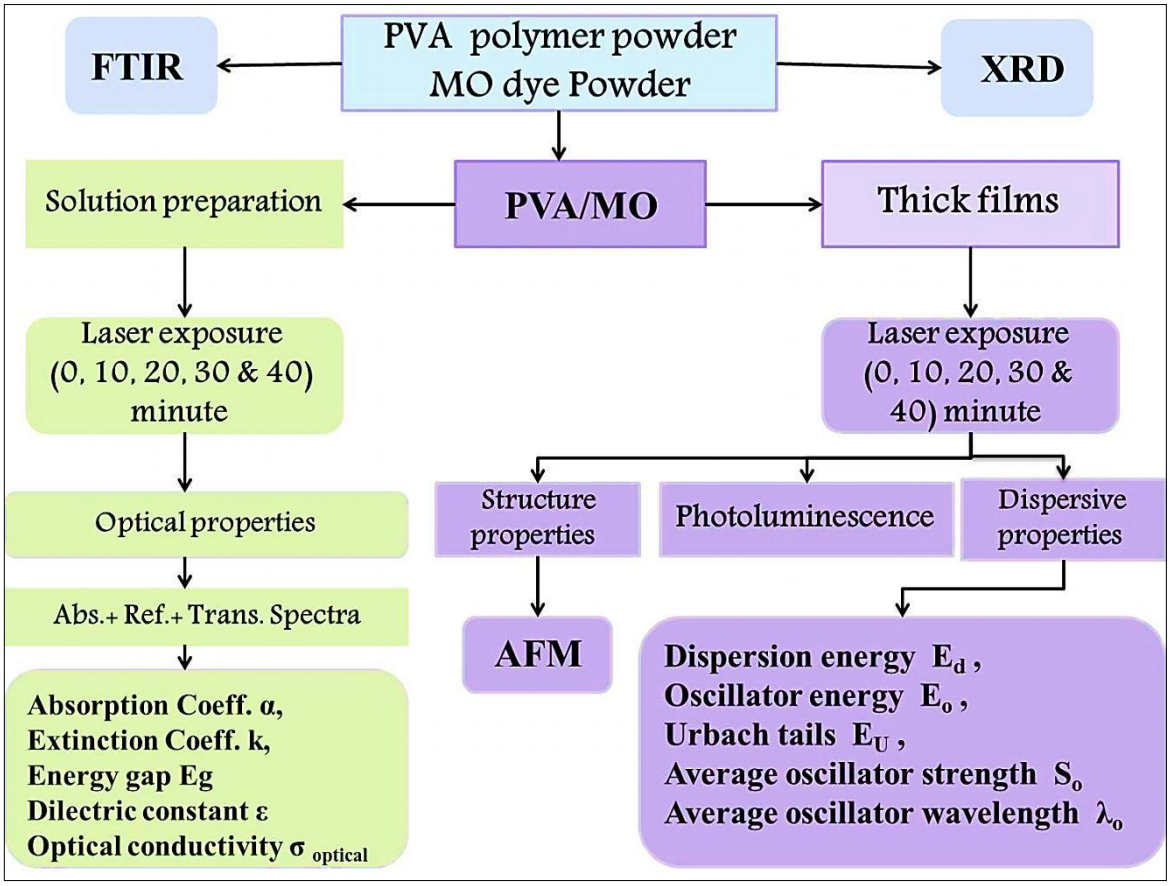

Figure (3-1): Schematic diagram of the experimental work.

3.2 Materials

Polyvinyl alcohol (PVA) polymer with molecular weight (10000 g/mole), supplied by (Sigma-Aldrich company) with high purity (99.999%) were used as matrix polymeric materials in this work. The dehydrated Methyl orange (MO) with

molecular weight 372.33g/mole was also supplied from Sigma-Aldrich Company, Japan. PVA and MO were prepared by dissolving them separately in distilled water.

3.3 FTIR Measurements

The structure of the PVA and methyl orange powder, which are mixed with KBr, was investigated by FTIR Fourier transform infrared spectrometer IR Affinity-1 (Shimadzu Company) Japanese. The measurments were made at Materials Department - College of Engineering - University of Babylon. The FTIR diagram of the technique is shown in Figure(3-2).

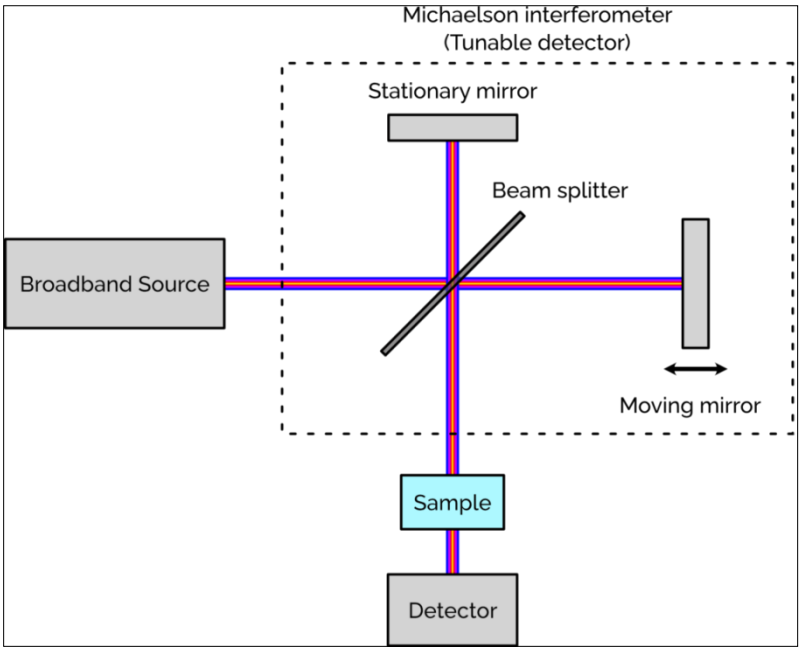

Figure (3-2): FTIR spectrophotometer diagram.

3.4 X–Ray Diffraction

The structures of PVA and MO Powder were investigated using (Lab X XRD-6000 SHIMADZU) at Materials Department - College of Engineering - University of Babylon. The measurements are done by the XRD system with wavelength of λ=1.5406 Å in a geometry of reflection. The operational voltage is

30 kV and current of 20 mA. The data here are recorded with the diffraction angle 2θ. The grain size was computed from the interplanar distance (d) for different planes.

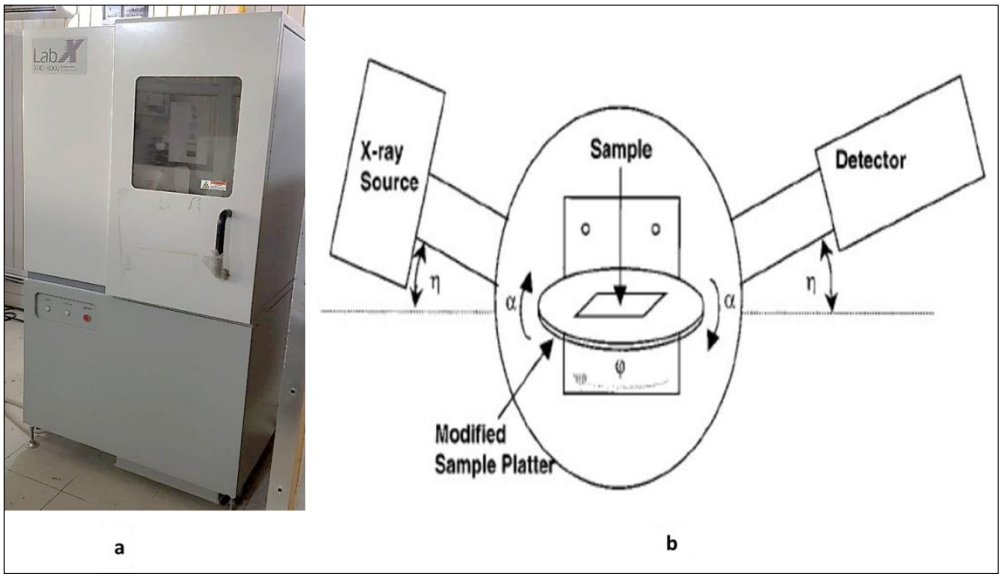

Figure (3-3): (a)X-ray exterior cover. (b) A Schematic diagram of XRD [68]**.**

3.5 Preparation of Samples

3.5.1 The Solutions

The samples were prepared in the form of solution by dissolving a 500mg of PVA in 50 ml of distilled water at 90^{o}C. The prepared solution was with a concentration of 10g/l. A 30mg of MO is accurately weighed and transferred into 10ml of distilled water at 50^{o}C. After that, the solution is diluted to reach 0.01g/l. concentration by using the equation ($C_1V_1=C_2V_2$). Then, 1 ml of PVA solution with concentration 10 g/l is mixed with 1 ml of MO solution with concentration 0.01g/l to obtain a PVA/MO composite solution. A magnetic stirrer is used for the purpose of homogenizing the solution of PVA, MO and PVA/MO at a temperature of 80^{o}C for 10 minutes.

Figure (3-4): The solution of methyl orange, PVA and PVA/MO composite.

3.5.2 The Thick Films

Different percentages of powder PVA and MO were weighed in different quantities to produce films of various thicknesses, as can be seen in the Table (3-1). All weights were dissolved in distilled water at 90°C for PVA and 50°C for MO then placed in a magnetic stirrer for 10 minutes. The solutions were poured into a Petri dish with a diameter of 5 cm, as the decanting procedure was utilized. Then, it is allowed to be dried at room temperature for three days. the method used to measure thickness is the weight method by using the equation:

$$t = \frac{m}{\rho A} \dots\dots\dots\dots\dots (3-2)$$

Where t the thickness of the sample.

m: the weight (mg).

ρ: the density of PVA, MO and PVA/MO.

A: the area of Petri dish**.**

Table (3-1) Thickness measurments of PVA, MO and PVA/MO thickfilms.

Powder	Weight (mg)	Thickness (nm)
PVA	0.006	2000
	0.008	3000
MO	0.0050	2000
	0.0075	3000
PVA/MO	0.004 (PVA) 0.0025(MO)	2000
	0.006 (PVA) 0.0050 (MO)	4000
	0.008 (PVA) 0.0075(MO)	6000

3.6 Laser Source

The system consists of a violet laser, two convex lenses with 10 cm focal length, and a flat mirror placed below the sample to reflect the laser beam back. The distance between the laser and the sample is 70 cm, while laser spot diameter about 5 cm .The experimental setup is located at Physics Department - College of Science - University of Babylon. The solution and thick films were irradiated at different intervals (10, 20, 30 and 40 minutes) for each concentration.

Table (3-2) discription of the laser used.

Characteristic	Value
Wevelength (λ)	405 nm
Power	60 mW
Intensity	3.05 mW/cm^3
Photon energy	3.06 eV
Stabilty time	> 60 minute

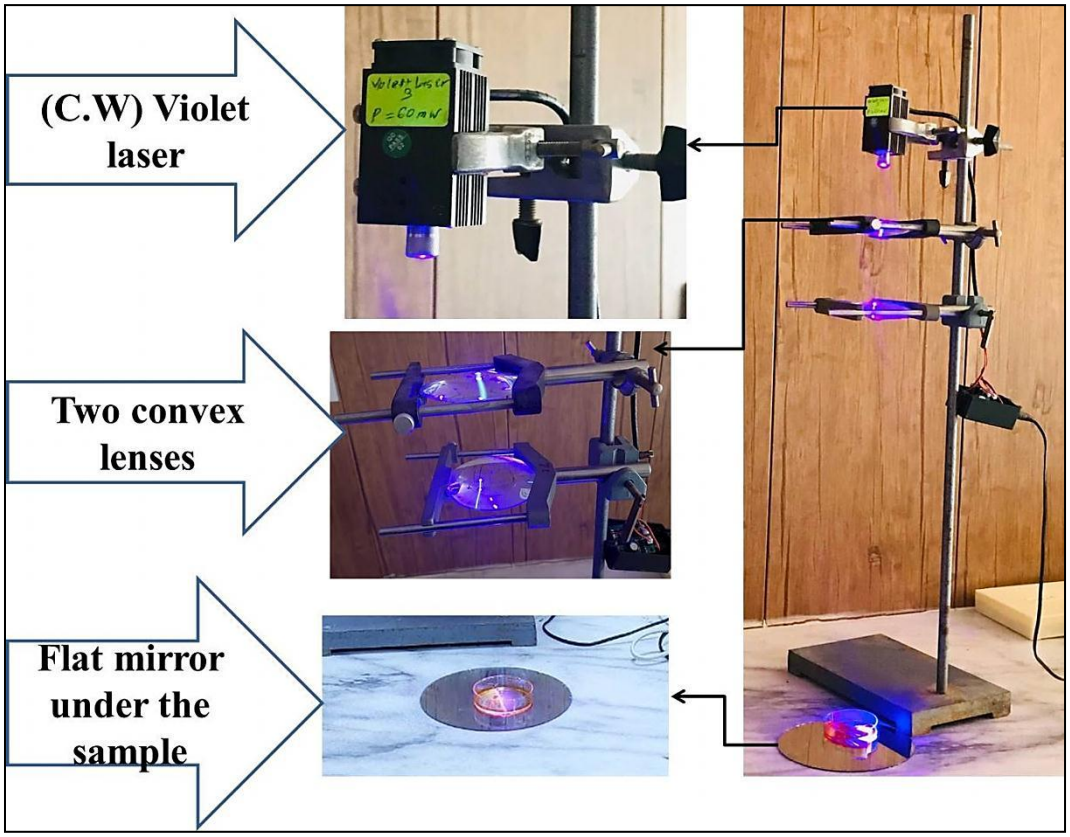

Figure (3-5): Laser Irradiation system.

3.7 The UV-Visible Absorption Spectroscopy

The optical properties of the prepared solutions and thick film are determined by UV-Visible spectrophotometer that located at Physics Department - College of Education for Pure science - University of Babylon. This spectrophotometer contains two light sources, deuterium and halogen lamps to provide the range of wavelength in the range (190-1100) nm. This gadget is a double-beam device, with one beam passing through the film under examination (optical measurements) and the other passing through the instrument's glass slide, using the output data of wavelength, transmittance, and absorbance in computer software. A Local Excel software is used to calculate the optical constants before and after irradiation such as energy band gap.

3. 8 AFM Measurements

Surface morphological measurements for PVA, MO, and PVA/MO thick films with varying thicknesses and substrate temperatures were performed using an Angstrom Advanced Inc. TT-2 AFM mode spectrometer. Computerized roughness and diameter of grains were acquired, as well as 2D images of all examined films.

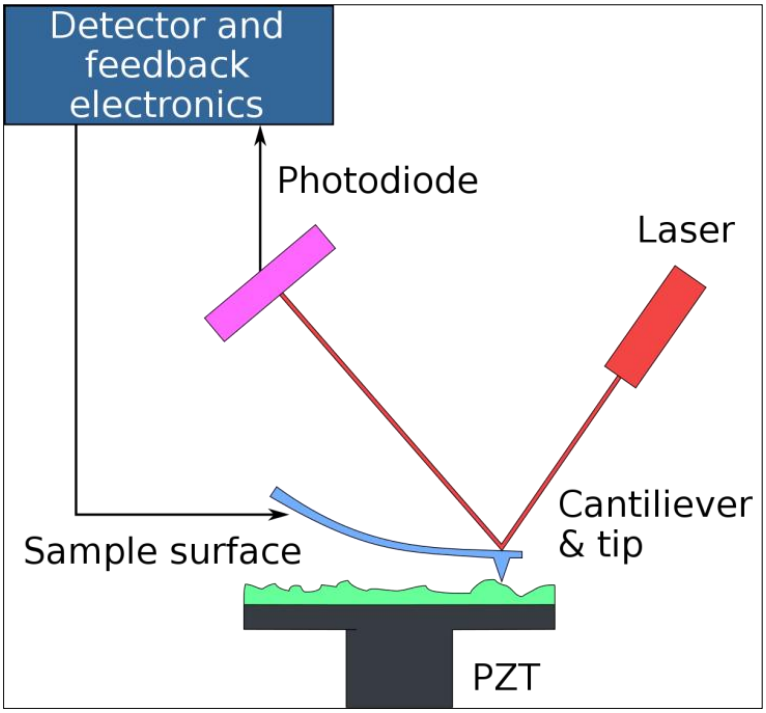

Figure(3-6): A diagram of atomic force microscopy.

3.9 photoluminescence Spectrophotometer

Fluorescence is based on photoluminescence, which is the physical process of releasing light after it has been absorbed by a substance. The fluorescence intensity indicates the amount of light (photons) emitted. It is the excited states that govern the amount of emission. The device is from SCINCO Fs-2, Korea, that is located at the Ministry of Science and Technology.

3.10 Excel programs

The optical constants such as absorption coefficient, extinction coefficient, dielectric constants and refractive index, as well as the dispersion parameters, such as dispersion energy, single oscillator energy, average oscillator strength and oscillator wavelength are calculated using two local Excel programs:

1- Optical properties program for solutions, AD-UV-Vis.-SOL-2023-ver.4.

2- Optical properties program for thin & thick films, AD-UV-Vis.-TF-2021-ver.3.

3- Dispersion properties program, AD-DCP-TF-2021-ver.2

CHAPTER FOUR

RESULTS & DISCUSSION

4.1 Introduction

This chapter presents the results and the analysis of the findings of (PVA, MO, and PVA/MO) for both solutions and thick films. The films are prepared by casting method in a petri dish and left to be dried at room temperature. The C.W. laser of 405 nm wavelength and 60 mW power is used to irradiate the samples in different times.

4.2 FTIR Measurements of the Powder

The main purpose of the FTIR test is to ascertain the identity of the original substance through its chemical affinities.

4.2.1 FTIR of the PVA Powder

FTIR Spectrum of PVA powder is showed in Figure (4-1) since the PVA spectrum has five major frequencies corresponding to the molecular bonds as shown in Table (4-1) [69].

Table (4-1): the analysis of FTIR for PVA:

Wave number cm^{-1}	Bound	Type of bonds vibration
800	C-C	stretching
1263.42	C-O	wagged vibration
1375.29	C-H	wagged vibration
1570.11	CH_2	rocking
1722.49	C=O	bending

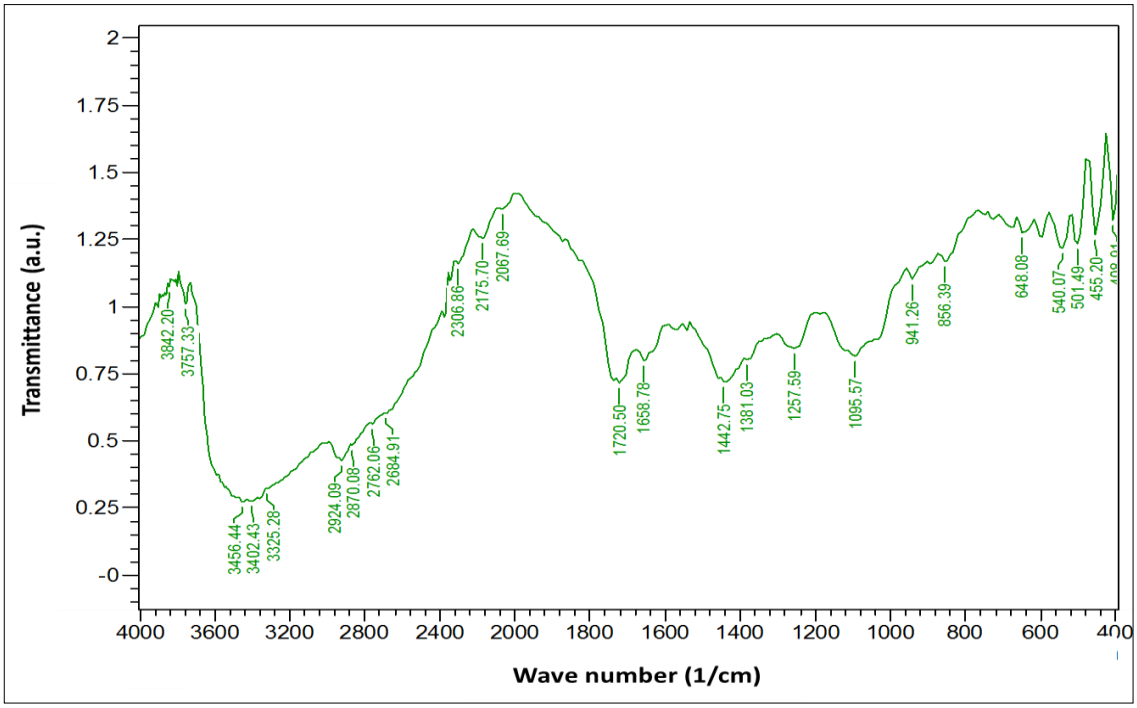

Figure (4-1): The FTIR transmittance spectra of PVA powder.

4.2.2 FTIR of the Methyl Orange Powder

The FTIR spectrum of the MO powder is shown in Figure (4-2). The strong peak existence of around 1280 cm^{-1} may be due to the C-S bond of the sulfonate group. Also, the presence of weak bond around 3300 cm^{-1} shows the existence of amine group. Because of the C-N stretch of aromatic amine, strong peaks around 1350 cm^{-1} can be seen which regarded as a certain indicator of existence of the aromatic amine in the compound. In addition, the peak presence around 1290 cm^{-1} indicates the presence of S-O [70].

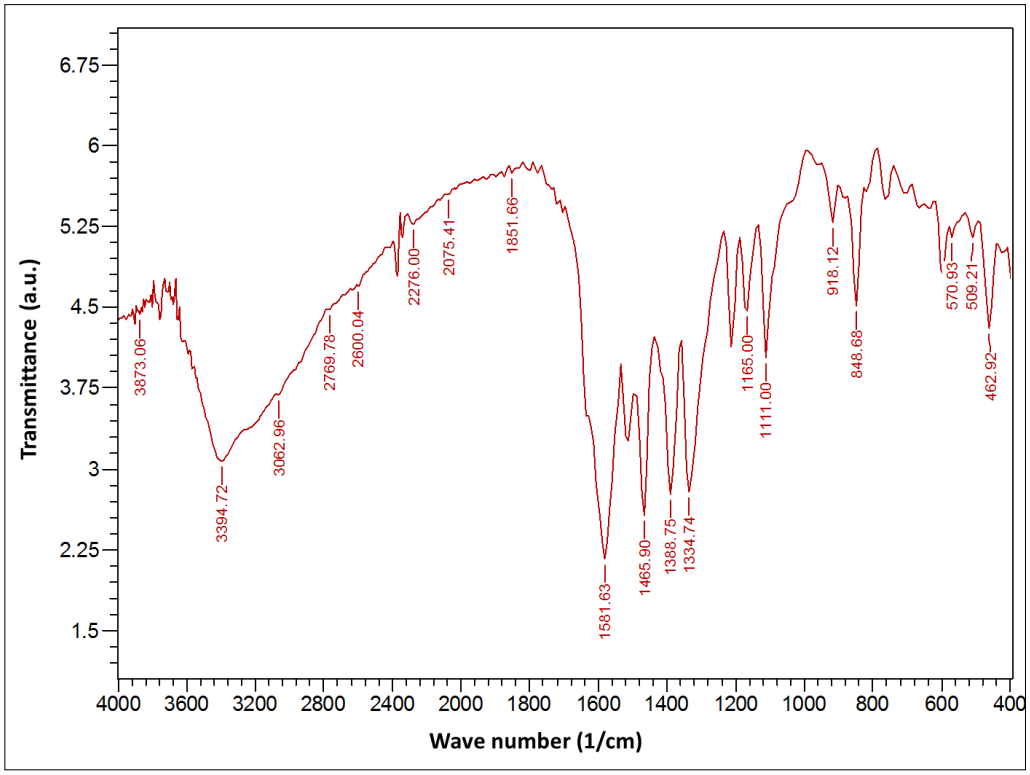

Figure (4-2): The FTIR spectrum of MO powder.

4.3 XRD of the Powder

X-ray diffraction is investigated to identify the crystal structure and calculate the average crystal size of each of the polymer and methyl orange.

4.3.1 XRD of the PVA

The PVA powder XRD data is displayed in Figure (4-3). The maximum diffraction peak, that produced using Match!3 software, is located at ($2\theta = 19.44$), (d = 0.45 nm) and Millar indices of (101).The crystal structure is a monoclinic unit cell. This is an evidence of that PVA powder exhibits crystalline X-ray diffraction[71]. Scherrer's equation (2-26) [72] is used to determine the average crystal size based on the observed X-ray diffraction patterns. The XRD data is illustrated in Table (4-2).

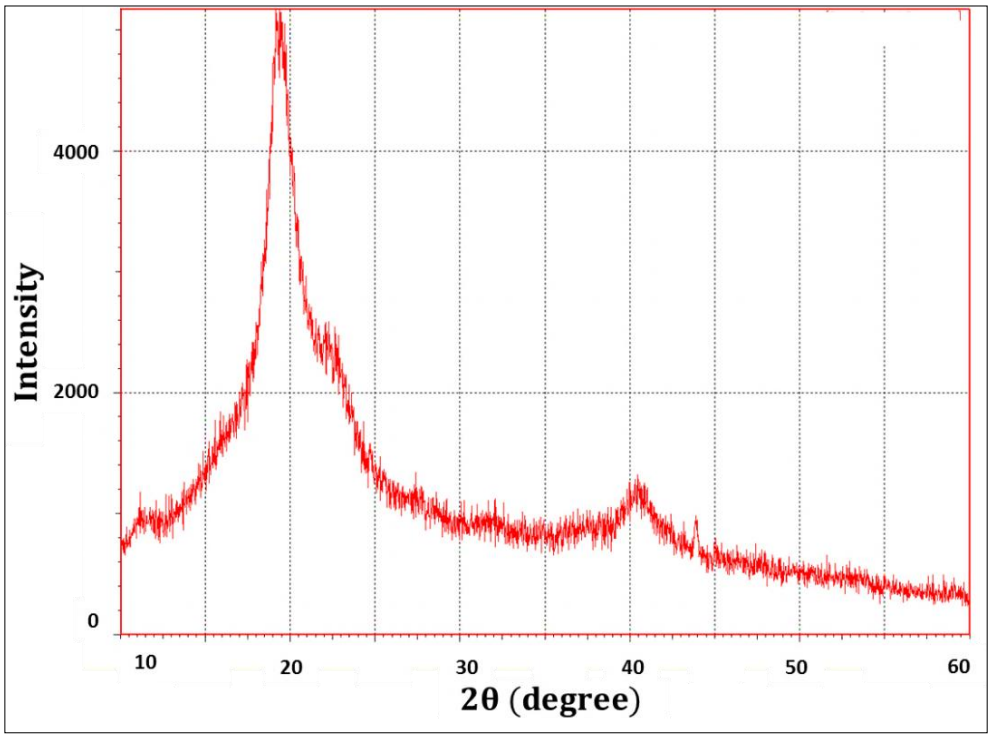

Figure (4-3): The XRD for PVA powder.

Table (4-2): XRD measurement of PVA powder:

2θ degree	d nm	I	I/I_o %	FWHM degree	β rad	Average crystal Size nm
19.44	0.456	366.89	100	2.08	0.036	38.75
40.46	0.222	49.27	10.7	0.36	0.006	23.52
43.90	0.206	42.97	11.71	0.23	0.004	37.24

4.3.2 XRD of the Methyl Orange Powder

The XRD data for the MO powder are shown in Figure (4-4). The major diffracting peaks are found using the Match!3 software, and it is roughly located at ($2\theta = 26.92$) with (d = 15.71 nm), ($2\theta = 44$) with (d=30.91 nm), and ($2\theta = 64.34$) with (d=39.09 nm). The unit cell of the crystal is monoclinic [73]. Based

on the observed X-ray diffraction patterns, the crystallite's grain size is calculated using Scherrer's equation (2-26) [72]. Table (4-3) presents the relevant data derived from MO powder XRD studies.

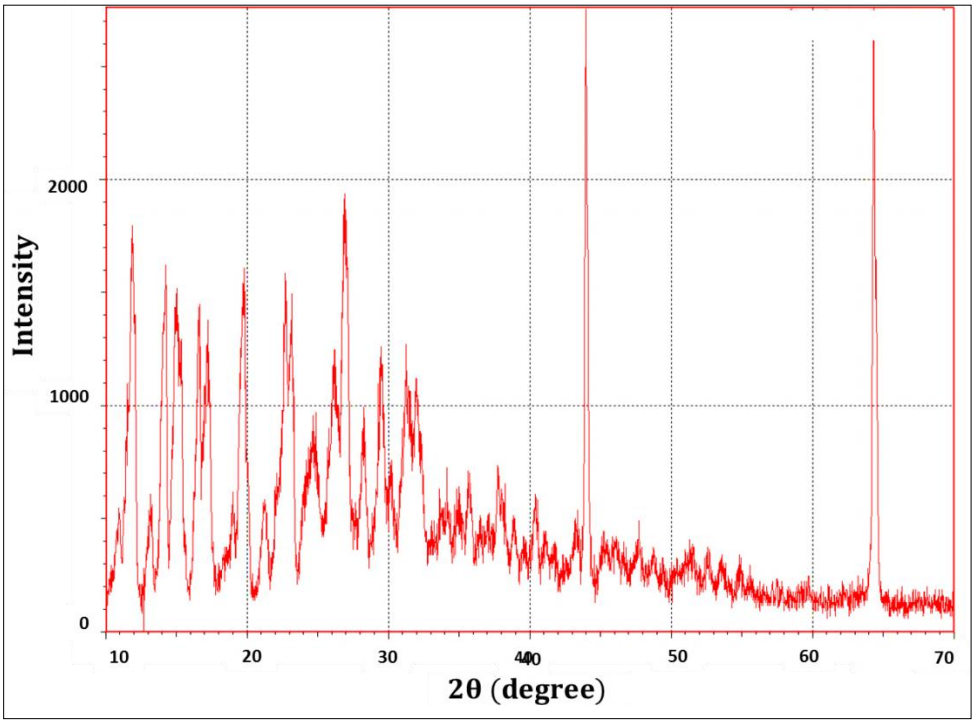

Figure (4-4): The XRD of MO powder.

Table (4-3): XRD measurement of MO powder:

2θ degree	d nm	I	I/I_o %	FWHM degree	β rad	Average crystal Size nm
10.96	0.806	50.20	8.87	0.28	0.004	28.5
15	0.590	180.49	476.5	0.44	0.007	18.21
17.20	0.515	149.86	367.3	0.44	0.007	18.26
26.92	0.331	270.25	60.64	0.52	0.009	15.71
44	0.205	409.89	91.97	0.20	0.003	30.91
64.34	0.144	445.69	100	0.24	0.004	39.09

4.4 Atomic Force Microscope (AFM)

Atomic force microscopy (AFM) is used to evaluate the surface structure of the PVA, MO and PVA/MO composite thick films before and after irradiation with different thickness using a violet laser source as shown in Figures (4-5 - 4-10). The findings revealed that the surfaces become less roughness, the grain size increased. The result shows that the laser beam irradiation improves the uniformity of the surfaces of the films because it acts to recrystallize them. The drop in average grain size values is related to the atoms inability to merge with one another due to strain between the crystalline boundaries in those films. The AFM results for each thick films are listed in Table (4-4).

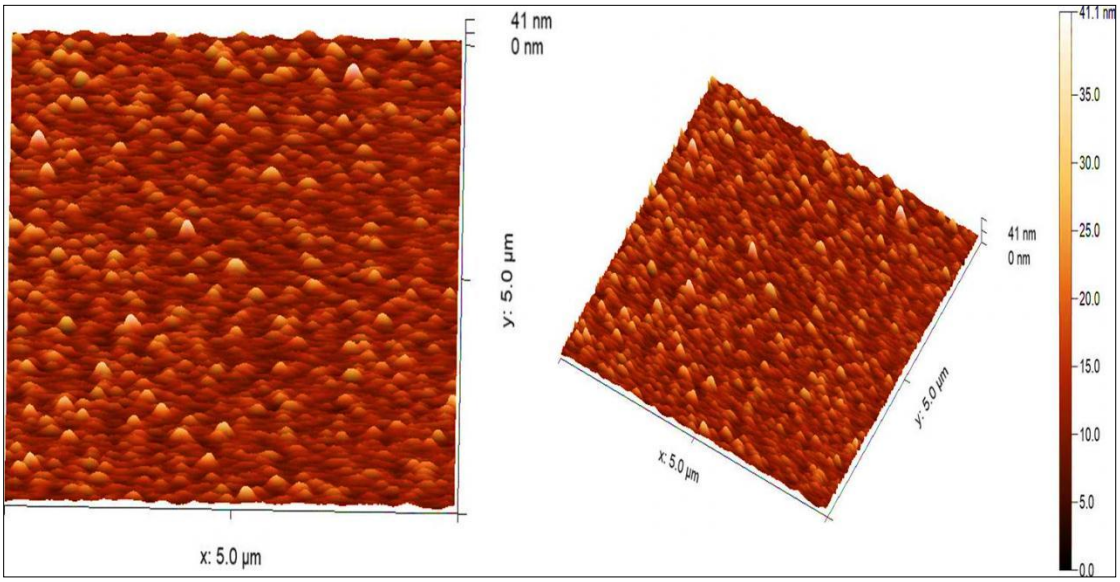

Figure (4-5): AFM for non-irradiated PVA thick film at thickness 3000 nm.

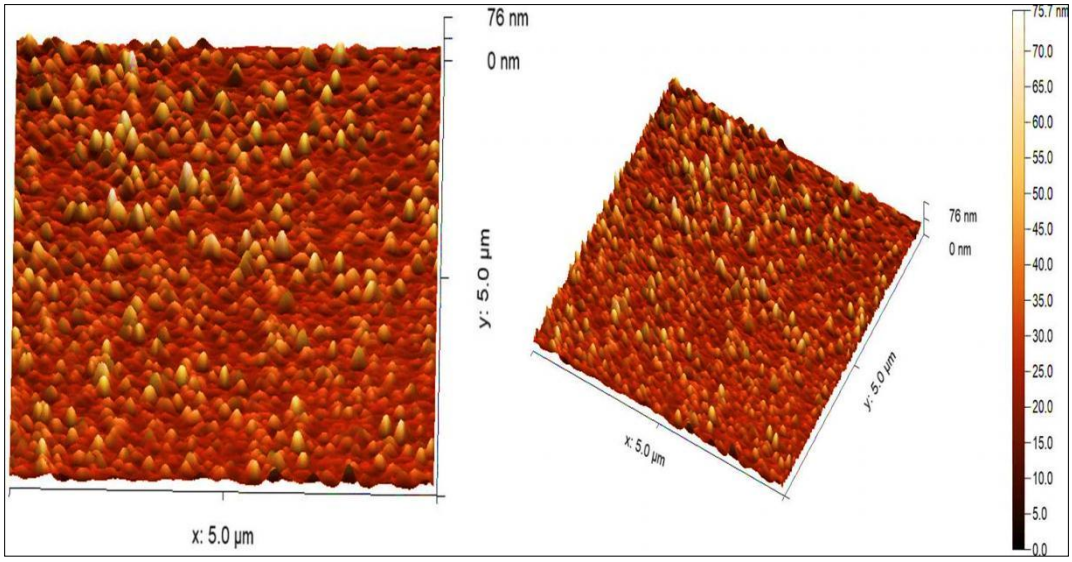

Figure (4-6): AFM for PVA thick film with thickness 3000nm irradiated for 40 min by a 405 nm violet laser.

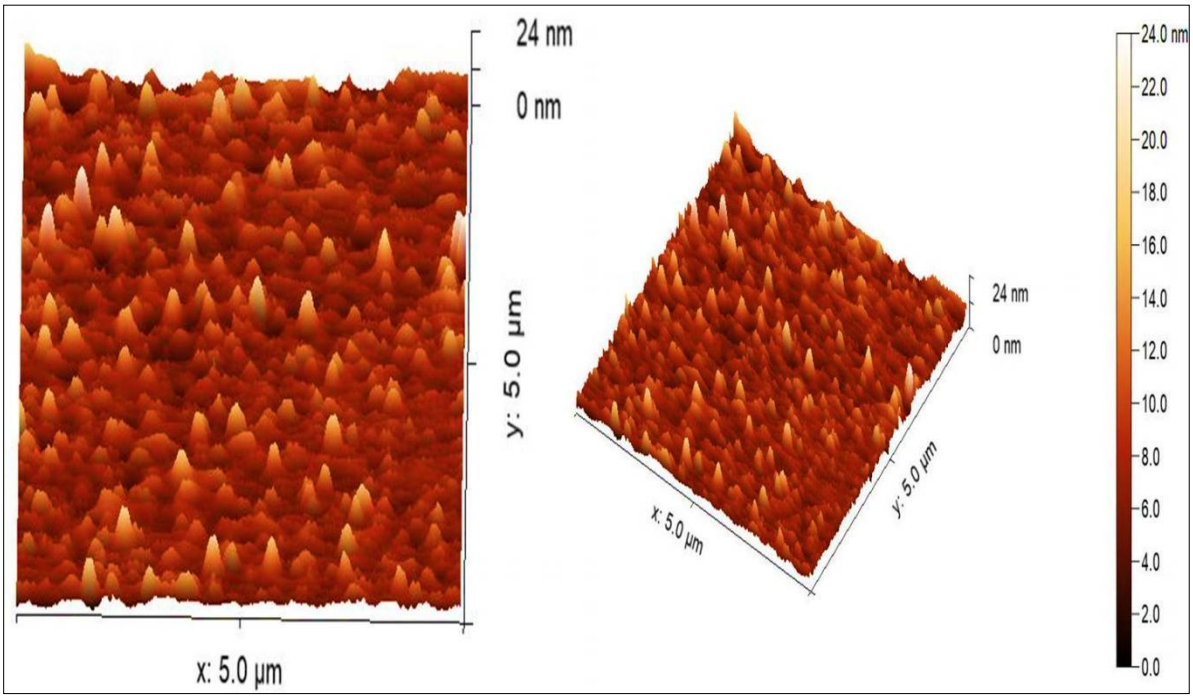

Figure (4-7): AFM for MO thick film with thickness 3000 nm for non-irradiated sample.

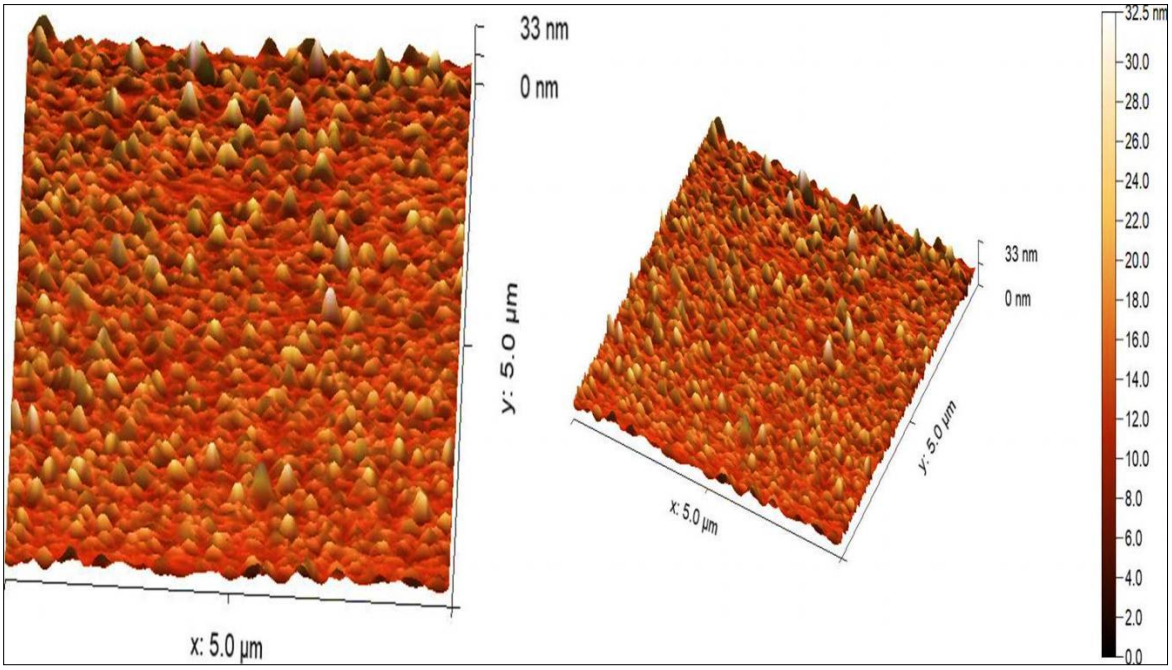

Figure (4-8): AFM for MO thick film with thickness 3000 nm and time irradiated 40 min by 405 nm violet laser.

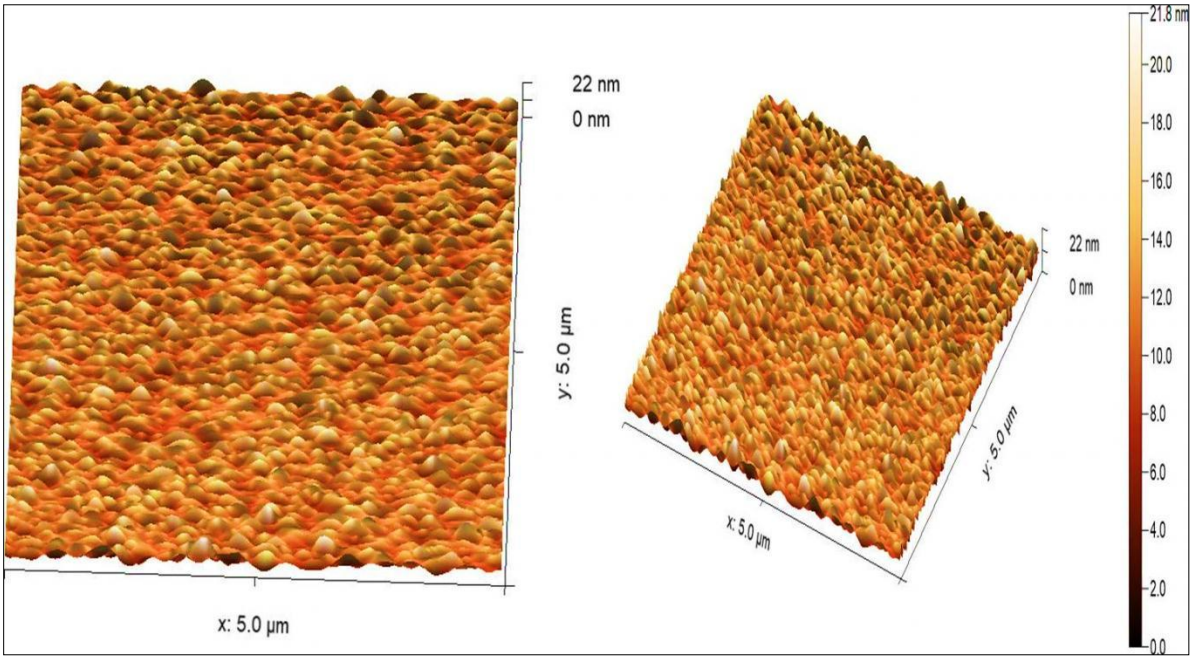

Figure (4-9): AFM for PVA/MO thick film with thickness 6000 nm for non-irradiated sample.

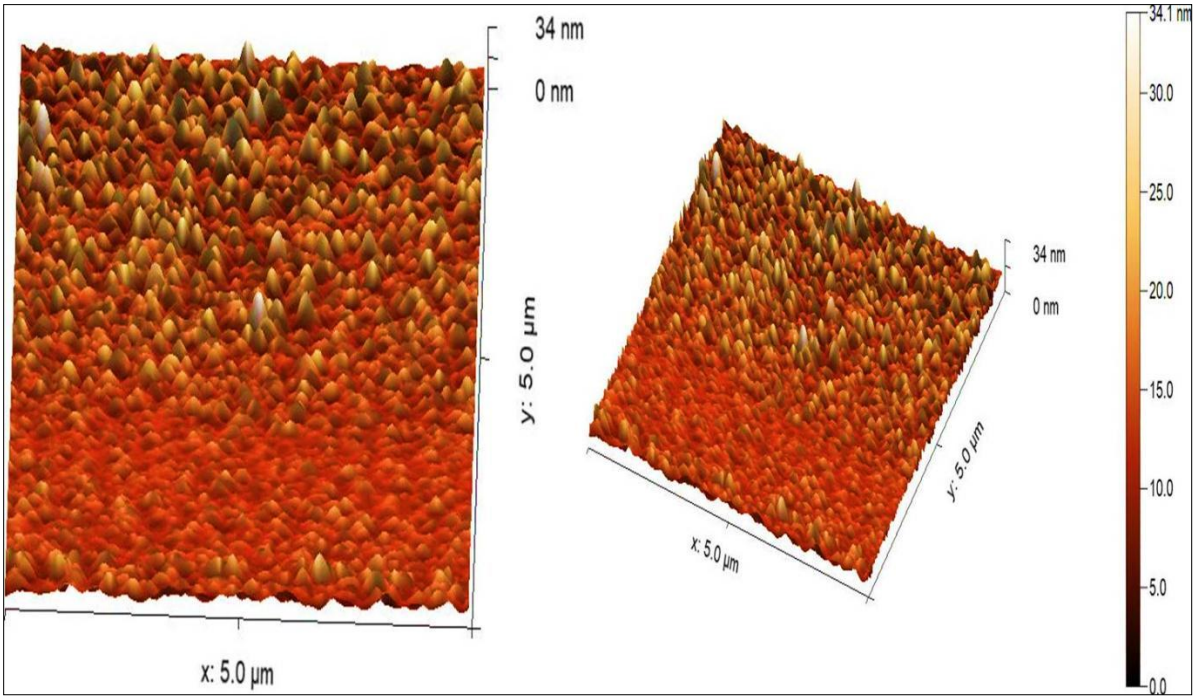

Figure (4-10): AFM for PVA/MO thick film with thickness 6000 nm and time irradiated 40 min by 405 nm violet laser.

Table (4-4): AFM measurements of PVA, MO and PVA/MO thick films before and after 405 nm laser irradiating.

Thick film	Thickness nm	Irradiating time min.	Average diameter nm	Roughness nm	Average Value nm	Root mean square nm
PVA	3000	0	86.345	5.568	22.059	39.27
		40	75.711	3.83	21.148	11.50
MO	3000	0	32.525	2.380	11.850	39.38
		40	24.024	1.469	6.710	11.61
PVA/MO	6000	0	34.075	2.754	11.554	56.16
		40	21.766	2.180	10.243	34.83

4.5 Optical Properties

4.5.1 The Solutions

The absorbance spectra of PVA, MO and PVA/MO solutions are recorded in the wavelength range (190-1100) nm before and after the laser irradiation. The data are illustrated in Figures (4-11a, 4-12a and 4-13a) for PVA, MO and PVA/MO respectively. PVA spectra show the absorption in the range (240–330) nm, the highest absorbance was recorded at the wavelength of 280 nm, While the wavelength from 360 nm there is no absorbance. For MO the absorbance spectra at (390 - 510) nm, the highest absorbance appears at the wavelength of 469 nm and from 530 nm there aren't absorption. In the case of composite PVA/MO, the absorbance spectrum appears at (260 - 520) nm, and it becomes clear that there are two high values of absorbance, the first at 270 nm and the second at 479 nm, while the wavelength that are not affected by absorbance are at 530 nm.

It can be seen from the absorbance spectra that increasing the irradiating laser time causes decreasing in the solution absorption obeying Beer – Lambert law. This behavior is attributed to breaking the molecules bonding due to the intense laser energy which is a strong indicator that laser beam has an effect on the absorbance. As a result, the irradiating by violet laser shows a red shift.

Figures (4-11b, 4-12b and 4-13b) indicate that the absorbance of the non-irradiated samples is bigger than the laser irradiated samples. It decreases with increasing the laser exposure time of the solution because of the longer time, the greater bonds dissociation.

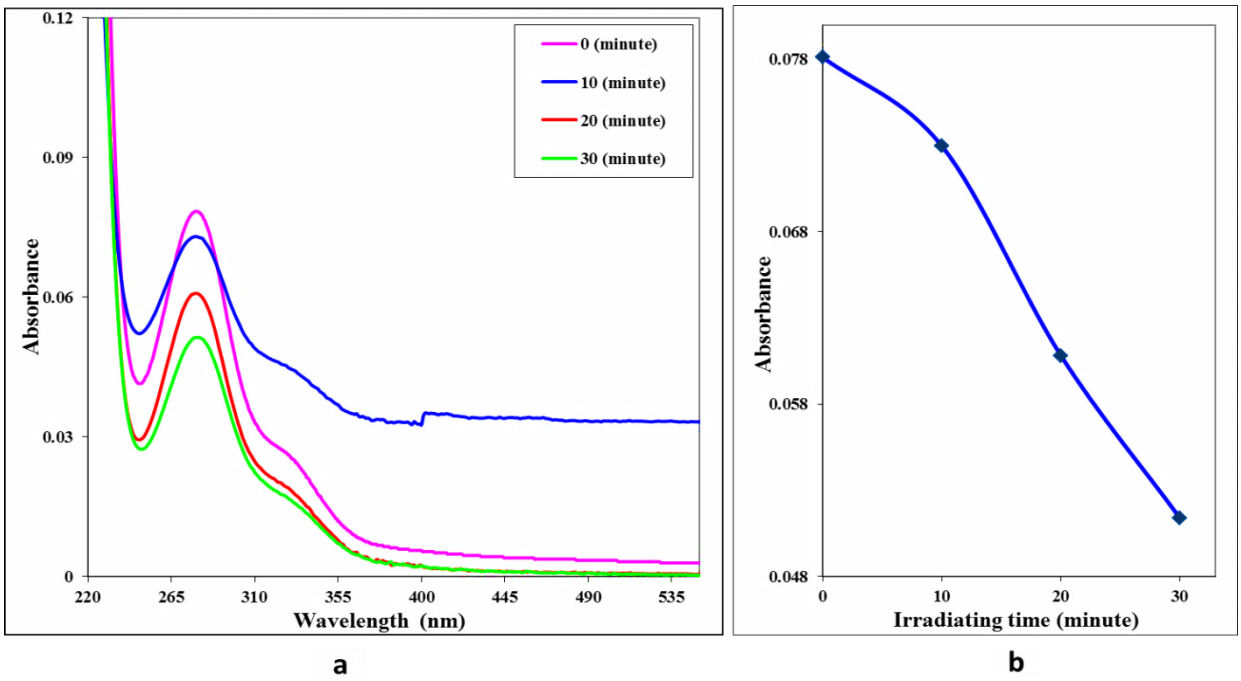

Figure(4-11): (a) The PVA absorbance spectra for different laser exposure times (0, 10, 20 and 30) min. (b) The absorbance as a function of irradiating time at 405 nm wavelength.

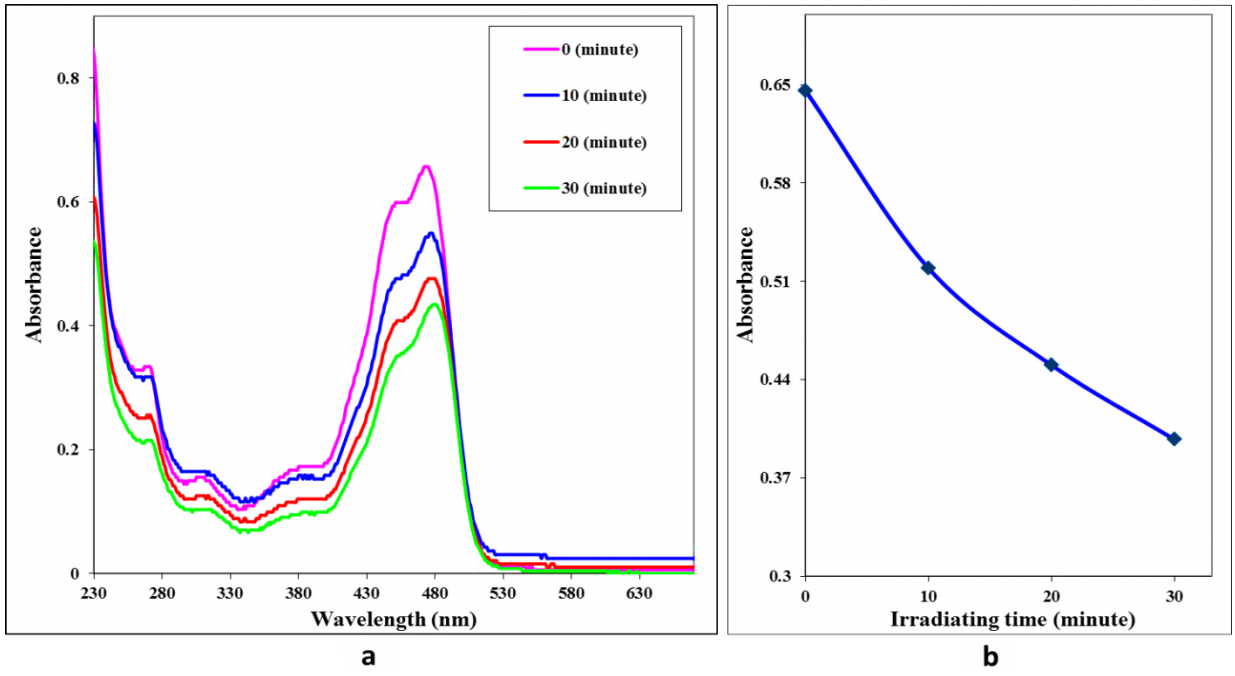

Figure (4-12):(a) The MO absorbance spectra for different irradiating times (0, 10, 20 and 30 minute). (b) The absorbance as a function of irradiating time at 405 nm wavelength.

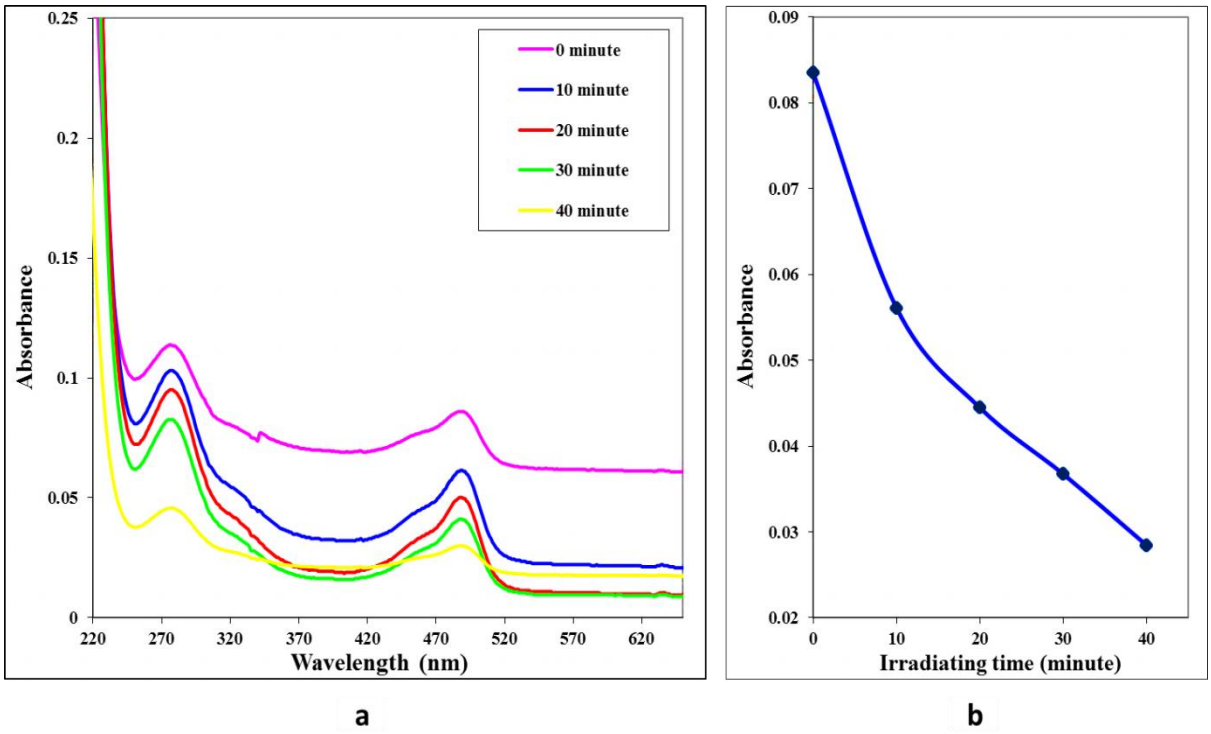

Figure (4-13): (a) The PVA/MO absorbance spectra for different irradiating times (0, 10, 20 and 30) min. (b) The absorbance as a function of irradiating time at 405 nm wavelength.

The indirect energy gap is excluded from Figures (4-14a, 4-15a and 4-16a) utilizing Tauc equation. $(\alpha h\upsilon)^{1/2}$ is plotted as a function of the solution band gap. Obviously, the rapid increase in the absorption coefficient is where it can deduce the absorption edge.

Figures (4-14a, 4-15a and 4-16a) explain the band gap behavior when the irradiation times increase. This energy gap control by laser irradiation can be used as an optical filter application.

The optical properties of PVA, MO and PVA/MO solutions appeared that decreasing in the absorbance and reflectance with increasing the laser irradiation times while the transmittance increases. The energy gap rises with increasing the irradiation times while the results show that the optical constants decrease as shown in tables (4-5, 4-6, 4-7).

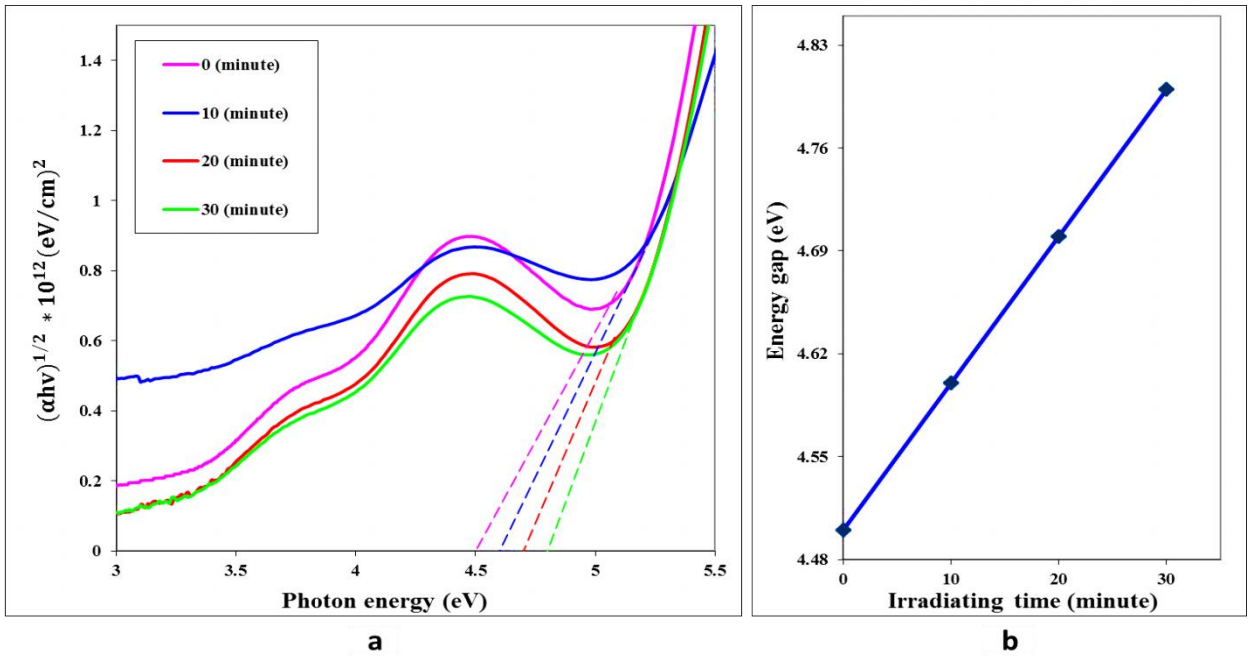

Figure(4-14):(a)The PVA $(\alpha hv)^{1/2}$ as a function of the photon energy for different irradiating times (0, 10, 20 and 30) min. (b) The indirect energy gap as a function of irradiating time at 405 nm wavelength.

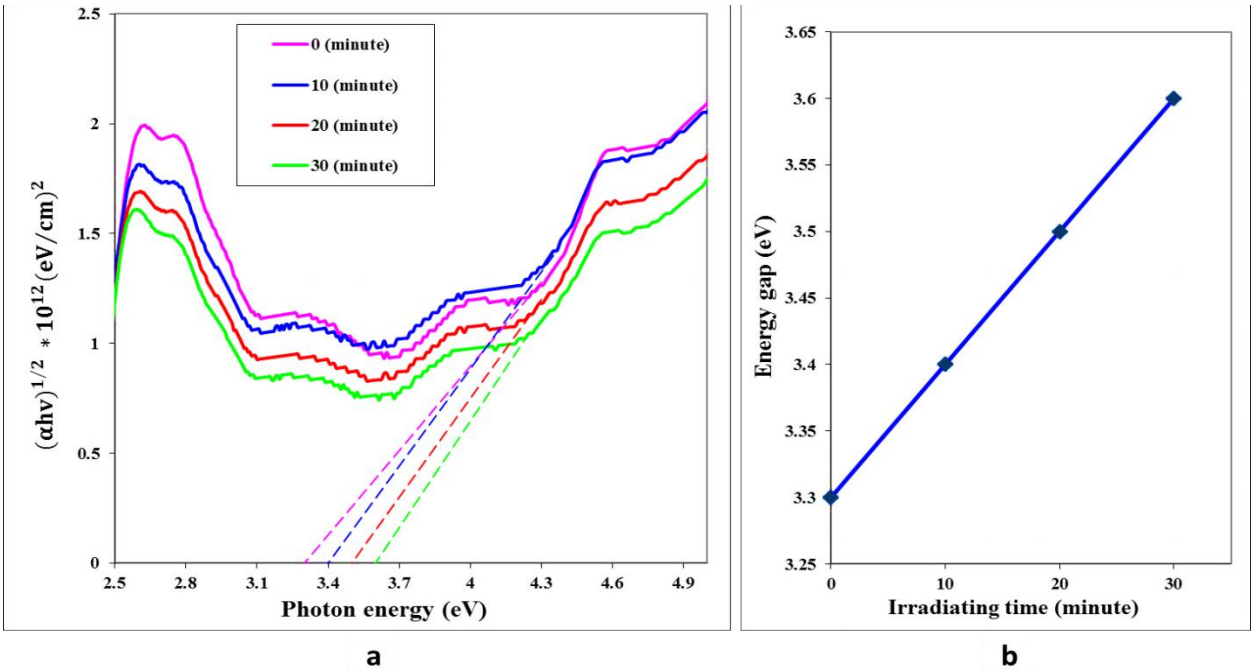

Figure (4-15): (a) The MO $(\alpha hv)^{1/2}$ as a function of the photo energy for different irradiating times (0, 10, 20 and 30) min. (b) The indirect energy gap as a function of irradiating time at 405 nm wavelength.

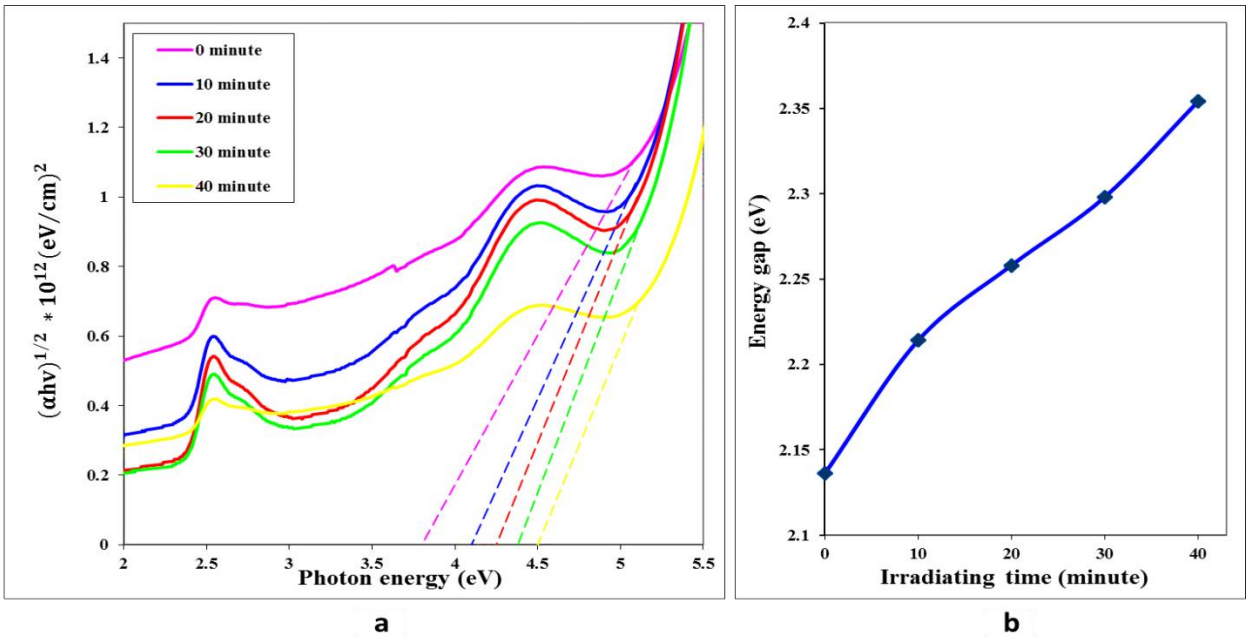

Figure (4-16): (a) The PVA/MO $(\alpha hv)^{1/2}$ as a function of the photo energy for different irradiating times (0, 10, 20 and 30) min. (b) The indirect energy gap as a function of irradiating time at 405 nm wavelength.

Table(4-5): The optical constants of PVA solution for different irradiating times at wavelength 280 nm.

Time min.	α cm^{-1}	K $\times 10^{-4}$	n	ε_{real}	$\varepsilon_{im} \times 10^{-4}$	Eg eV	σ optical $\times 10^{-6}$ s^{-1}
0	0.18	4.01	1.57	2.46	1.26	4.5	6.74
10	0.17	3.73	1.53	2.35	1.15	4.6	6.16
20	0.14	3.11	1.45	2.10	0.903	4.7	4.85
30	0.12	2.63	1.38	1.92	0.728	4.8	4.23

Table(4-6): The optical constants of MO solution for different irradiating times at wavelength 469 nm:

Time min.	α cm^{-1}	K $\times 10^{-4}$	n	ε_{real}	$\varepsilon_{im} \times 10^{-4}$	Eg eV	σ optical $\times 10^{-6}$ s^{-1}
0	1.49	5.55	1.88	3.54	2.09	3.2	6.69
10	1.20	4.46	2.30	5.30	2.06	3.3	6.57
20	1.04	3.87	2.45	6.03	1.90	3.5	6.08
30	0.91	3.42	2.52	6.35	1.72	3.6	5.51

Table(4-7): The optical constants of PVA/MO solution for different irradiating times at wavelength 479 nm:

Time min.	α cm^{-1}	K $\times 10^{-4}$	n	ε_{real}	$\varepsilon_{im} \times 10^{-4}$	Eg eV	σ optical $\times 10^{-6}$ s^{-1}
0	0.19	7.33	1.60	2.57	2.35	3.8	7.36
10	0.13	4.92	1.42	2.01	1.40	4.1	4.37
20	0.10	3.90	1.33	1.78	1.04	4.25	3.26
30	0.08	3.23	1.28	1.63	8.25	4.38	2.58
40	0.07	2.50	1.22	1.48	6.08	4.5	1.90

4.5.2 The Thick Films

PVA, MO and PVA/MO thick films are deposited by casting coating method at room temperature with different thickness on a petri dish.

PVA thick films have absorbance spectrum around (280- 380) nm for both thickness 2000 and 3000 nm. High absorption appears at 350 and 360 nm, respectively, for both thicknesses.

For MO at thickness 2000 and 3000 nm the spectrum recording in (400- 560)nm and (420- 580) nm, while the high wavelength in 480nm and 490 nm respectively

In the composite PVA/MO thick films for thickness 2000 nm (460- 550) with high absorption 500nm, 4000nm (470- 560)nm with high absorption 520nm and 6000 nm (370- 570)nm with high absorption 560nm.

The absorption spectrum are show in Figures (17 a - 23 a) before and after laser irradiation for the polymer, methyl orange, and their composite with different thicknesses, respectively.

As for the Figures (17 b - 23 b), they show the relationship between the absorption spectrum and the irradiation time (0, 10, 20, 30 and 40) minutes, as the absorption spectrum decreases with increasing irradiation time due to the breaking of bonds.

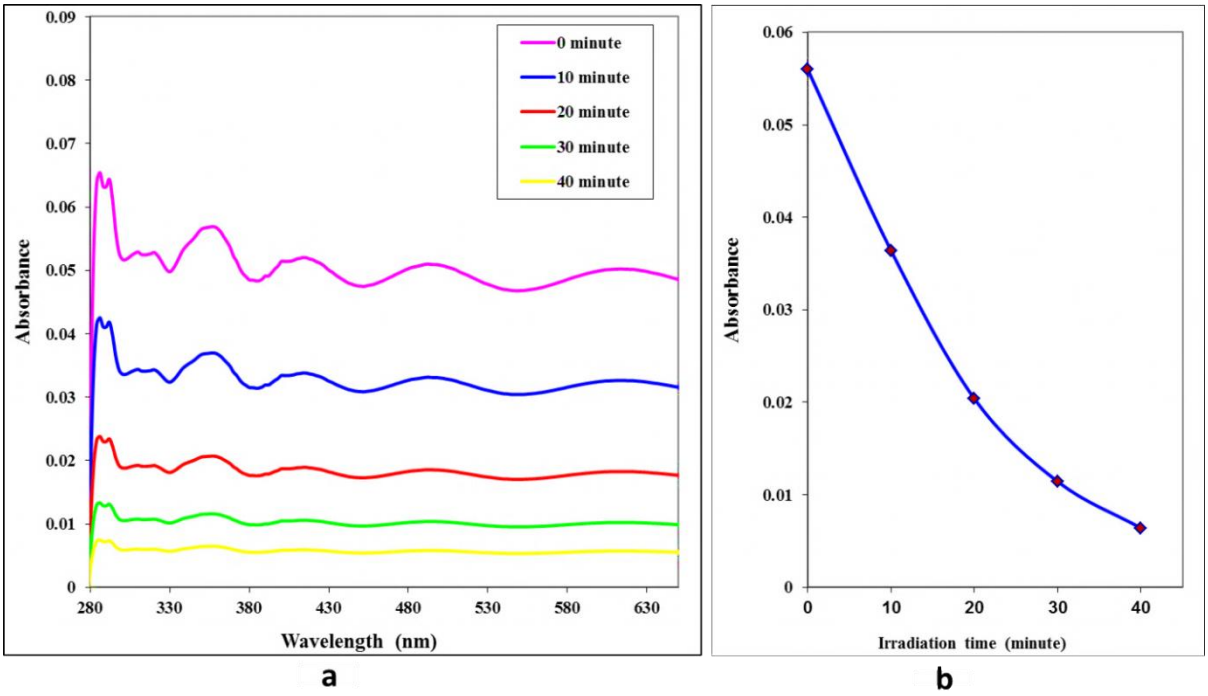

Figure (4-17): (a) The absorbance spectra of PVA thick films with 2000 nm thickness for different irradiating times (0, 10, 20, 30 and 40) min. (b) The absorbance as a function of irradiating time at 405 nm wavelength.

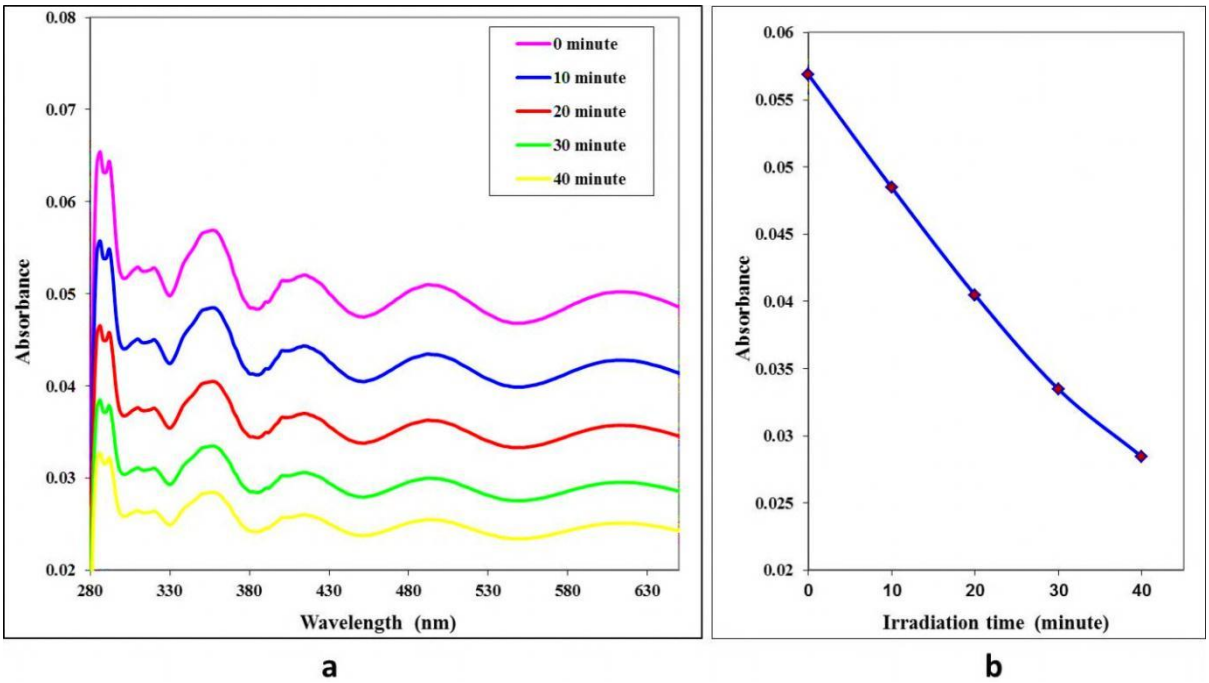

Figure (4-18): (a) The absorbance spectra of PVA thick films with 3000 nm thickness for different irradiating times (0, 10, 20, 30 and 40) min. (b) The absorbance as a function of irradiating time at 405 nm wavelength.

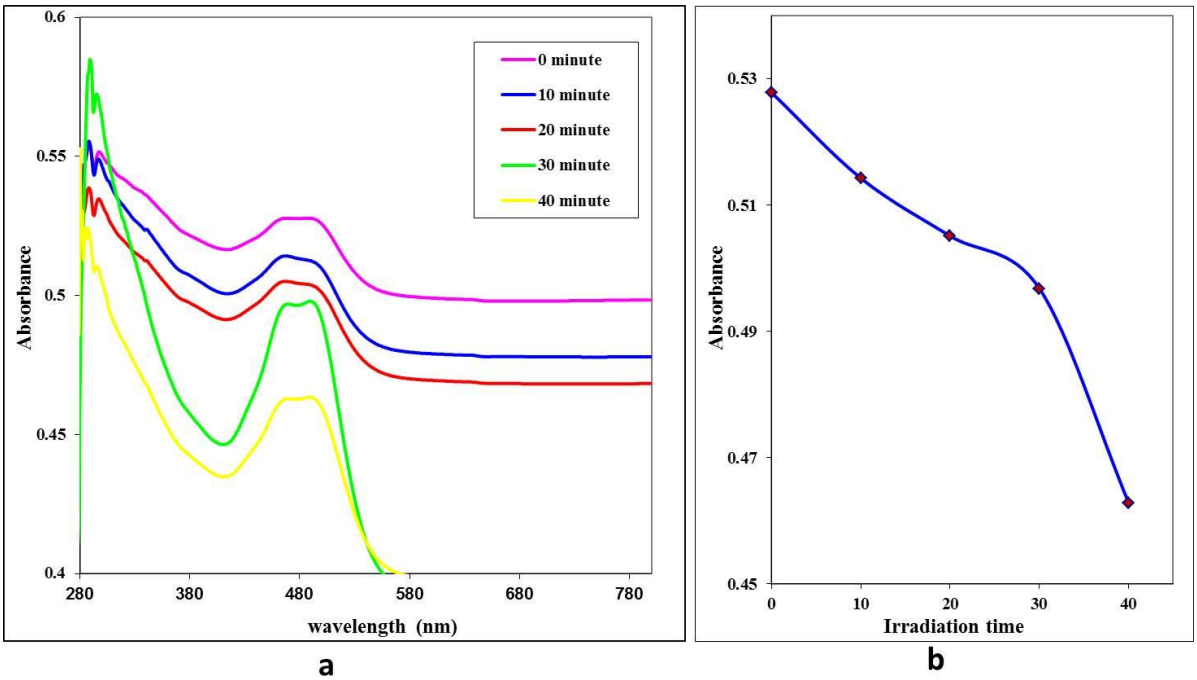

Figure (4-19): (a) The absorbance spectra of MO thick films with 2000 nm thickness for different irradiating times (0, 10, 20, 30 and 40) min. (b) The absorbance as a function of irradiating time at 405 nm wavelength.

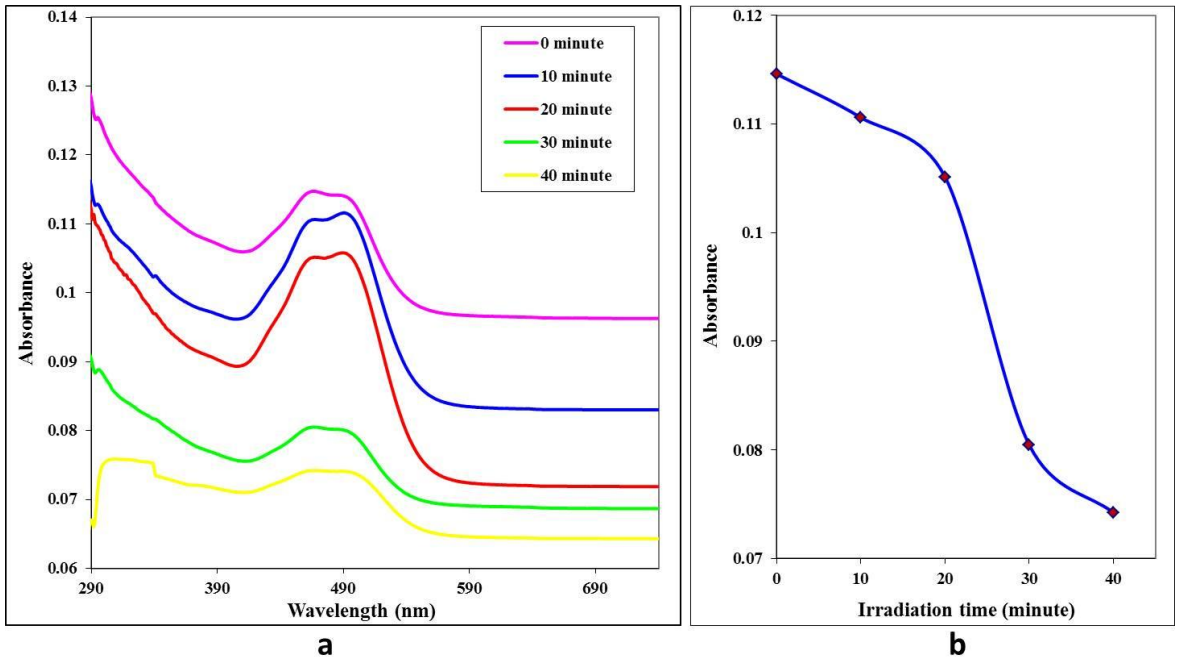

Figure (4-20): (a) The absorbance spectra of MO thick films with 3000 nm thickness for different irradiating times (0, 10, 20, 30 and 40) min. (b) The absorbance as a function of irradiating time at 405 nm wavelength.

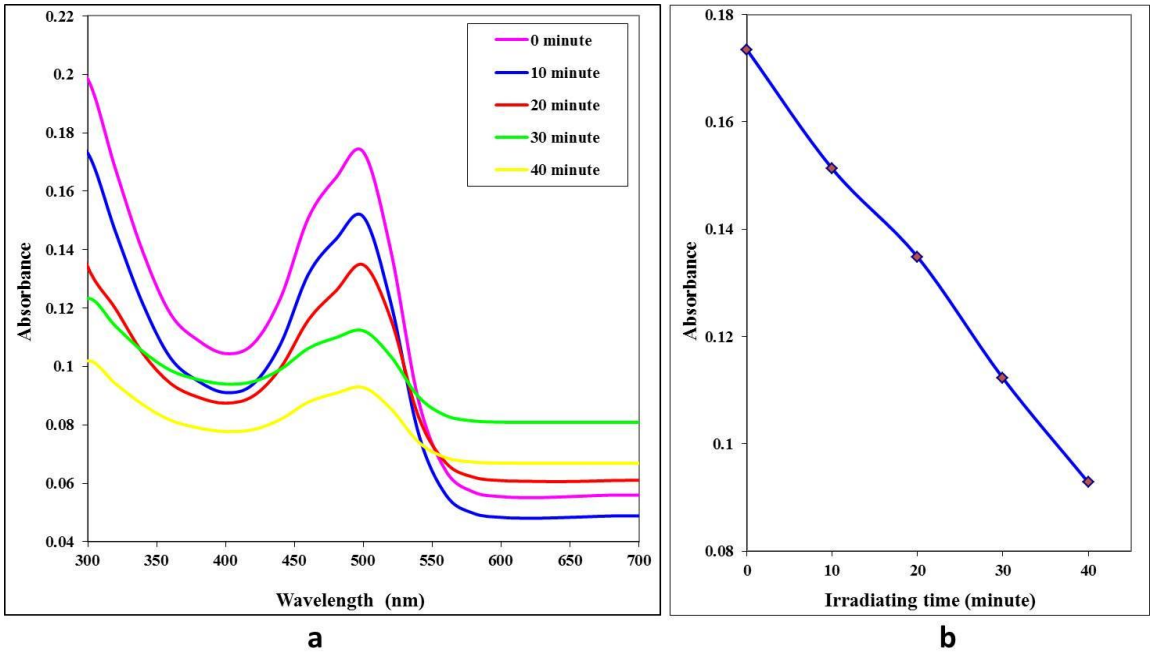

Figure (4-21): (a) The absorbance spectra of PVA/MO thick films with 2000 nm thickness for different irradiating times (0, 10, 20, 30 and 40) min. (b) The absorbance as a function of irradiating time at 405 nm wavelength.

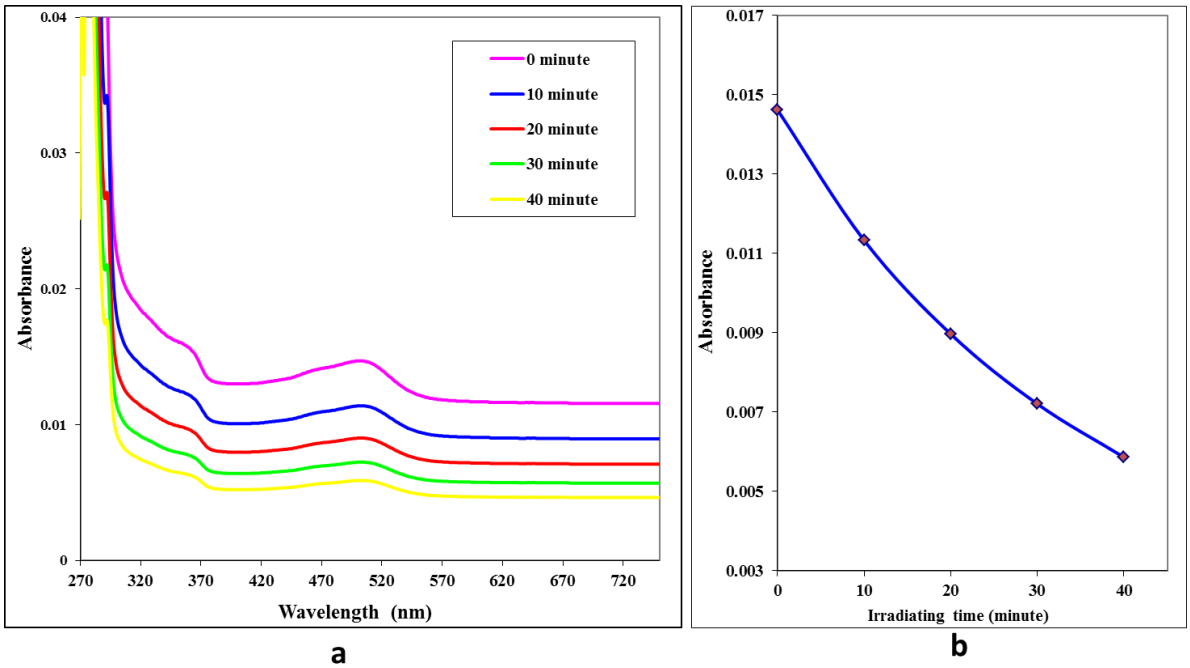

Figure (4-22): (a) The absorbance spectra of PVA/MO thick films with 4000 nm thickness different irradiating times (0, 10, 20, 30 and 40) min. (b) The absorbance as a function of irradiating time at 405 nm wavelength.

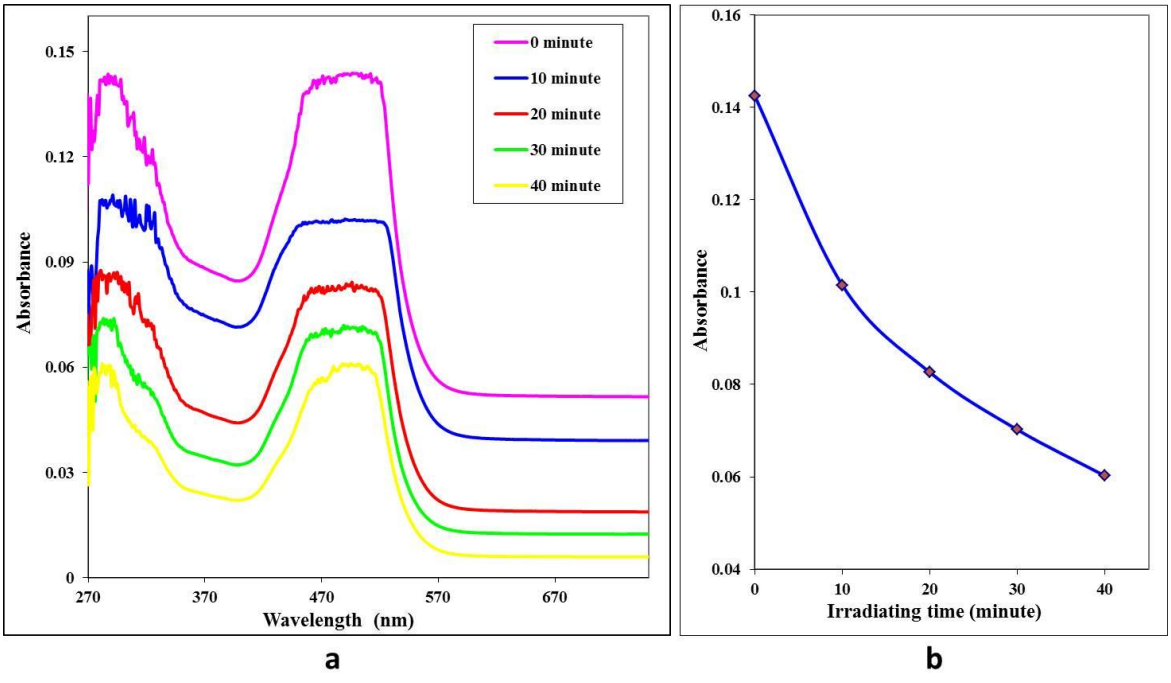

Figure (4-23): (a) The absorbance spectra of PVA/MO thick films with 6000 nm thickness for different irradiating times (0, 10, 20, 30 and 40) min. (b) The absorbance as a function of irradiating time at 405 nm wavelength.

The energy band gap (direct) with photon energy as shown in Fig. (4-27 – 4 33). the photon energy value of PVA, MO and PVA/MO thick film of ~ 2000, 3000 *nm* thickness for each PVA and MO and about 2000, 4000 and 6000 nm for PVA/MO, irradiated at wavelength 405 *nm* at time 0,10,20,30 and 40 *min*. We notice that the optical energy gap increases slightly with the increase in the time irradiation. Optical parameters as (absorption coefficient, refractive index, extinction coefficient, dielectric constants, optical conductivity and direct energy gap) for all thick films are listed in Tables (4-8 - 4-14).

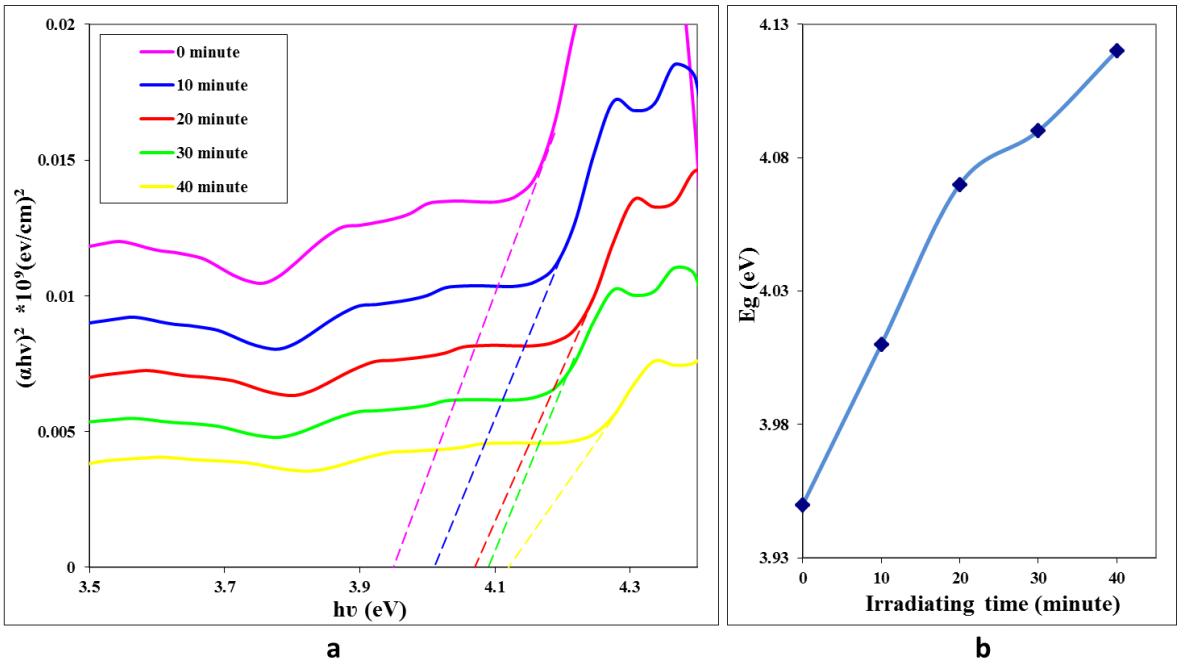

Figure (4-24): (a) The PVA at thickness 2000nm $(\alpha h\upsilon)^2$ as a function of the photo energy for different irradiating times (0, 10, 20, 30 and 40) min. (b) The direct energy gap as a function of irradiating time at 405 nm wavelength.

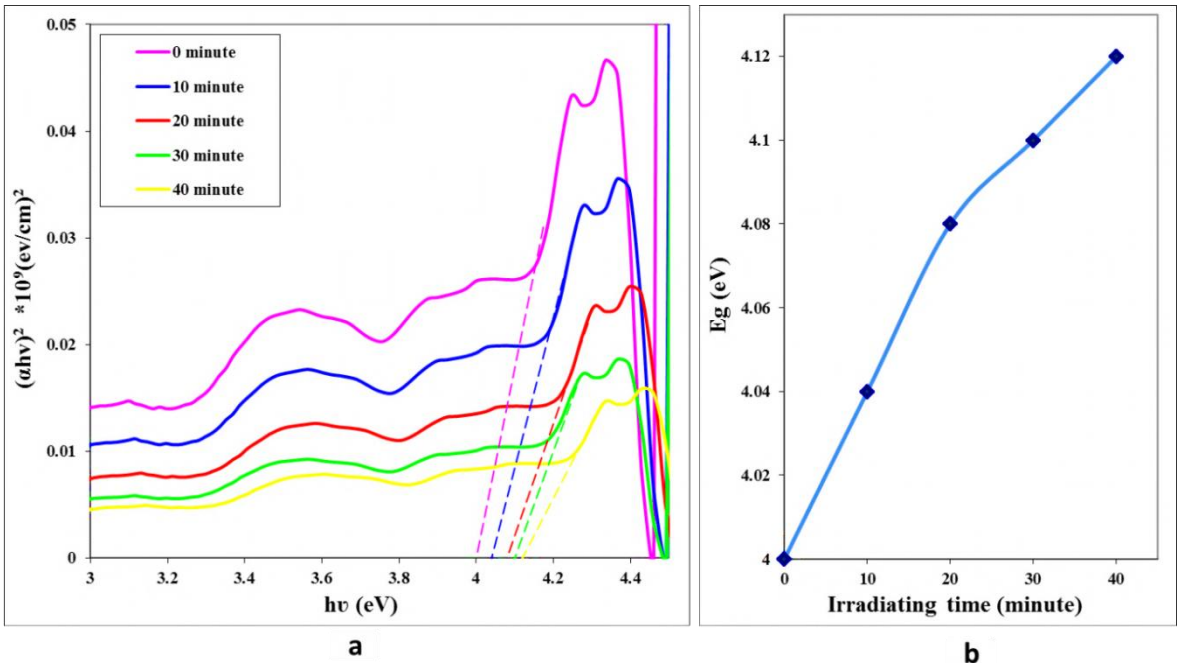

Figure (4-25): (a) The PVA at thickness 3000nm $(\alpha h\nu)^2$ as a function of the photo energy for different irradiating times (0, 10, 20, 30 and 40) min. (b) The direct energy gap as a function of irradiating time at 405 nm wavelength.

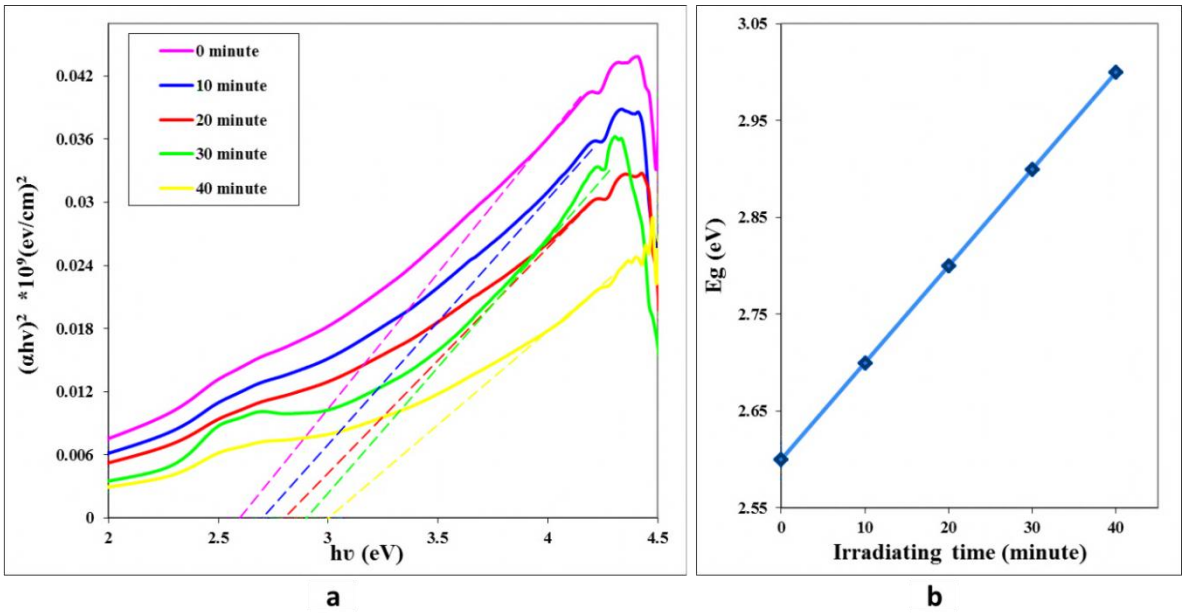

Figure (4-26): (a) The MO at thickness 2000nm $(\alpha h\nu)^2$ as a function of the photo energy for different irradiating times (0, 10, 20, 30 and 40) min. (b) The direct energy gap as a function of irradiating time at 405 nm wavelength.

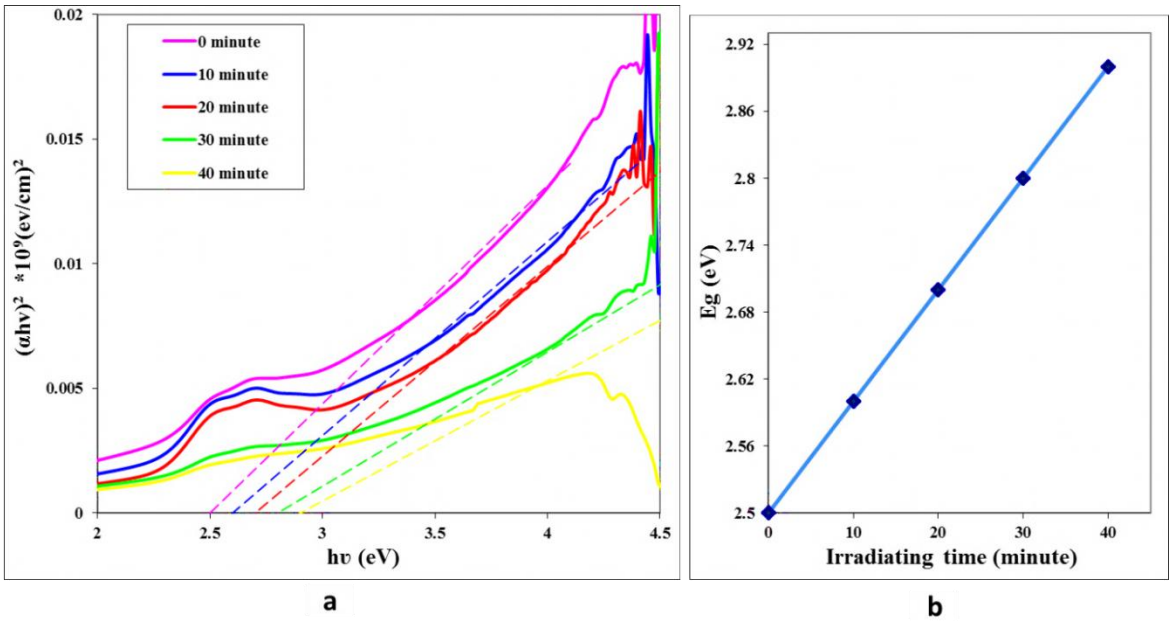

Figure (4-27): (a) The MO at thickness 3000nm $(\alpha h\upsilon)^2$ as a function of the photo energy for different irradiating times (0, 10, 20, 30 and 40) min. (b) The direct energy gap as a function of irradiating time at 405 nm wavelength.

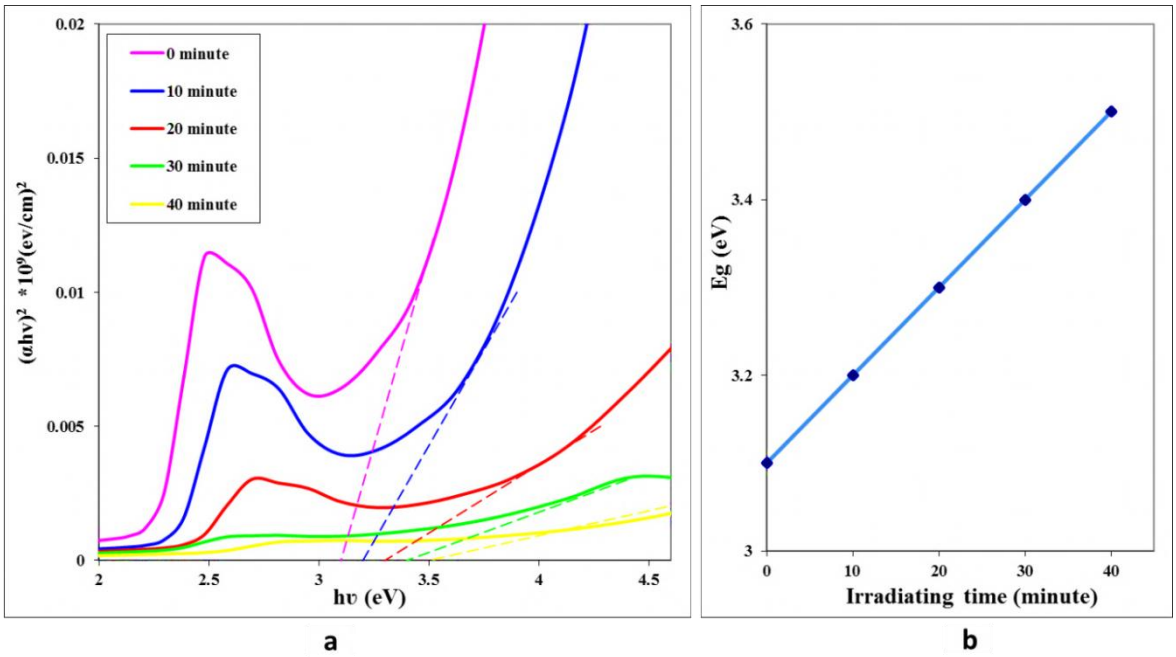

Figure (4-28): (a) The PVA/MO at thickness 2000nm $(\alpha h\upsilon)^2$ as a function of the photo energy for different irradiating times (0, 10, 20, 30 and 40) min. (b) The direct energy gap as a function of irradiating time at 405 nm wavelength.

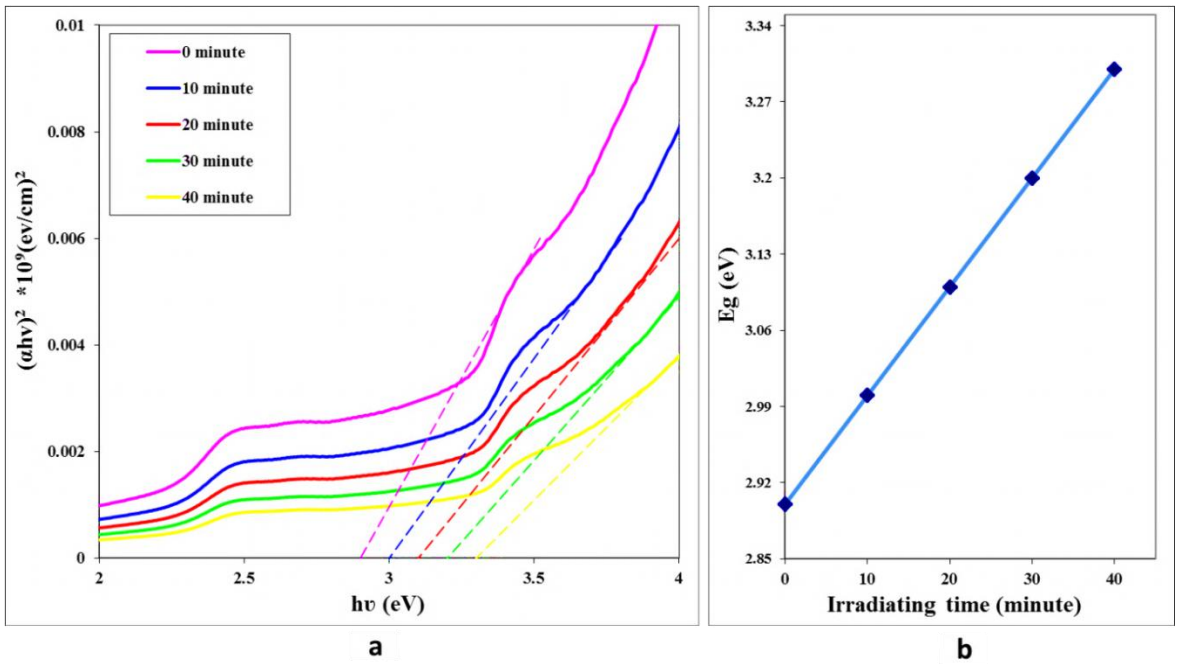

Figure (4-29): (a) The PVA/MO at thickness 4000nm $(\alpha h\nu)^2$ as a function of the photo energy for different irradiating times (0, 10, 20, 30 and 40) min. (b) The direct energy gap as a function of irradiating time at 405 nm wavelength.

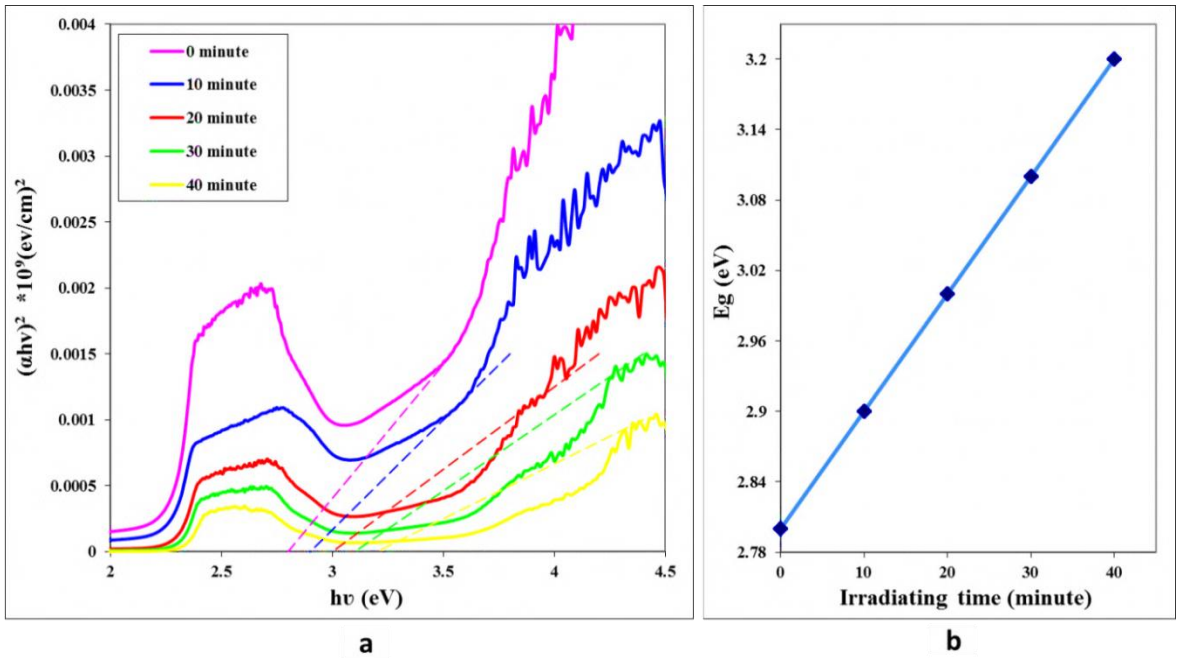

Figure (4-30): (a) The PVA/MO at thickness 6000nm $(\alpha h\nu)^2$ as a function of the photo energy for different irradiating times (0, 10, 20, 30 and 40) min. (b) The direct energy gap as a function of irradiating time at 405 nm wavelength.

Table(4-8): The optical constants of PVA thick film with 2000 nm for different irradiating times at wavelength 350 nm.

Time min.	α cm^{-1}	K $\times 10^{-4}$	n	ε_{real}	$\varepsilon_{im} \times 10^{-4}$	Eg eV	$\sigma_{optical} \times 10^{-6}$ s^{-1}
0	0.0645	17.87	1.41	2	50.6	3.95	21.8
10	0.0419	11.6	1.27	1.62	29.6	4.01	12.7
20	0.0234	6.50	1.15	1.33	15.05	4.07	6.48
30	0.0131	3.64	1.08	1.18	7.93	4.09	3.41
40	0.0073	2.04	1.04	1.10	4.28	4.12	1.84

Table(4-9): The optical constants of PVA thick film with 3000 nm for different irradiating times at wavelength 360 nm.

Time min.	α cm^{-1}	K $\times 10^{-4}$	n	ε_{real}	$\varepsilon_{im} \times 10^{-4}$	Eg eV	$\sigma_{optical} \times 10^{-6}$ s^{-1}
0	0.0436	12.44	1.42	2.02	35.42	4	14.84
10	0.0372	10.60	1.36	1.85	28.92	4.04	12.11
20	0.0310	8.85	1.30	1.70	23.12	4.08	9.68
30	0.0256	7.32	1.25	1.57	18.36	4.1	7.69
40	0.0218	6.22	1.21	1.48	15.15	4.13	6.34

Table(4-10): The optical constants of MO thick film with 2000 nm for different irradiating times at wavelength 480 nm.

Time min.	α cm^{-1}	K ×10^{-4}	n	ε_{real}	$\varepsilon_{im} \times 10^{-4}$	Eg eV	σ optical×10^{-6} s^{-1}
0	0.6076	23.22	2.43	5.91	10.58	2.6	33.06
10	0.5909	22.58	2.35	5.56	10.46	2.7	32.71
20	0.5806	22.19	2.34	5.47	10.38	2.8	32.46
30	0.5718	21.85	2.31	5.37	10.31	2.9	32.22
40	0.5329	20.36	2.27	5.19	9.9	3	30.96

Table(4-11): The optical constants of MO thick film with 3000 nm for different irradiating times at wavelength 490 nm.

Time min.	α cm^{-1}	K ×10^{-4}	n	ε_{real}	$\varepsilon_{im} \times 10^{-4}$	Eg eV	σ optical×10^{-6} s^{-1}
0	0.0879	32.98	1.79	3.23	11.85	2.5	37.76
10	0.0848	31.83	1.77	3.14	11.29	2.6	35.96
20	0.0807	30.26	1.74	3.02	10.53	2.7	33.55
30	0.0617	23.16	1.58	2.50	7.33	2.8	23.36
40	0.0569	21.36	1.54	2.37	6.58	2.9	20.98

Table(4-12): The optical constants of PVA/ MO thick film with 2000 nm for different irradiating times at wavelength 500 nm.

Time min.	α cm^{-1}	K $\times 10^{-4}$	n	ε_{real}	$\varepsilon_{im} \times 10^{-4}$	Eg eV	σ optical $\times 10^{-6}$ s^{-1}
0	0.1997	79.51	2.10	4.44	33.51	3.1	10.05
10	0.1741	69.34	1.99	3.99	27.73	3.2	8.32
20	0.1552	61.79	1.91	3.65	23.64	3.3	7.09
30	0.1292	51.45	1.78	3.18	18.35	3.4	5.50
40	0.1068	42.54	1.66	2.76	14.15	3.5	4.24

Table(4-13): The optical constants of PVA/ MO thick film with 4000 nm for different irradiating times at wavelength 520 nm.

Time min.	α cm^{-1}	K $\times 10^{-4}$	n	ε_{real}	$\varepsilon_{im} \times 10^{-4}$	Eg eV	σ optical $\times 10^{-6}$ s^{-1}
0	0.0084	33.08	1.11	1.23	73.64	2.9	22.36
10	0.0065	25.63	1.08	1.18	55.77	3	16.93
20	0.0051	20.29	1.06	1.14	43.41	2.917	13.18
30	0.0041	16.30	1.05	1.11	34.44	2.945	10.45
40	0.0033	13.26	1.04	1.09	27.74	3	8.42

Table(4-14): The optical constants of PVA/ MO thick film with 6000 nm for different irradiating times at wavelength 560 nm.

Time min.	α cm^{-1}	K $\times 10^{-4}$	n	ε_{real}	$\varepsilon_{im} \times 10^{-4}$	Eg eV	σ optical $\times 10^{-6}$ s^{-1}
0	0.05464	20.88	1.95	3.81	81.60	2.8	25.50
10	0.0389	14.88	1.71	2.95	51.14	2.9	15.98
20	0.0317	12.11	1.59	2.55	38.72	2.917	12.10
30	0.0269	10.29	1.51	2.29	31.20	2.945	9.75
40	0.0231	8.83	1.44	2.09	25.55	3	7.98

4.6 Dispersive properties for thick films

To study the dispersive properties of PVA, MO and PVA/MO thick films, Urbach tails are calculated using the absorption data before and after violet laser exposure of 10, 20, 30 and 40 minute duration. ($\ln \alpha$) is plotted as a function of the photon energy (hυ) depending on equation (2-20), which was discussed in chapter two. The behaviour is shown in Figures (4-31a – 4-37a). The inverse slope represents Urbach tails.

The relationship between Urbach energy and irradiation times is shown in Figures (4-31b – 4-37b). It is found that increasing the irradiation time causes decreasing in the Urbach energy. This indicated that the crystallization of the irradiated thick films increases due to decreasing the crystal defects and the dislocations.

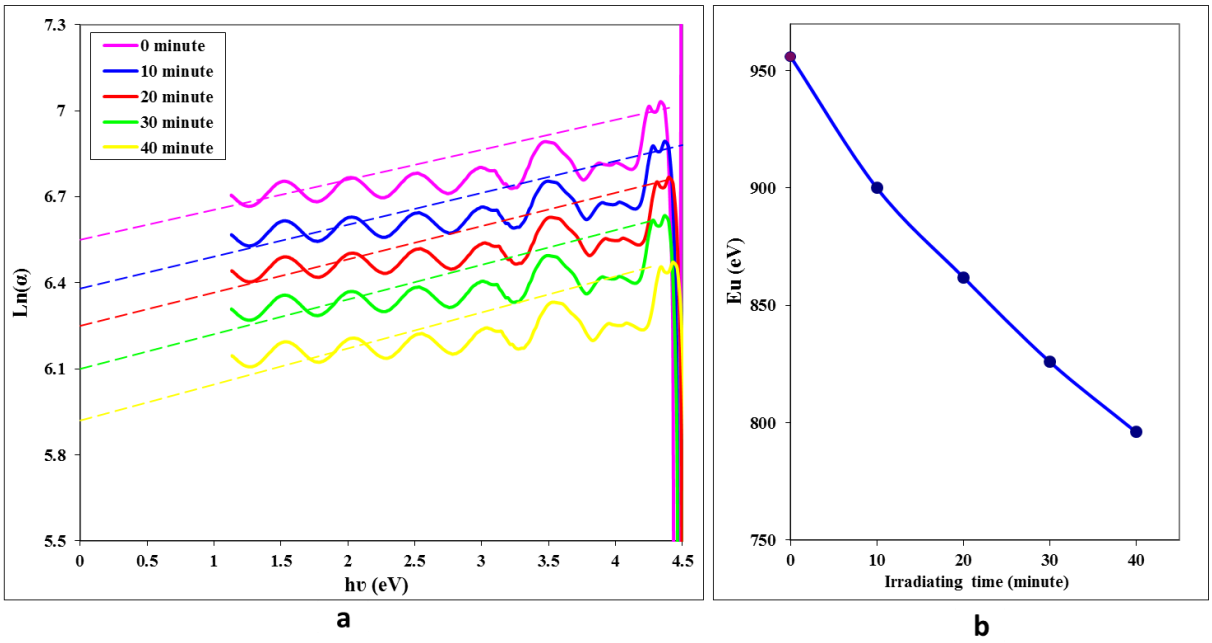

Figure (4-31): (a) ln α as a function of the photon energy of PVA thick film with 2000 nm thickness. (b) Urbach energy as a function of irradiating times.

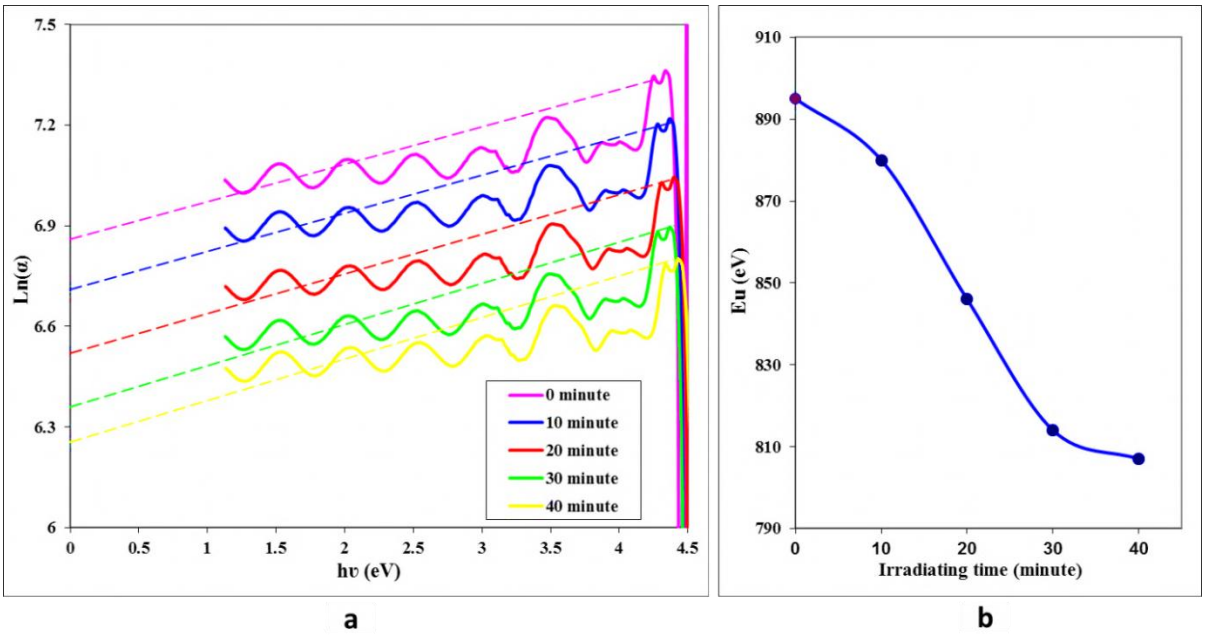

Figure (4-32): (a) ln α as a function of the photon energy of PVA thick film with 3000 nm thickness. (b) Urbach energy as a function of irradiating times.

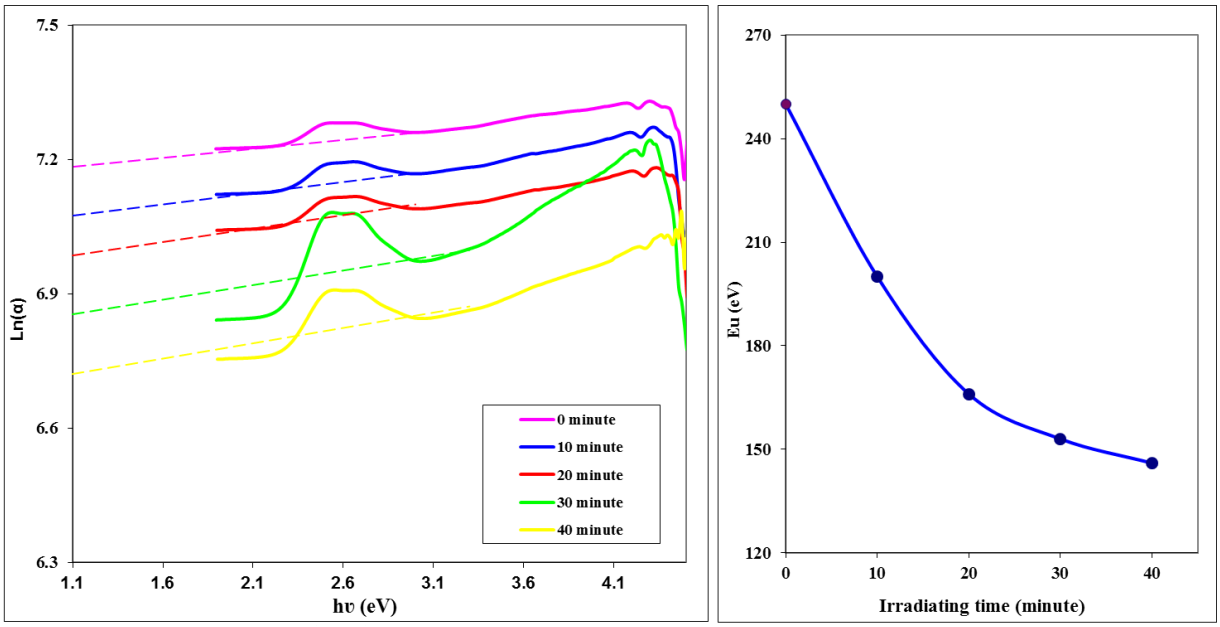

a b

Figure (4-33): (a) ln α as a function of the photon energy of MO thick film with 2000 nm thickness. (b) Urbach energy as a function of irradiating times.

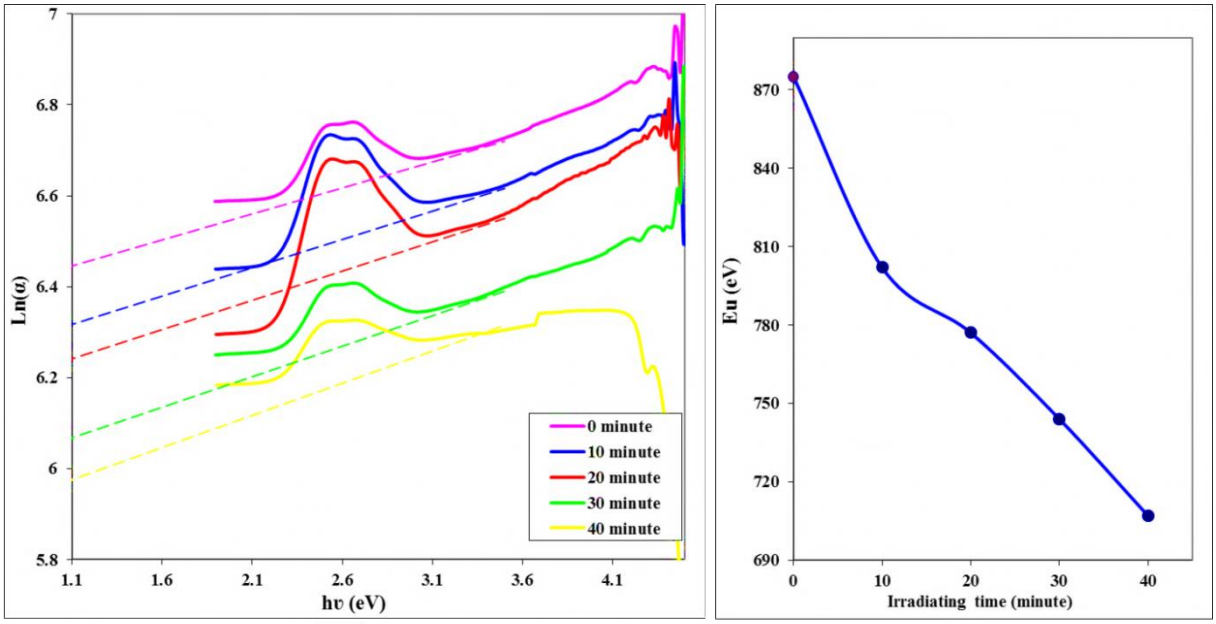

a b

Figure (4-34): (a) ln α as a function of the photon energy of MO thick film with 3000 nm thickness. (b) Urbach energy as a function of irradiating times.

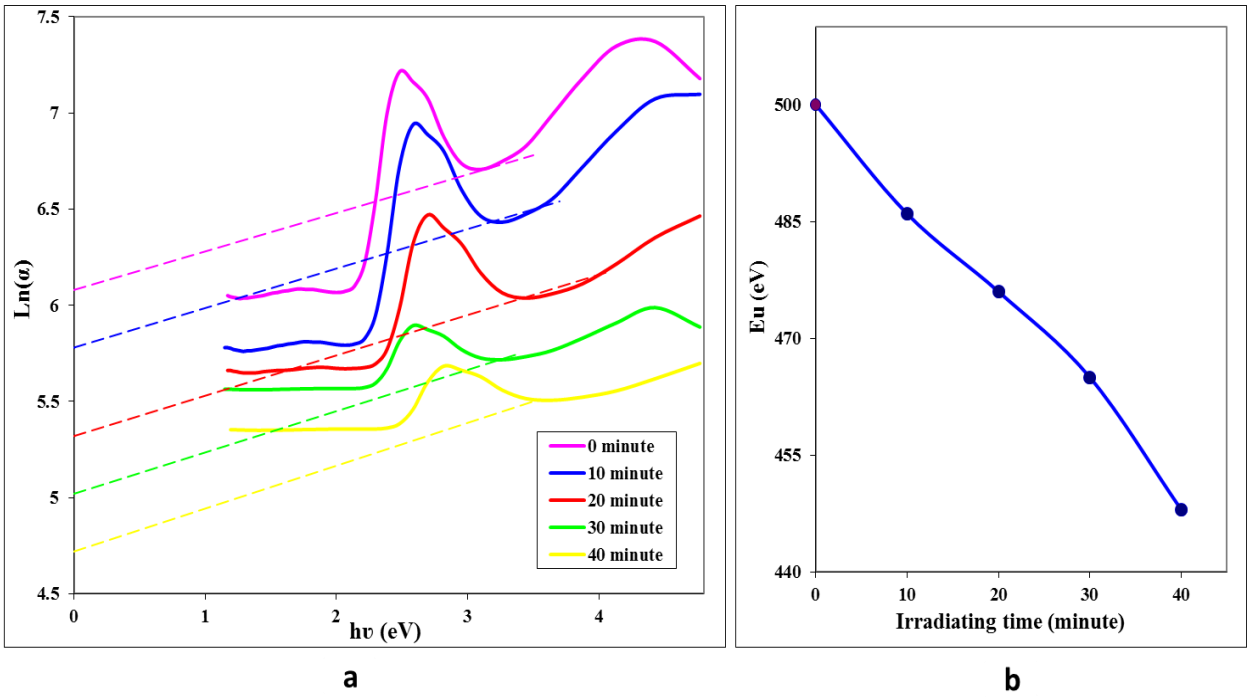

Figure (4-35): (a) ln α as a function of and photon energy of PVA/MO thick film with 2000 nm thickness (b) Urbach energy as a function of irradiating times.

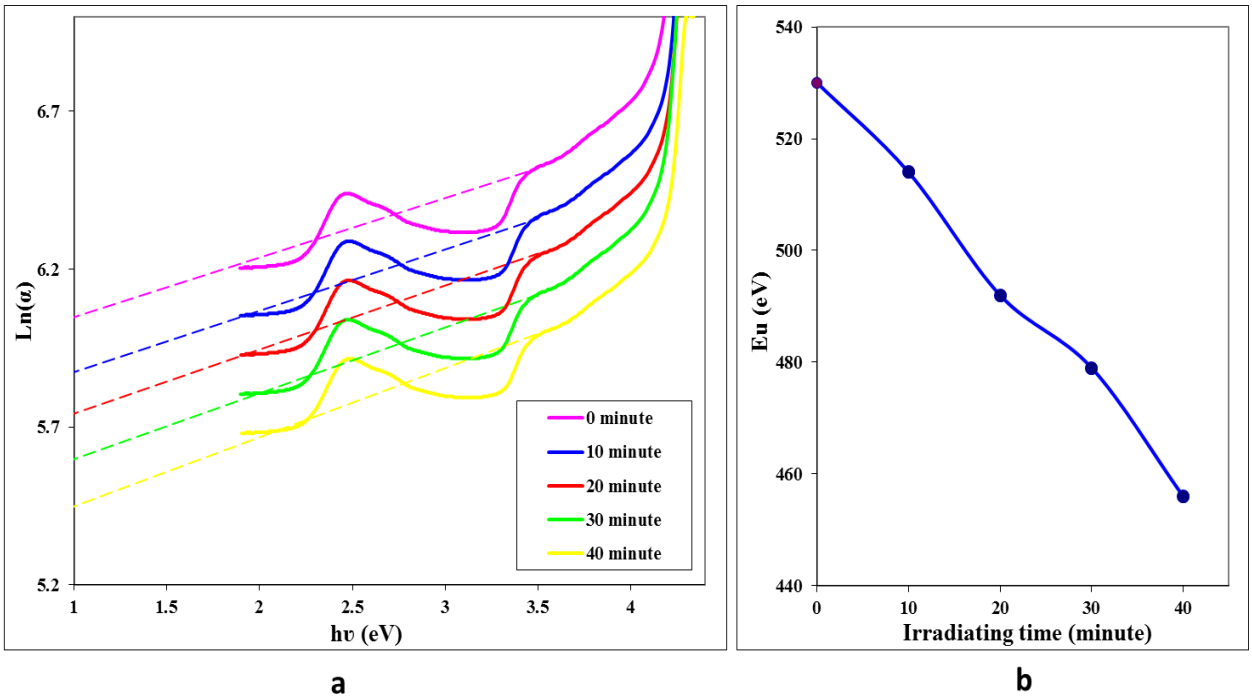

Figure (4-36): (a) ln α as a function of the photon energy of PVA/MO thick film with 4000 nm thickness. (b) Urbach energy as a function of irradiating times.

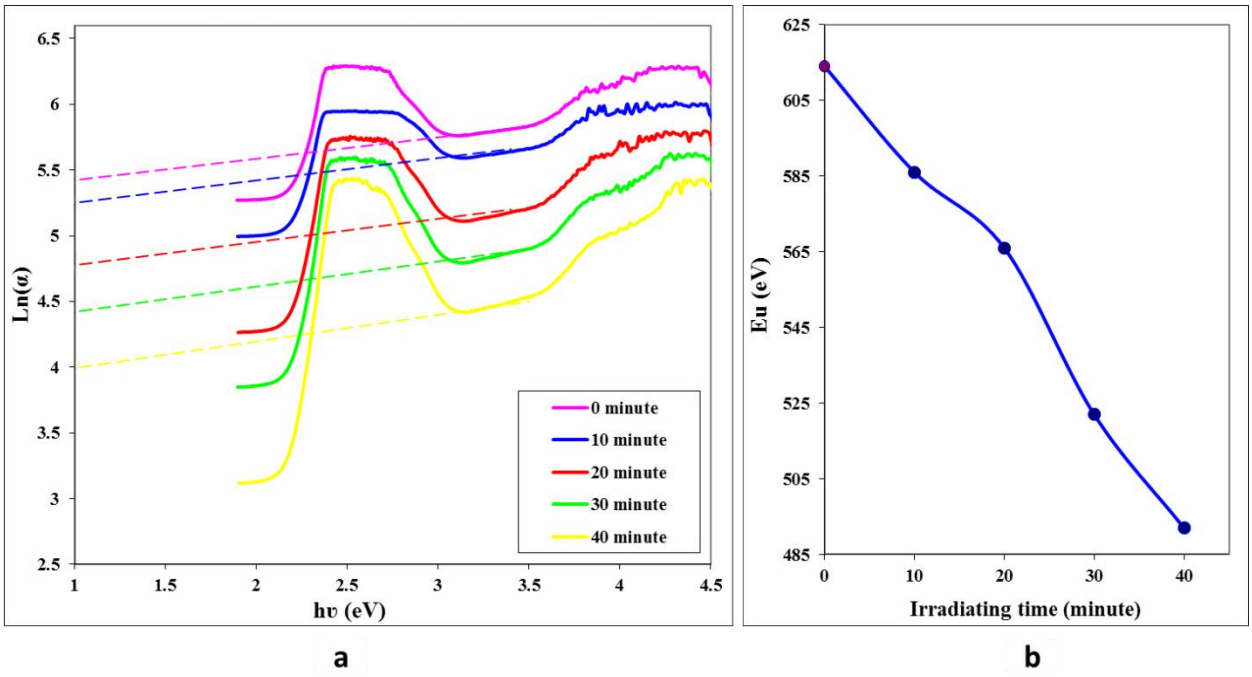

Figure (4-37): (a) ln α as a function of the photon energy of PVA/MO thick film with 6000 nm thickness. (b) Urbach energy as a function of irradiating times.

To find the single oscillator energy E_0 and the dispersion energy E_d of PVA, MO and PVA/MO, it is plotted between the invers of (n^2-1) and $((h\nu)^2$ according to (2-18) equation. The slope represents $(E_o\ E_d)^{-1}$ and the intercept value represents (E_0/E_d). The single oscillator energy E_0 is approximately as doubled as the energy gap value. This behaviour is shown in Figures (4-38, 4-40, 4-42, 4-44, 4-46, 4-48 and 4-50).

The dispersion energy and the single oscillator as a function of times explains in Figures (4-39, 4-41, 4-43, 4-45, 4-47, 4-49 and 4-51). Both of them will increases with the increase of time. Decreasing the energy gap belongs to increasing the absorbance which has an indirect effect on the single oscillator energy.

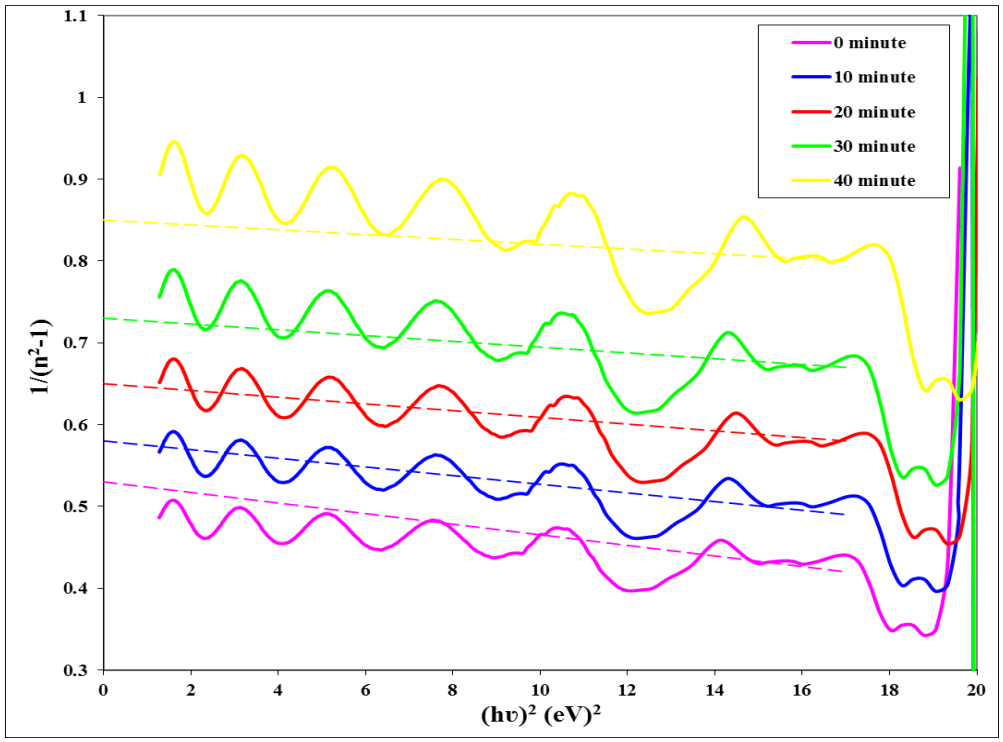

Figure(4-38): $1/(n^2-1)$ vs. Square photon energy of 2000 nm PVA thick film.

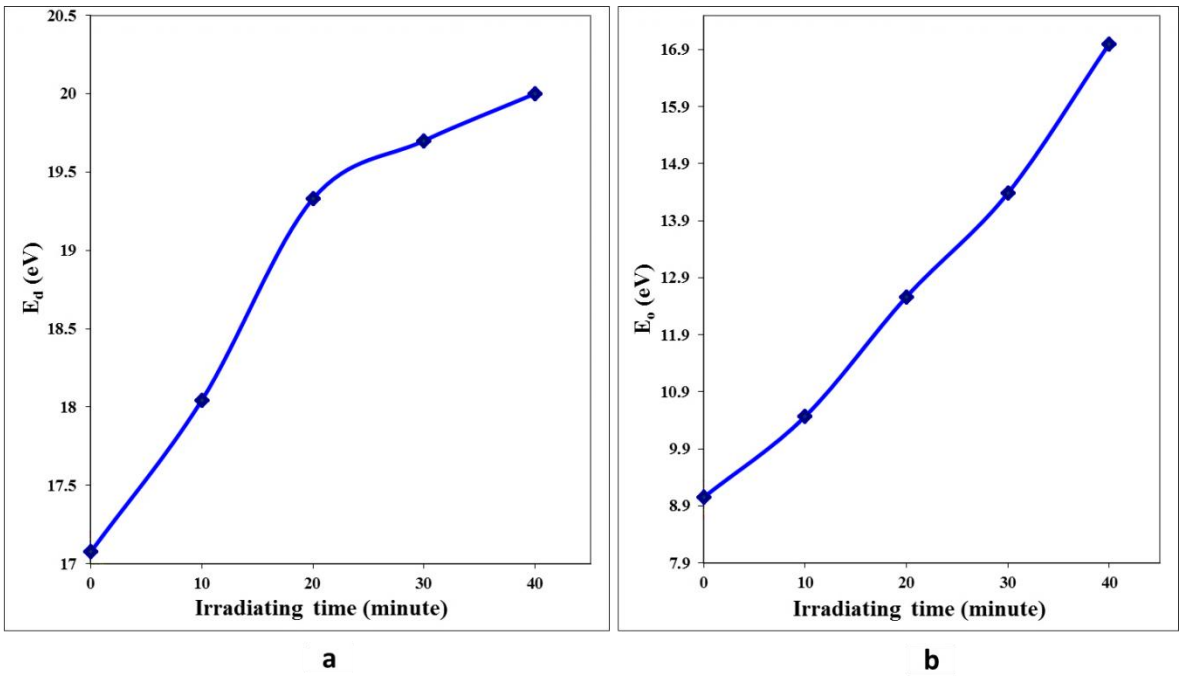

Figure (4-39):Laser irradiating time effect of 2000 nm PVA thick film on (a) The dispersion energy (b) Single oscillator energy.

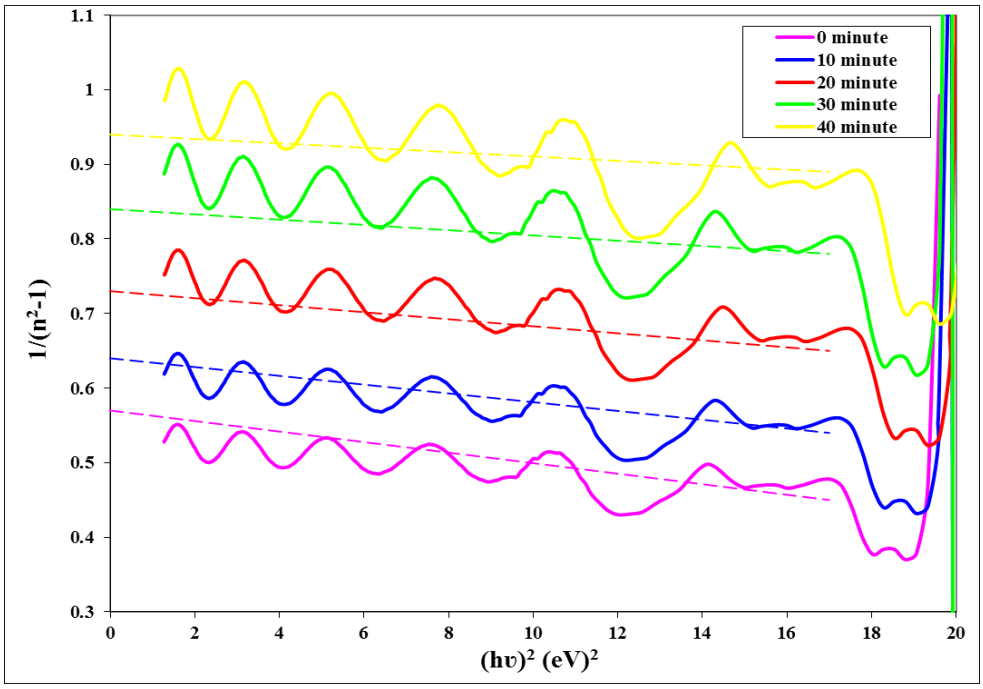

Figure (4-40): $1/(n^2-1)$ vs. Square photon energy of 3000 nm PVA thick film.

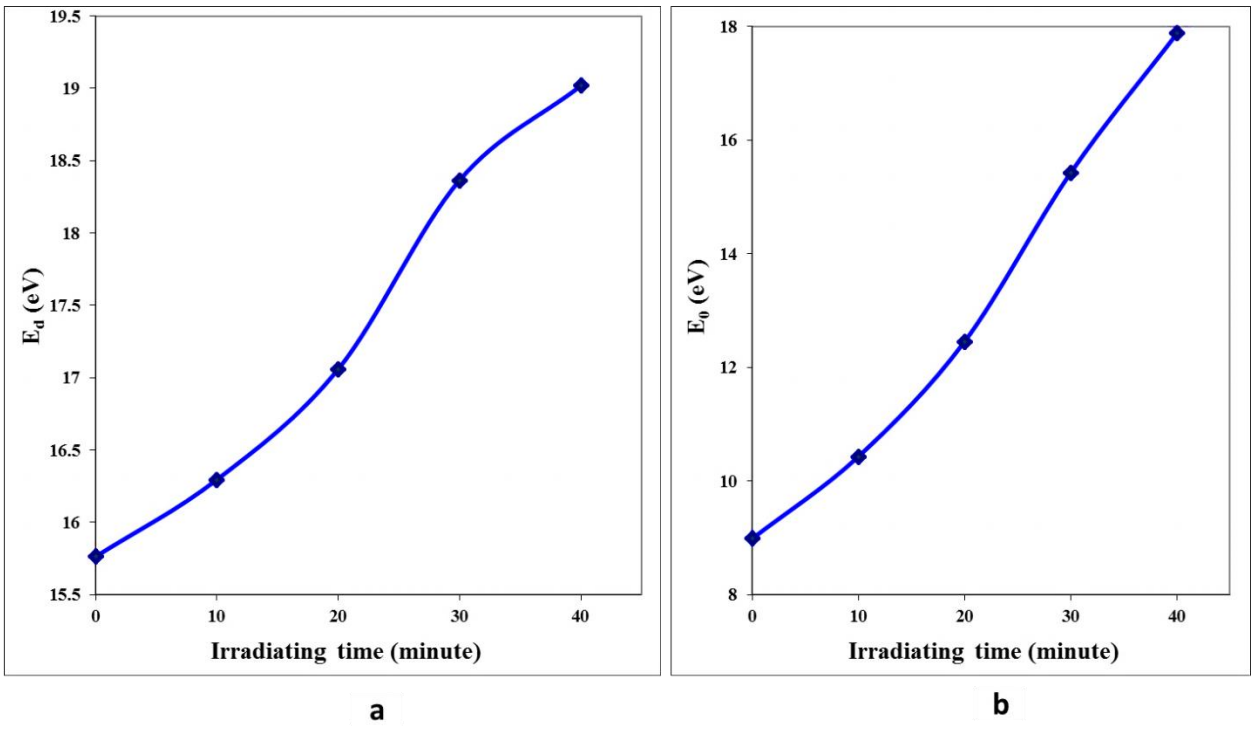

Figure (4-41) : Laser irradiating time effect of 3000 nm PVA thick film on (a) The dispersion energy (b) Single oscillator energy.

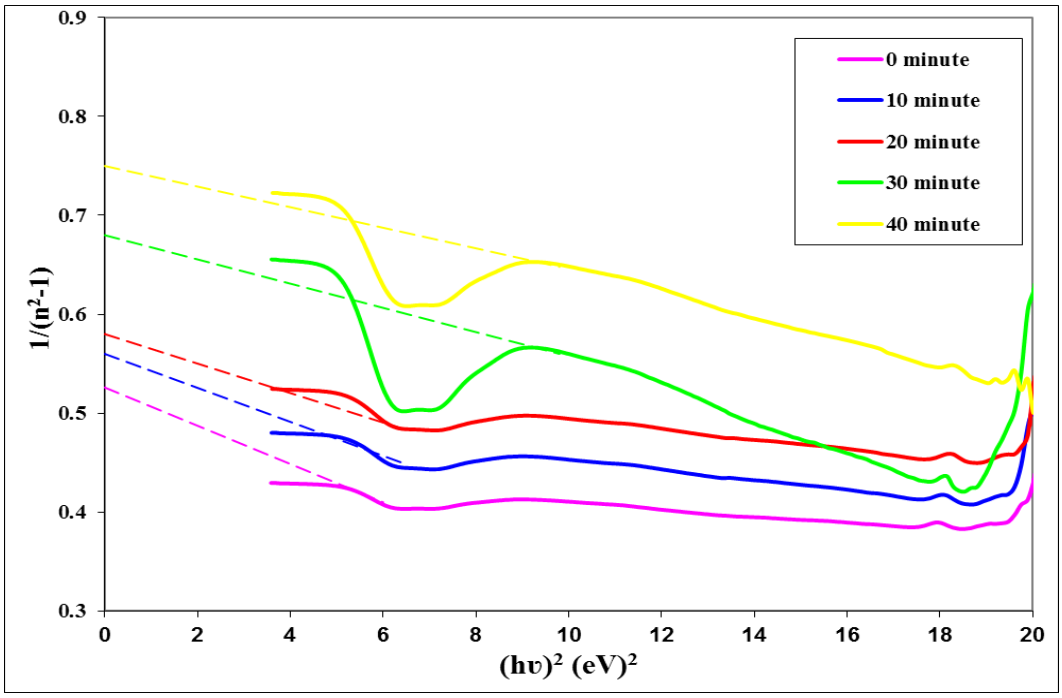

Figure (4-42): $1/(n^2-1)$ vs. Square photon energy of 2000 nm MO thick film.

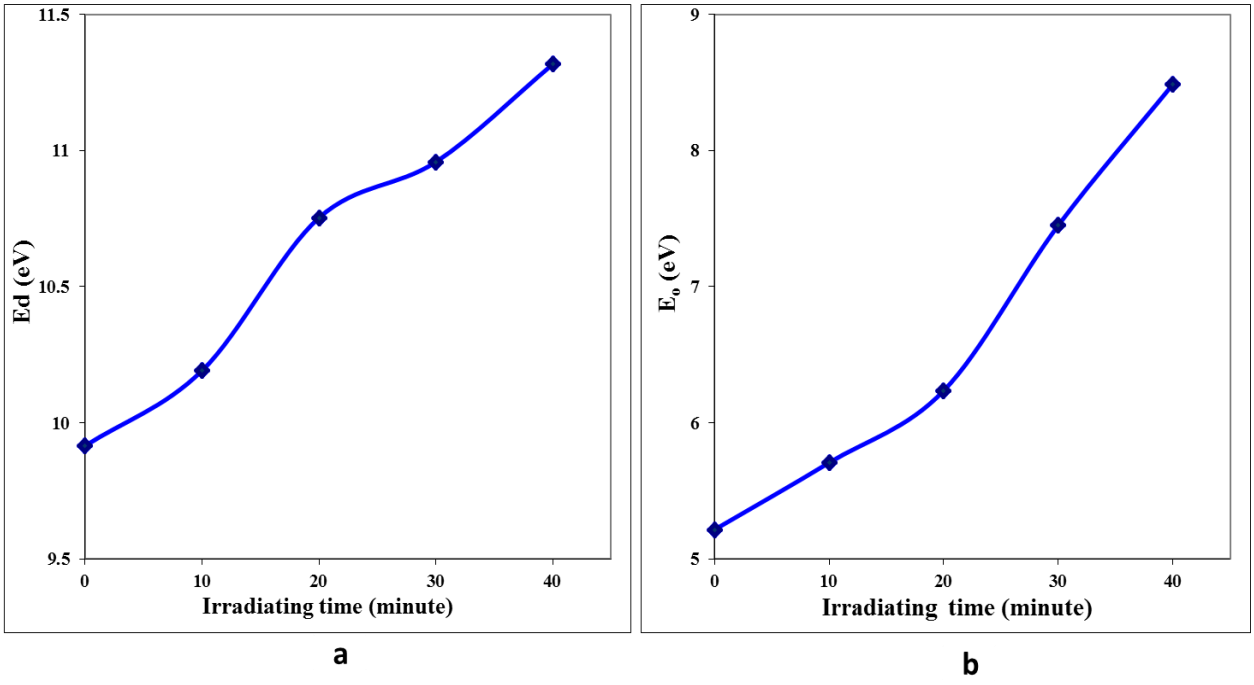

Figure (4-43): Laser irradiating time effect of 2000 nm MO thick film on (a) The dispersion energy (b) Single oscillator energy.

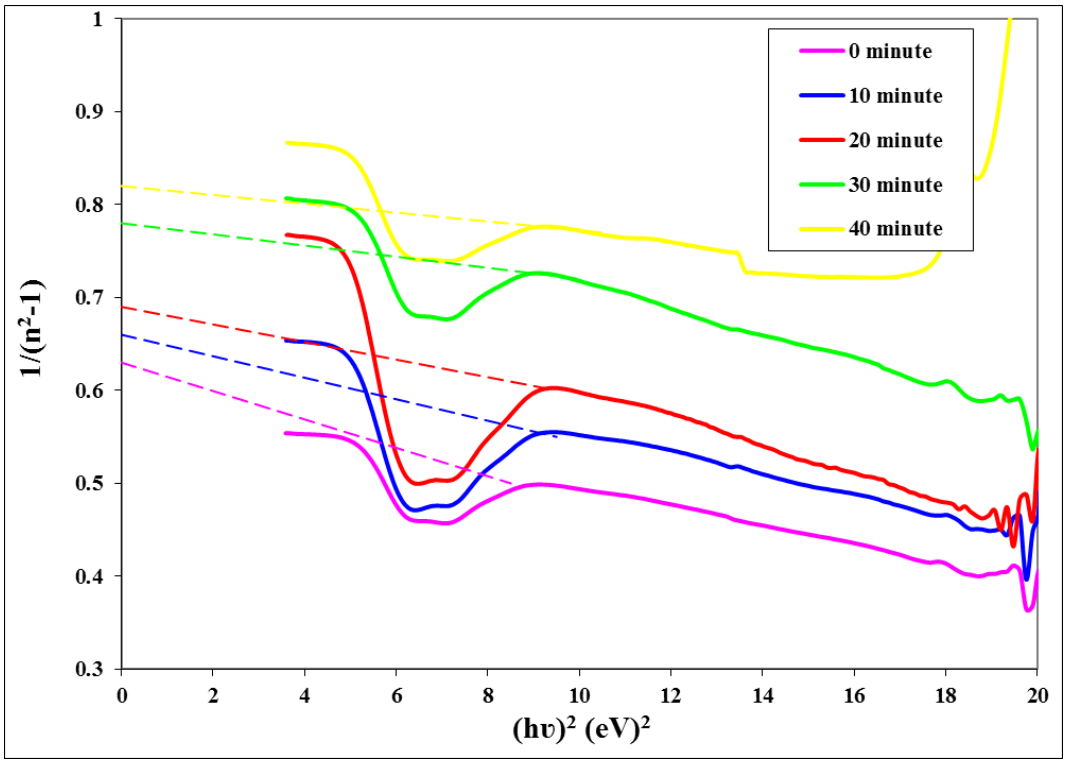

Figure (4-44) : $1/(n^2-1)$ vs. Square photon energy of 3000 nm MO thick film.

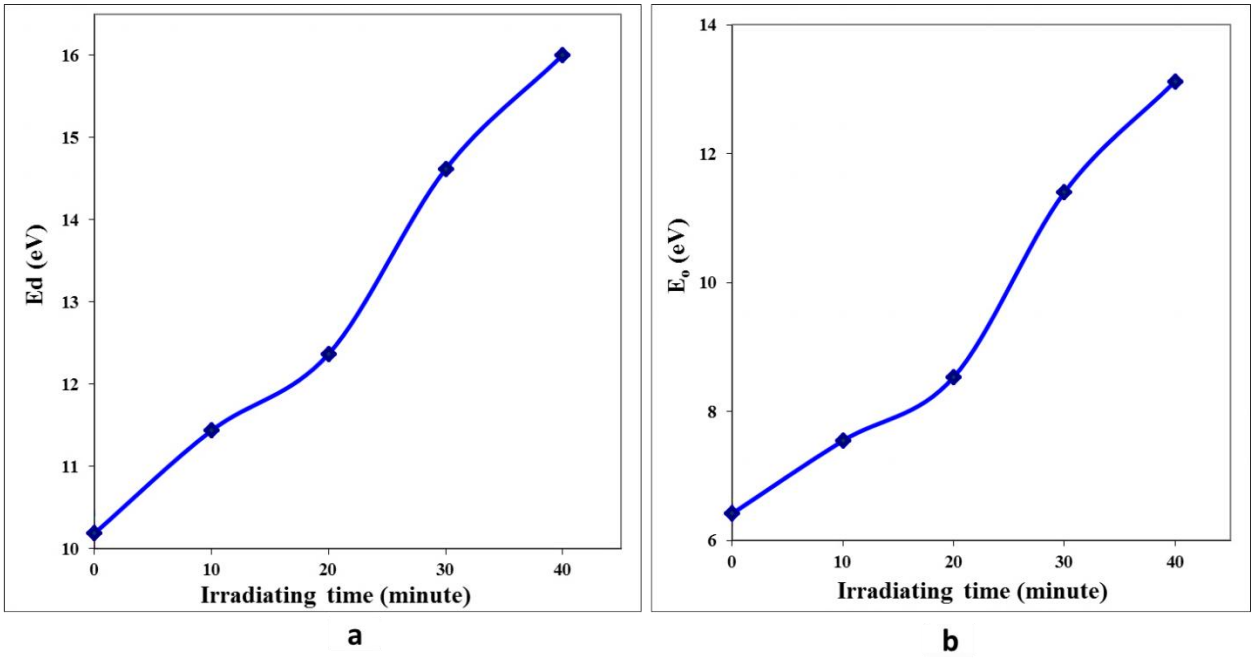

Figure (4-45) : Laser irradiating time effect of 3000 nm MO thick film on (a) The dispersion energy (b) Single oscillator energy.

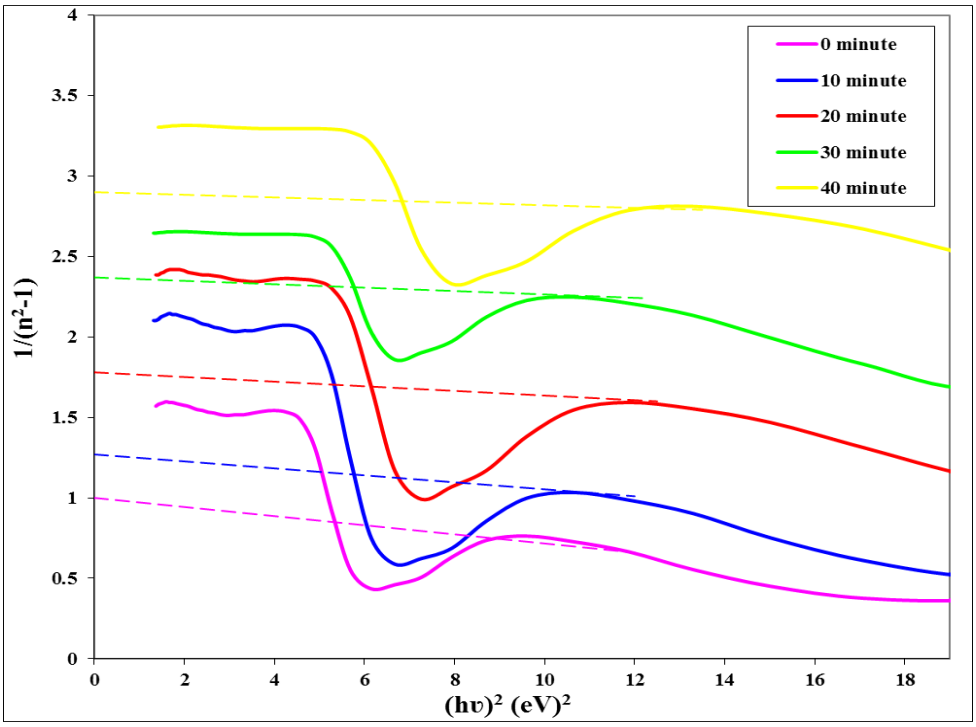

Figure (4-46): $1/(n^2-1)$ vs. Square photon energy of 2000 nm PVA/MO thick film.

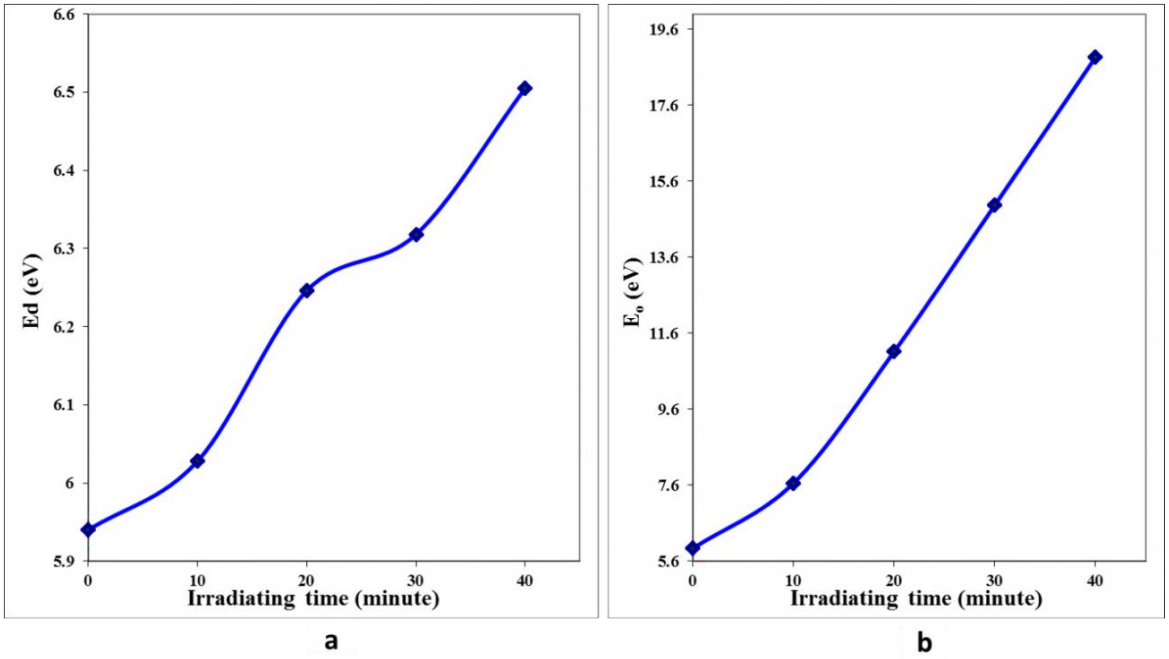

Figure (4-47): Laser irradiating time effect of 2000 nm PVA/MO thick film on (a) The dispersion energy (b) Single oscillator energy.

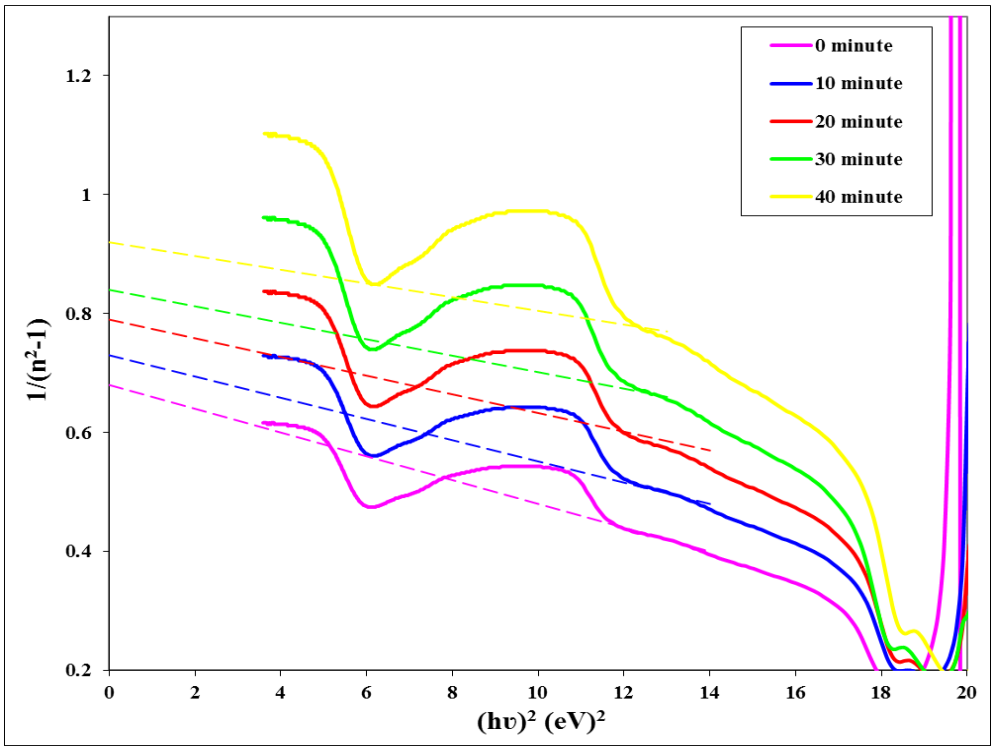

Figure (4-48): $1/(n^2-1)$ vs. Square photon energy of 4000 nm PVA/MO thick film.

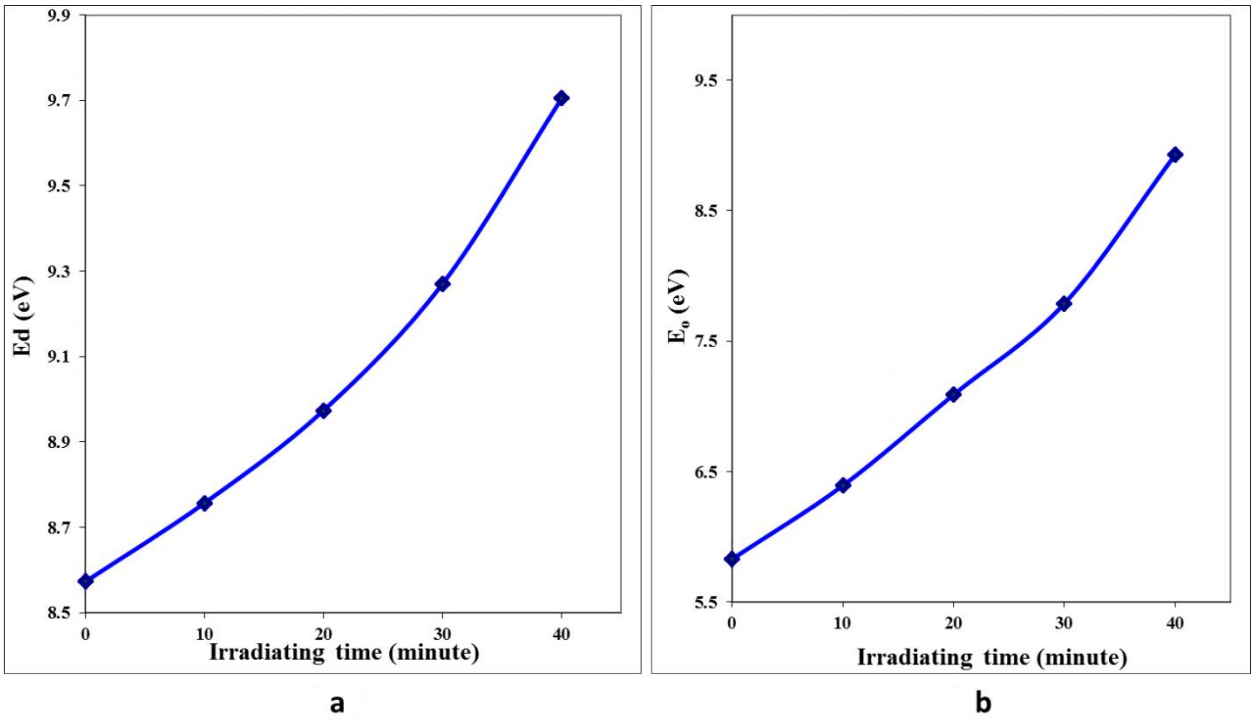

Figure (4-49): Laser irradiating time effect of 4000 nm PVA/MO thick film on (a) The dispersion energy (b) Single oscillator energy.

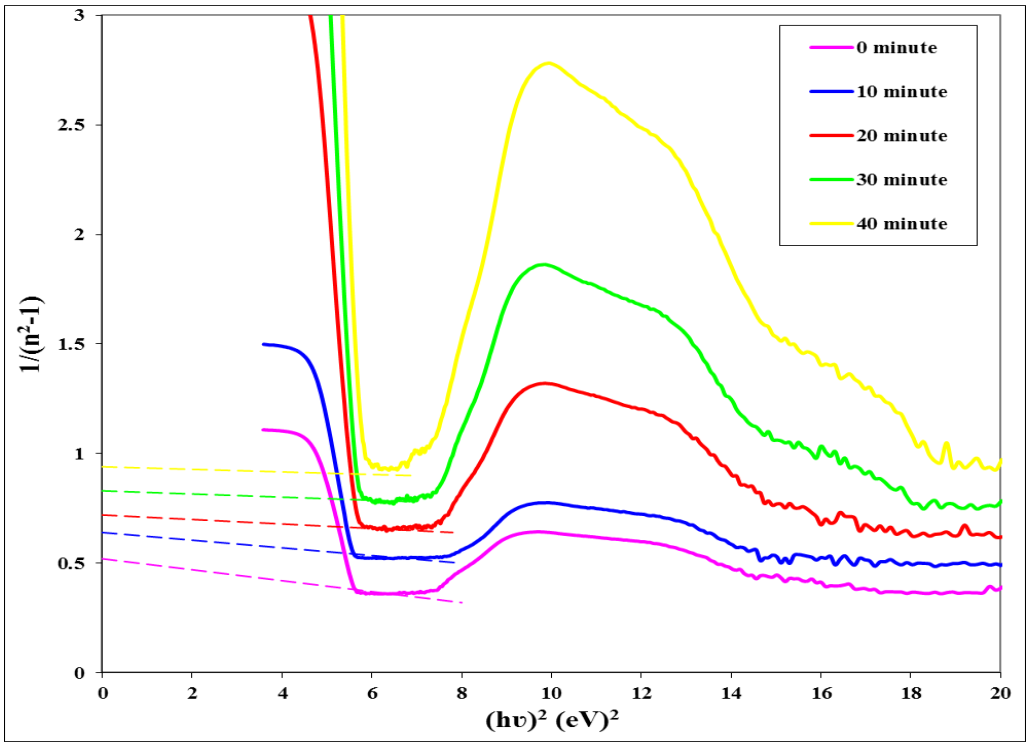

Figure (4-50) $1/(n^2-1)$ vs. Square photon energy of 6000 nm PVA/MO thick film.

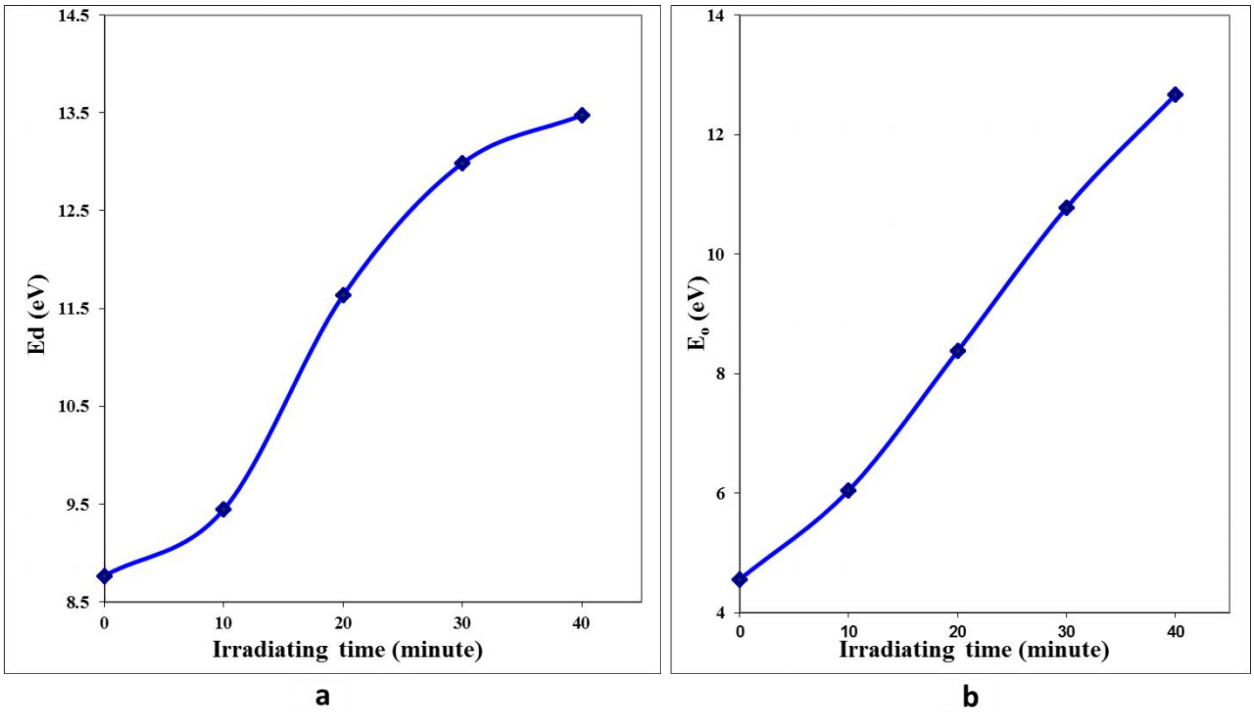

Figure (4-51): Laser irradiating time effect of 6000 nm PVA/MO thick film on (a) The dispersion energy (b) Single oscillator energy.

The relation between inverse drawing of (n^2-1) and (λ^2) for thick films are explained in Figures (4-52, 4-54, 4-56, 4-58, 4-60, 4-62 and 4-64), the slope represents the reciprocal of the average oscillator strength $(1/S_o)$ and the intercept represents average inter band oscillator wavelength $(1/S_o\lambda_\circ^2)$, as indicated in equation (2-22).

The average oscillator strength as a function of the irradiation time, which increases with the increase in the laser irradiation time and decreases with the increase in the thickness of the film but the average inter band oscillator wavelength is indicated as a function of the irradiation time, which shows an inverse relationship with average oscillator strength, as it decreases with increasing the irradiation time and increases with increasing thickness, which is shows in the Figures(4-53, 4-55, 4-57, 4-59, 4-61, 4-63 and 4-65).

The dispersion parameters, Urbach energy and the direct energy gap are shows in tables (15 - 21).

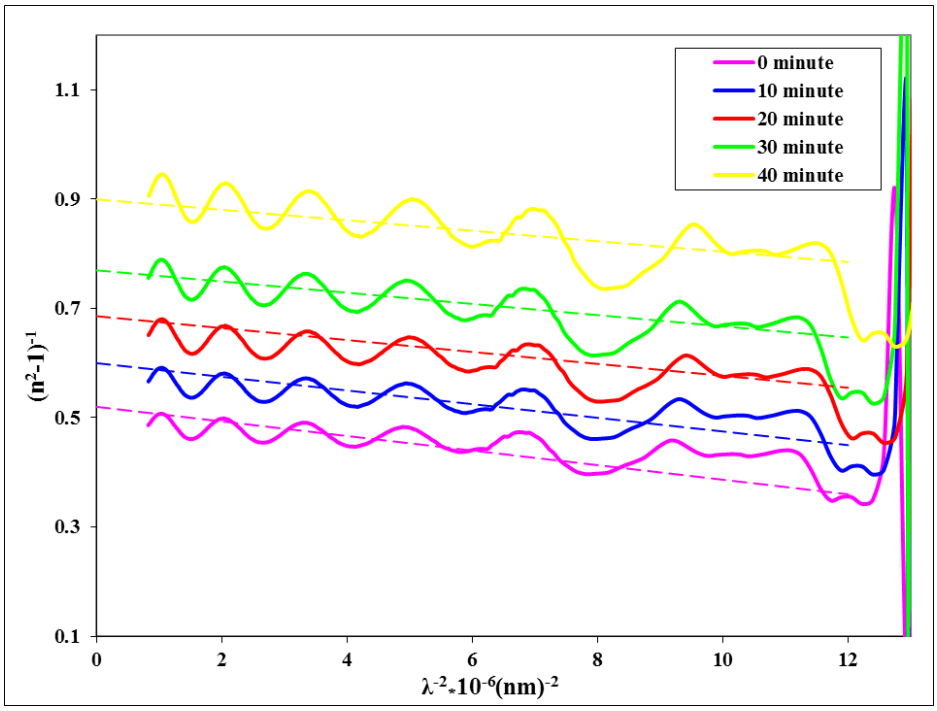

Figure (4-52): The relation between $1/(n^2-1)$ and $1/\lambda^2$ for PVA thick film at thickness 2000 nm.

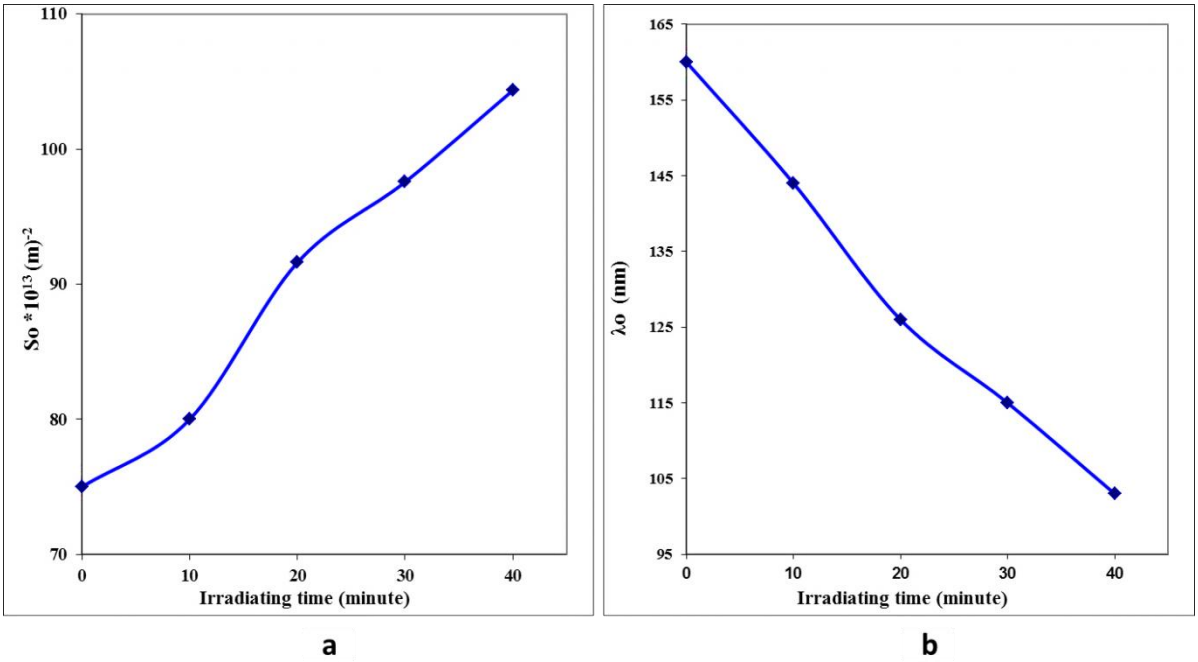

Figure (4-53):The PVA thick film 2000 nm (a) Average oscillator strength as a function of irradiating times. (b) Average inter band oscillator wavelength as a function of the irradiation time.

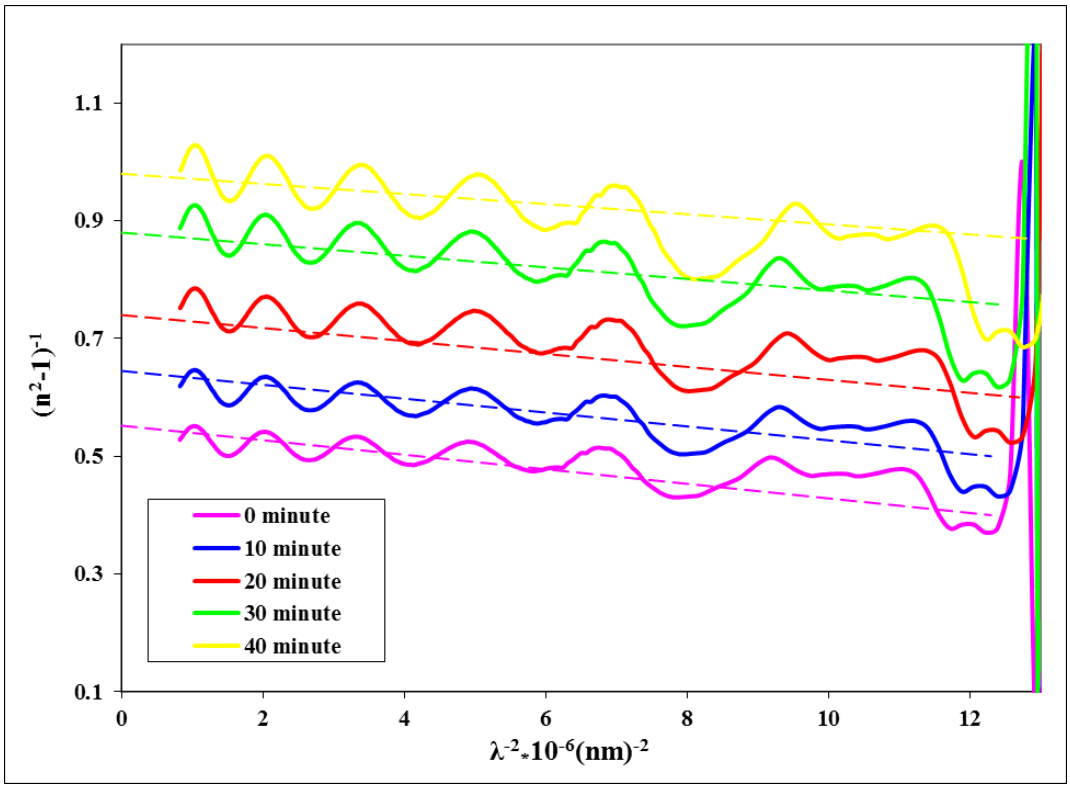

Figure (4-54): The relation between $1/(n^2-1)$ and $1/\lambda^2$ for PVA thick film at thickness 3000 nm.

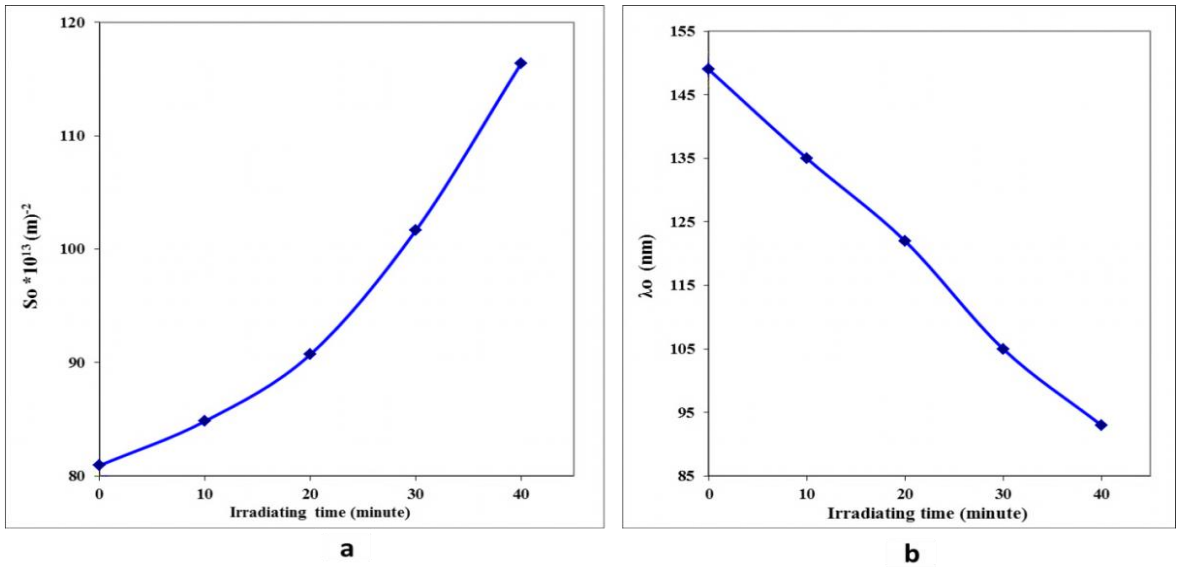

Figure (4-55):The PVA thick film 3000 nm (a) Average oscillator strength as a function of irradiating times. (b) Average inter band oscillator wavelength as a function of the irradiation time.

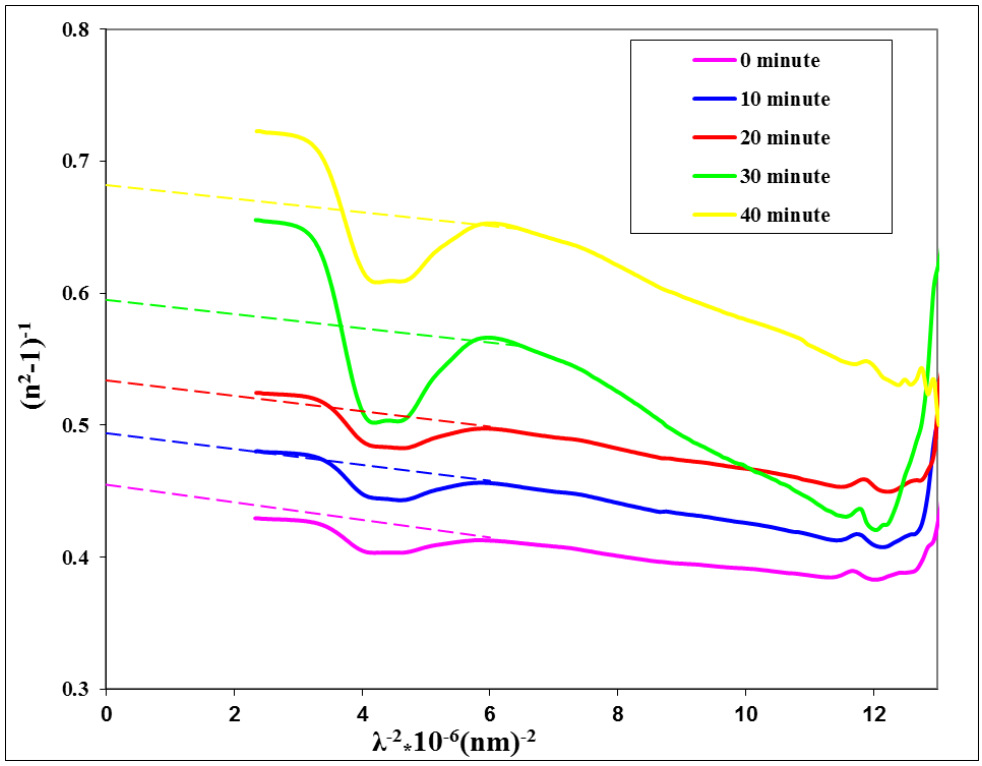

Figure (4-56): The relation between $1/(n^2-1)$ and $1/\lambda^2$ for MO thick film at thickness 2000 nm.

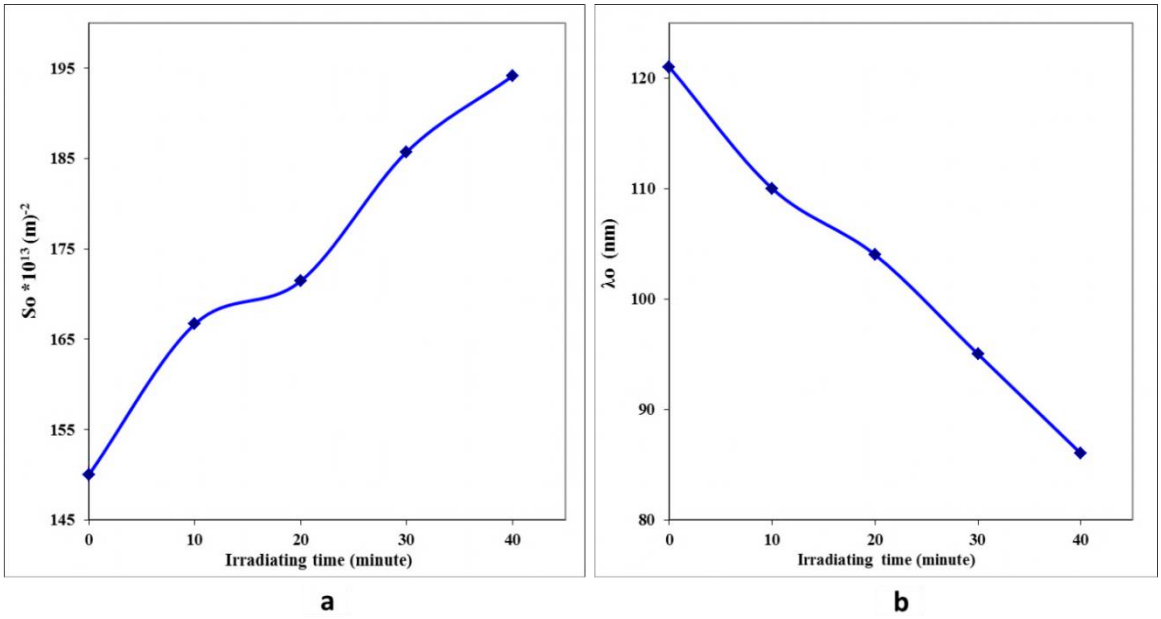

Figure (4-57): MO thick film 2000 nm (a) Average oscillator strength as a function of irradiating times. (b) Average inter band oscillator wavelength as a function of the irradiation time.

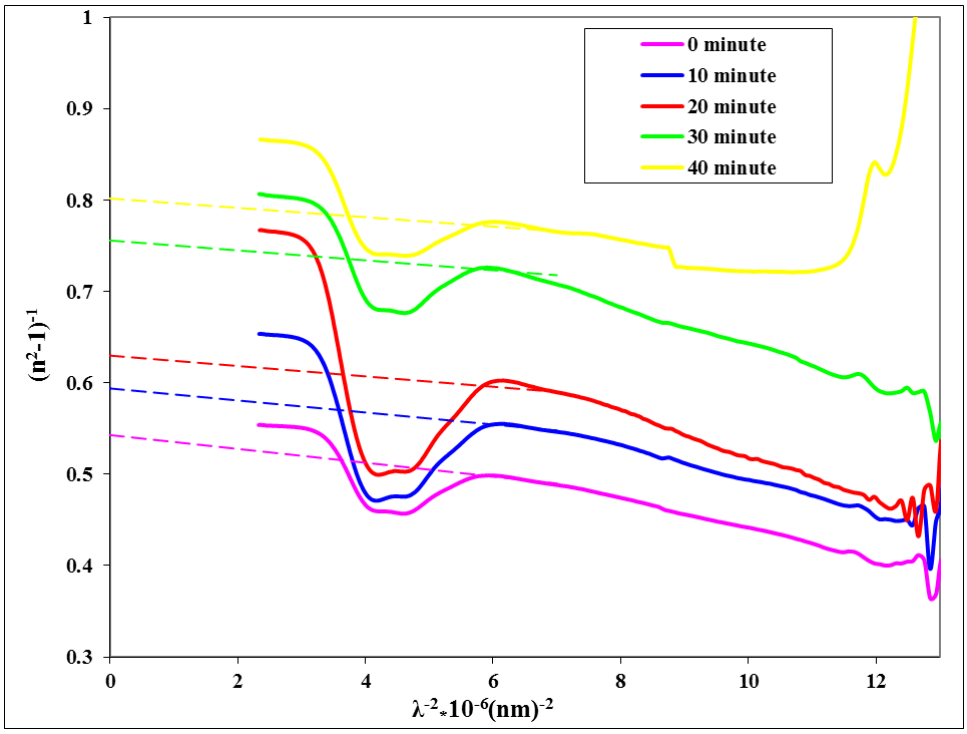

Figure (4-58): The relation between $1/(n^2-1)$ and $1/\lambda^2$ for MO thick film at thickness 3000 nm.

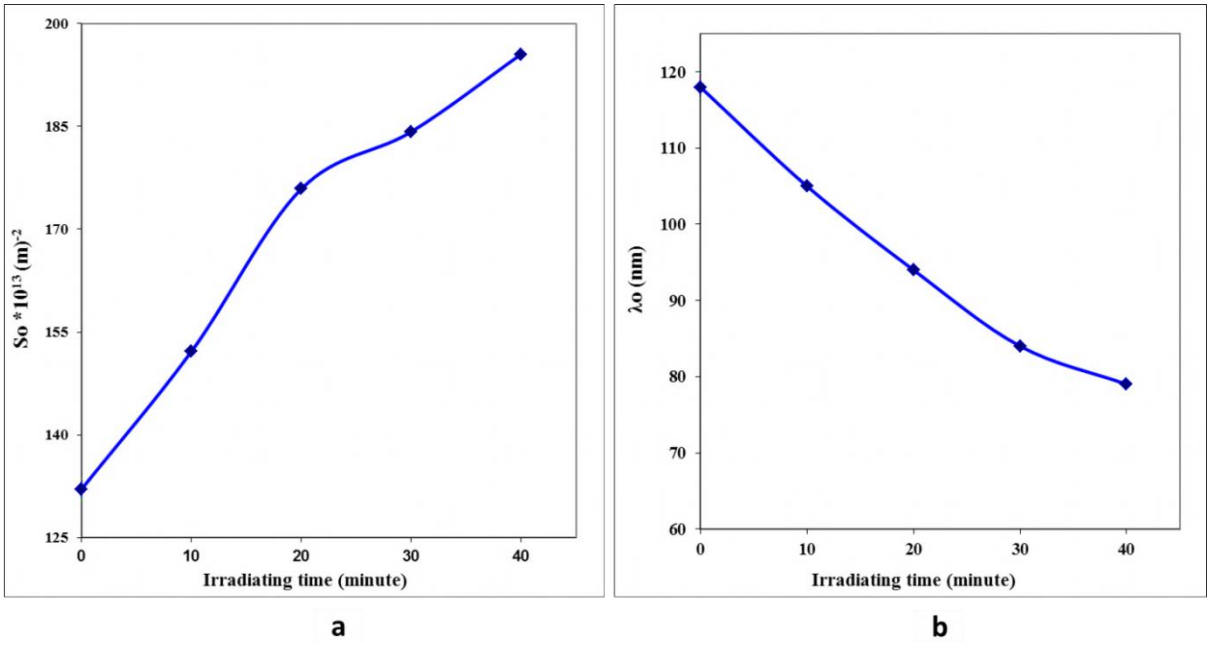

Figure (4-59): The MO thick film 3000 nm (a) Average oscillator strength as a function of irradiating times. (b) Average inter band oscillator wavelength as a function of the irradiation time.

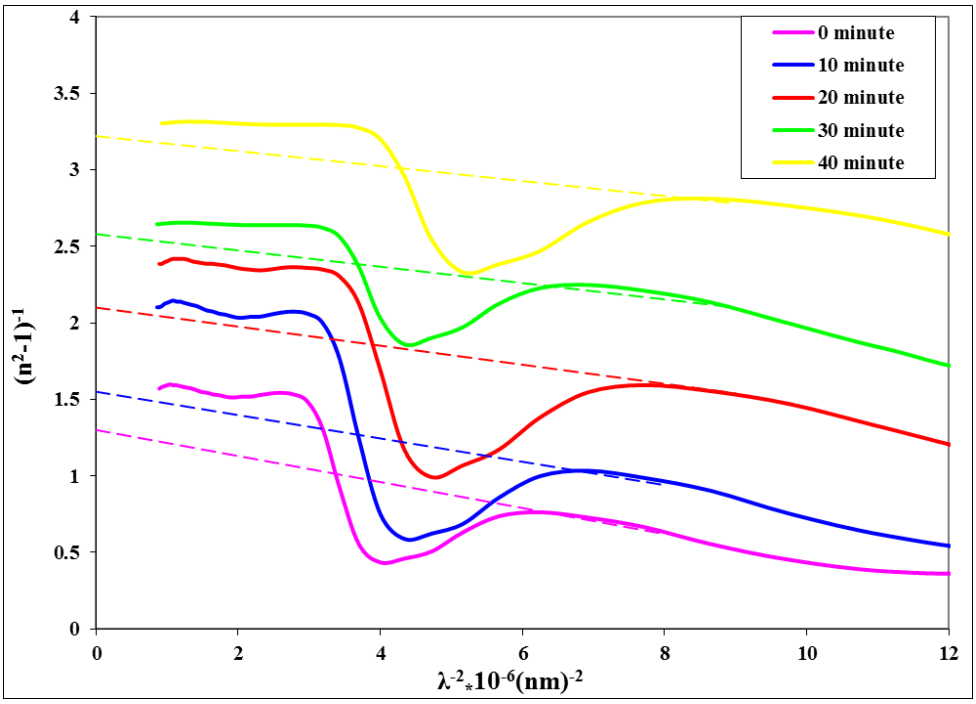

Figure (4-60):The relation between $1/(n^2-1)$ and $1/\lambda^2$ for PVA/MO thick film at thickness 2000 nm.

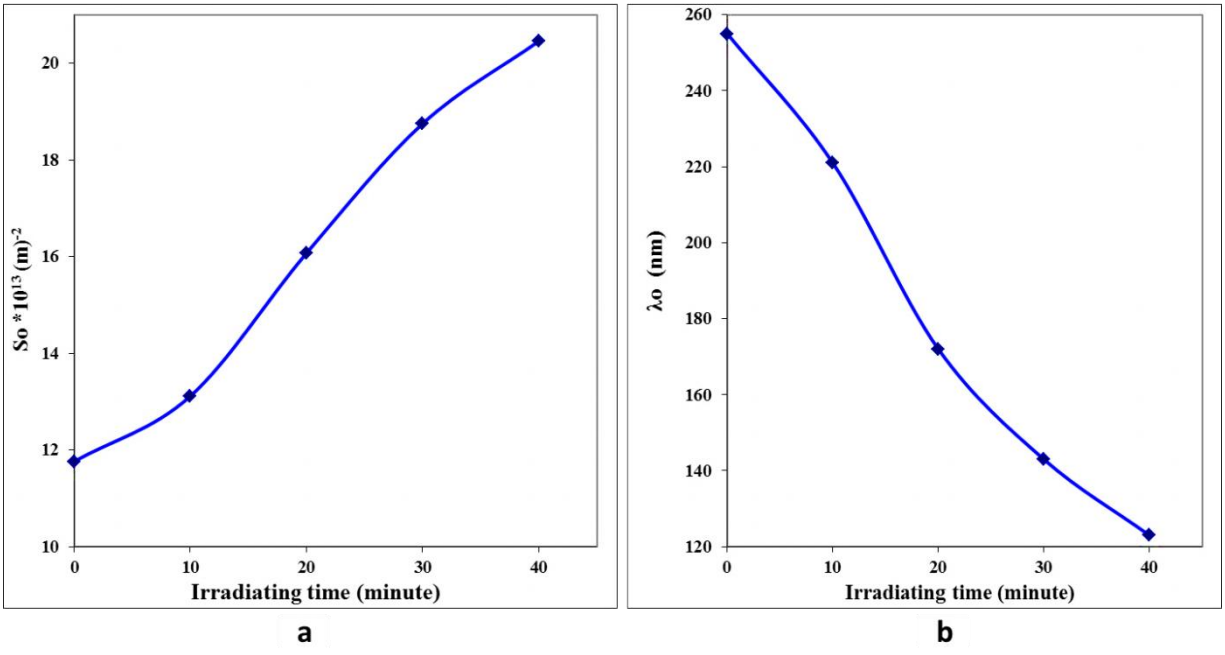

Figure (4-61): The PVA/MO thick film 2000 nm (a) Average oscillator strength as a function of irradiating times. (b) Average inter band oscillator wavelength as a function of the irradiation time.

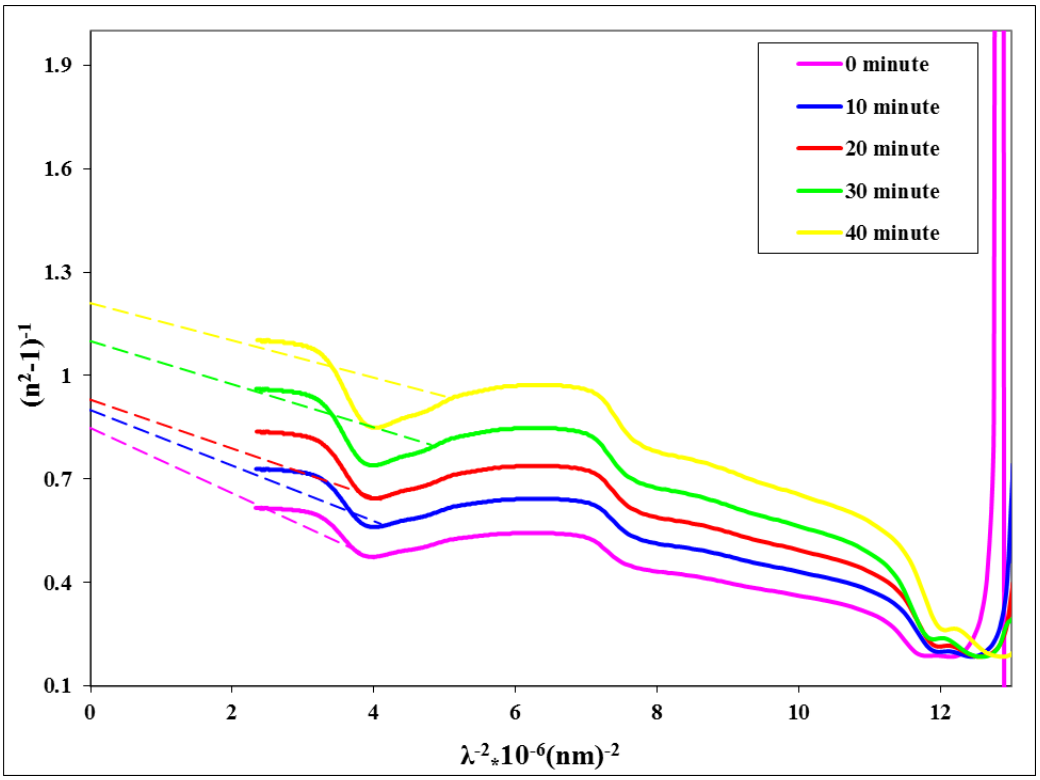

Figure (4-62):The relation between $1/(n^2-1)$ and $1/\lambda^2$ for PVA/MO thick film at thickness 4000 nm.

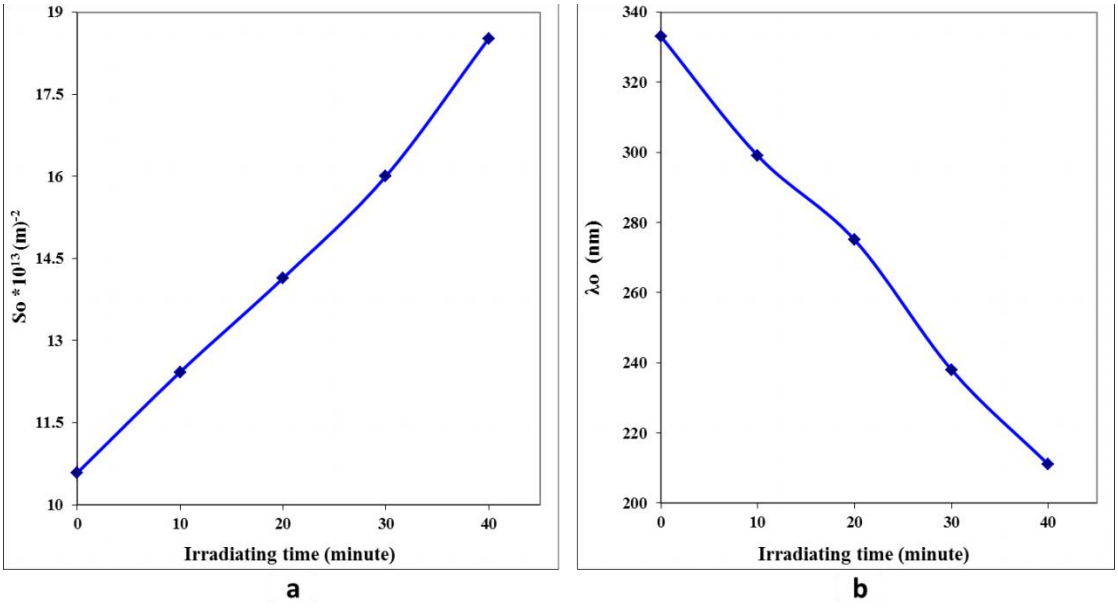

Figure (4-63):The PVA/MO thick film 4000 nm (a) Average oscillator strength as a function of irradiating times. (b) Average inter band oscillator wavelength as a function of the irradiation time.

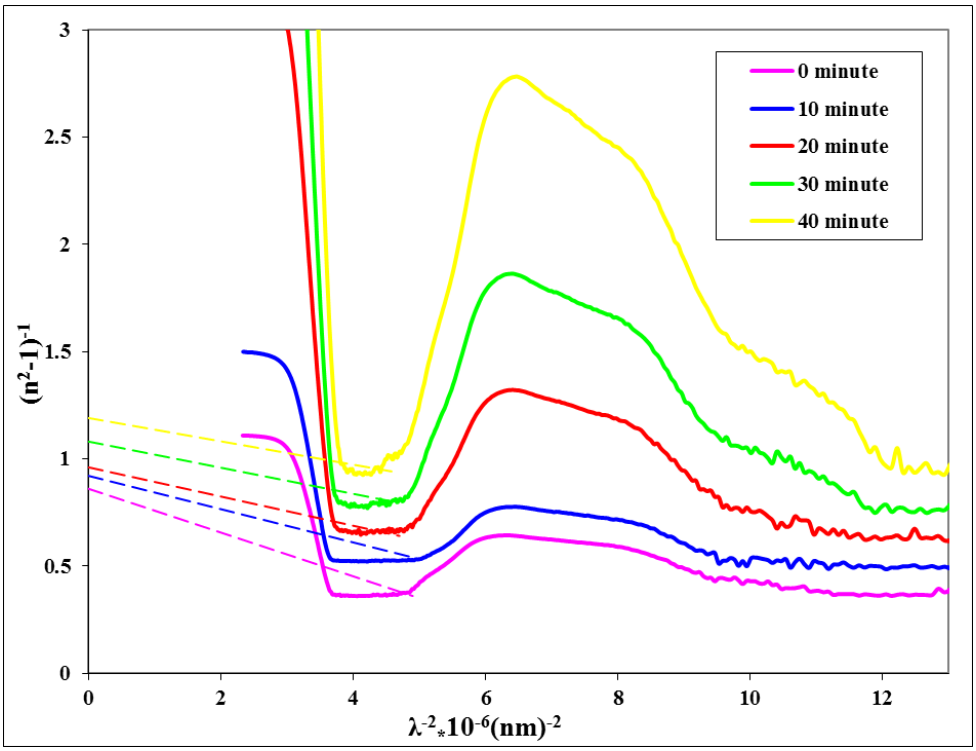

Figure (4-64):The relation between $1/(n^2-1)$ and $1/\lambda^2$ for PVA/MO thick film at thickness 6000 nm.

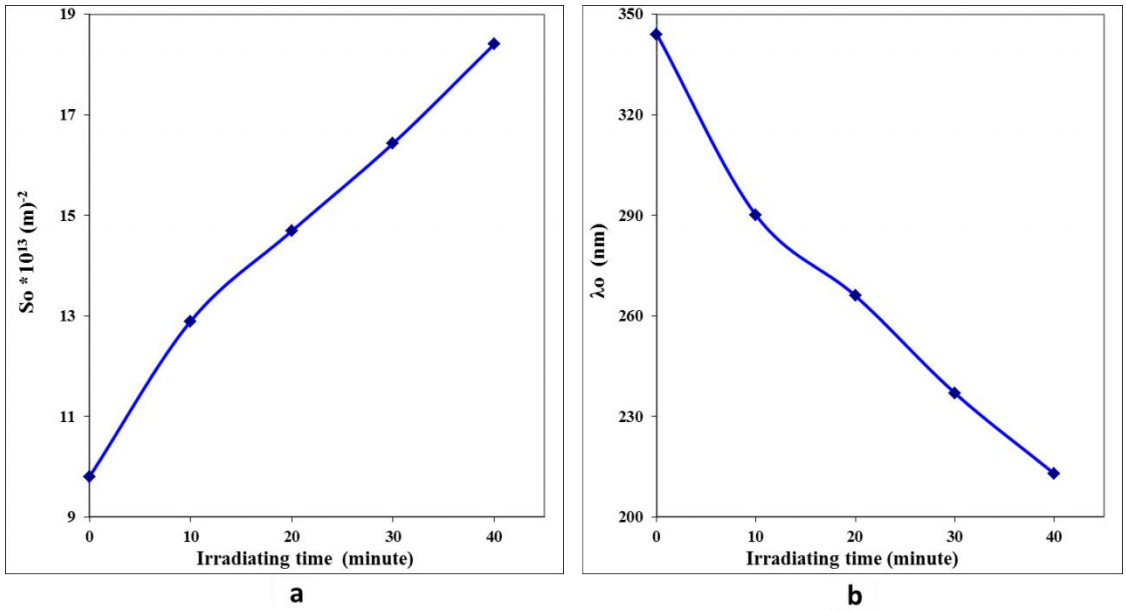

Figure (4-65):The PVA/MO thick film 6000 nm (a) Average oscillator strength as a function of irradiating times. (b) Average inter band oscillator wavelength as a function of the irradiation time.

Table (4-15): The dispersion parameters of PVA with 2000 nm thickness at wavelength 348 nm.

Time min.	E_o eV	Ed eV	Eg eV	Eu meV	$S_o * 10^{13}$ m^{-2}	λ_o nm	M_{-1}	M_{-3} eV^{-2}
0	9.05	17.07	3.95	956	75	160	1.88	0.023
10	10.46	18.04	4.01	900	80	144	1.72	0.015
20	12.56	19.32	4.07	862	91.603	126	1.53	0.009
30	14.38	19.7	4.09	826	97.56	115	1.36	0.006
40	17	20	4.12	796	104.347	103	1.176	0.004

Table (4-16): The dispersion parameters of PVA with 3000 nm thickness at wavelength 348 nm.

Time min.	E_o eV	Ed eV	Eg eV	Eu meV	$S_o * 10^{13}$ m^{-2}	λ_o nm	M_{-1}	M_{-3} eV^{-2}
0	8.98	15.76	4	895	80.921	149	1.75	0.021
10	10.43	16.29	4.04	880	84.827	135	1.56	0.014
20	12.45	17.06	4.08	846	90.714	122	1.37	0.008
30	15.42	18.36	4.1	814	101.639	105	1.19	0.005
40	17.87	19.01	4.12	807	116.363	93	1.06	0.003

Table (4-17): The dispersion parameters of MO with 2000 nm thickness at wavelength 470 nm.

Time min.	E_o eV	Ed eV	Eg eV	Eu meV	$S_o * 10^{13}$ m^{-2}	λ_o nm	M_{-1}	M_{-3} eV^{-2}
0	5.21	9.91	2.6	250	150	121	1.90	0.070
10	5.70	10.19	2.7	200	166.666	110	1.78	0.055
20	6.23	10.75	2.8	166	171.428	104	1.72	0.044
30	7.45	10.95	2.9	153	185.714	95	1.40	0.026
40	8.48	11.31	3	146	194.117	86	1.33	0.018

Table (4-18): The dispersion parameters of MO with 3000 nm thickness at wavelength 470 nm.

Time min.	E_o eV	Ed eV	Eg eV	Eu meV	$S_o * 10^{13}$ m^{-2}	λ_o nm	M_{-1}	M_{-3} eV^{-2}
0	6.41	10.18	2.5	875	132.075	118	1.58	0.038
10	7.54	11.43	2.6	802	152.173	105	1.51	0.026
20	8.53	12.36	2.7	777	175.879	94	1.44	0.019
30	11.40	14.61	2.8	744	184.21	84	1.28	0.009
40	13.12	16.00	2.9	707	195.53	79	1.21	0.007

Table (4-19): The dispersion parameters of PVA/MO with 2000 nm thickness at wavelength 500 nm.

Time min.	E_o eV	Ed eV	Eg eV	Eu meV	$S_o * 10^{13}$ m^{-2}	λ_o nm	M_{-1}	M_{-3} eV^{-2}
0	5.94	5.94	3.1	500	11.764	255	1	0.028
10	7.65	6.02	3.2	486	13.114	221	0.78	0.013
20	11.11	6.24	3.3	476	16.071	172	0.56	0.004
30	14.97	6.31	3.4	465	18.75	143	0.42	0.001
40	18.86	6.50	3.5	448	20.454	123	0.34	0.0009

Table (4-20): The dispersion parameters of PVA/MO with 4000 nm thickness at wavelength 495 nm.

Time min.	E_o eV	Ed eV	Eg eV	Eu meV	$S_o * 10^{13}$ m^{-2}	λ_o nm	M_{-1}	M_{-3} eV^{-2}
0	5.83	8.57	2.9	530	10.582	333	1.53	0.045
10	6.39	8.75	3	514	12.424	299	1.36	0.033
20	7.09	8.97	2.917	492	14.137	275	1.26	0.025
30	7.78	9.27	2.945	479	16	238	1.19	0.019
40	8.92	9.70	3	456	18.518	211	1.08	0.013

Table (4-21): The dispersion parameters of PVA/MO with 6000 nm thickness at wavelength 490 nm.

Time min.	E_o eV	Ed eV	Eg eV	Eu meV	$S_o * 10^{13}$ m^{-2}	λ_o nm	M_{-1}	M_{-3} eV^{-2}
0	4.56	8.76	2.8	614	9.8	344	1.92	0.092
10	6.04	9.44	2.9	586	12.894	290	1.56	0.042
20	8.37	11.63	2.917	566	14.687	266	1.38	0.019
30	10.77	12.98	2.945	522	16.428	237	1.20	0.010
40	12.66	13.47	3	492	18.4	213	1.06	0.006

4.7 Photoluminescence for Thick Films

The Photoluminescence spectra for PVA, MO, and PVA/MO thick films of different thicknesses: 3000nm for both PVA and MO, 6000nm for PVA/MO before and after laser exposure with irradiation times of 40 minutes at 405 nm laser wavelength, are presented in Figures. (4-66, 4-67 and 4-68). The comparison of the emission and excitation energy gaps is also shown in Table (4-22). The results show a convergence between the energy gap calculated using Tauc equation and the one calculated by the Photoluminescence.

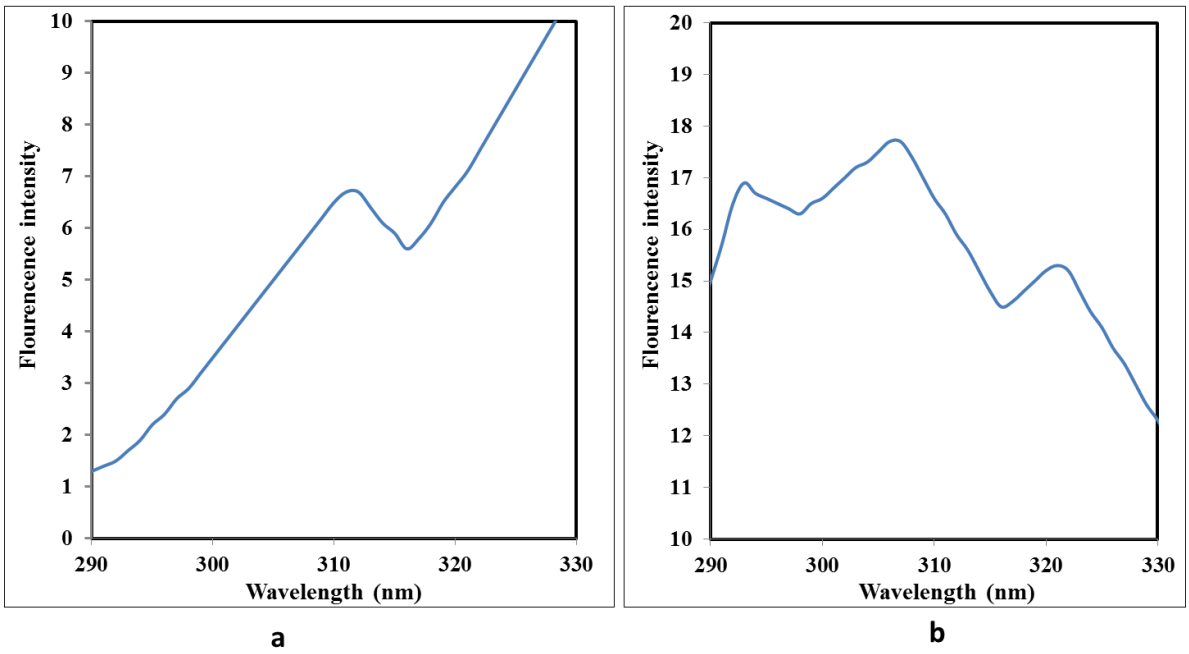

Figure (4-66): Emission spectra of PVA thick film at thickness 3000 nm irradiated by 405 nm laser (a) Before irradiating (b) After 40 minute irradiation time.

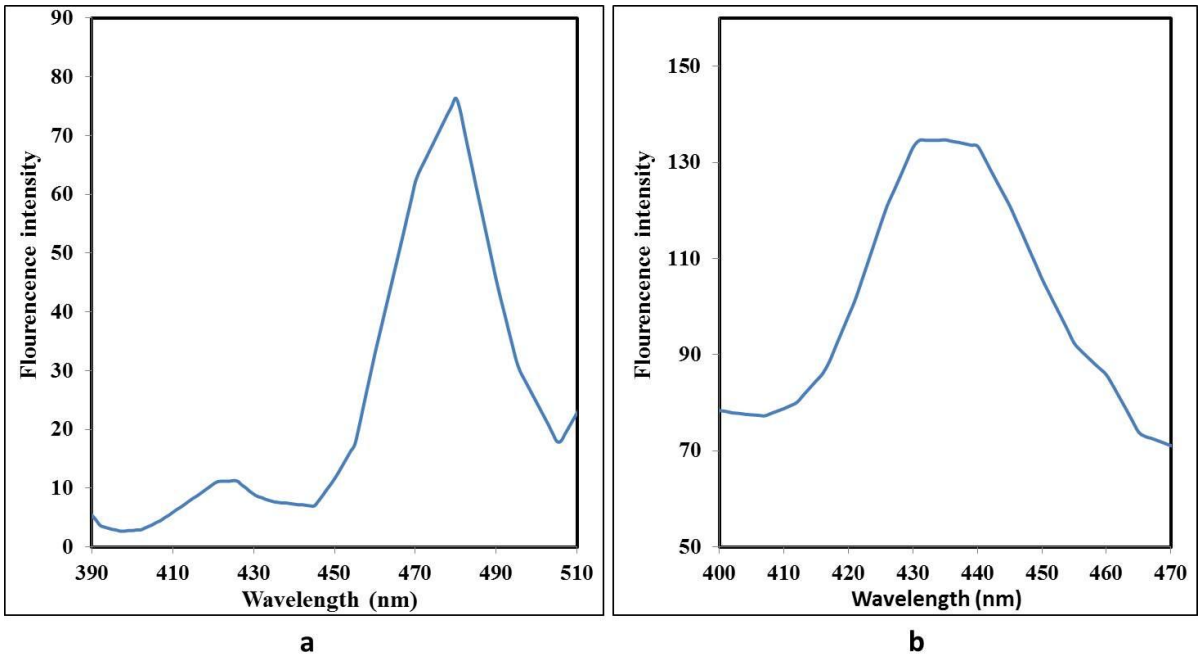

Figure (4-67): Emission spectra of MO thick film at thickness 3000 nm, irradiated by 405 nm laser (a) Before irradiating (b) After 40 minute irradiation time.

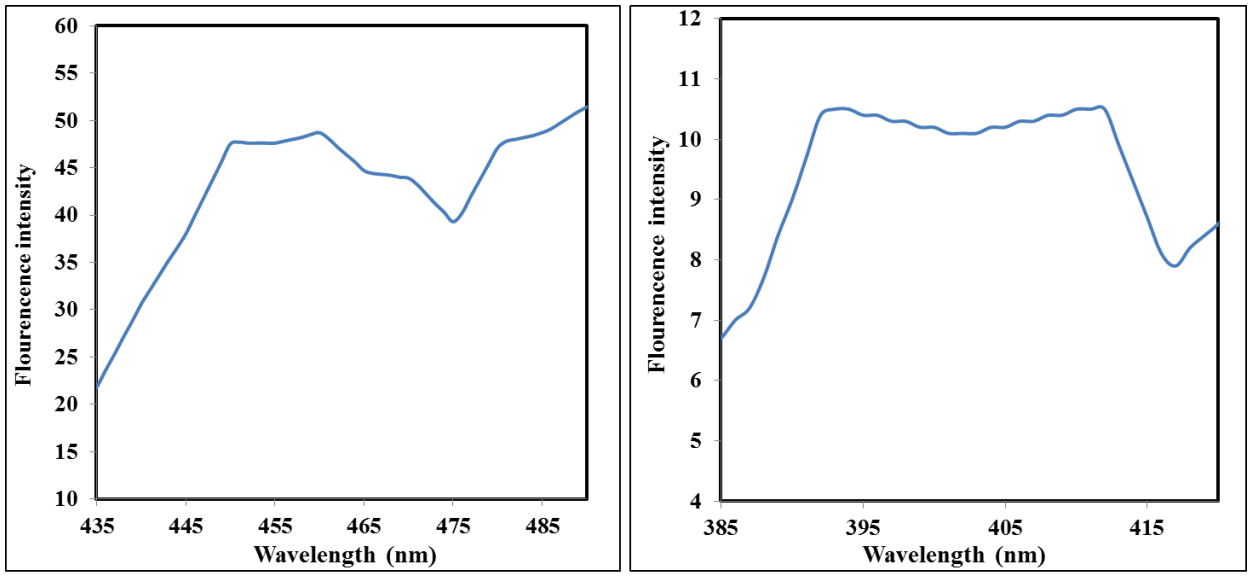

Figure (4-68): Emission spectra of PVA/MO thick film at thickness 6000 nm irradiated by 405 nm laser (a) Before irradiating (b) After 40 minute irradiation time.

Table(4-22): The energy gap of PVA, MO and PVA/MO thick film measured by Tauc and PL methods:

Thick film	Thickness nm	Irradiating time min.	Eg eV Tauc method	Eg eV PL	Error ± %
PVA	3000	0	3.95	3.83	3.13
		40	4.12	4	3.00
MO	3000	0	2.5	2.45	2.04
		40	2.9	2.83	2.47
PVA/MO	6000	0	2.8	2.74	2.18
		40	3.2	3.11	2.89
$\lambda\, nm = 405$ for violet laser					

CHAPTER FIVE

CONCLUSIONS & FUTURE WORKS

5.1 Conclusions

The key findings from this study are summarized in the following paragraphs:

1) The energy gap can be controlled by laser irradiation of PVA, MO and PVA/MO overlay between composite for both solutions and thick films which can be used as optical filters for physical and medical applications. in addition to the chemical characteristic, which has high sensitivity to the fluid acidity (PH).
2) Urbach energy of the thick films can be controlled by laser irradiation time to obtain an enhanced structure.
3) The average oscillator strength of the thick films increases while the average oscillator wavelength decreases due to the inverse relationship between them.
4) The dispersion coefficients can be controlled by laser irradiation, which can be used to modify geometric and optical specifications with applications and the need for medical applications.
5) According AFM results, the thick films surface after laser irradiation becomes smoother than before producing small surface area which will be appropriate for multi-layer filter.

5.2 Suggestions

1) Examination of solutions and films by UV-visble spectrophotometer immediately after laser irradiation.
2) The angle of diffraction of the laser should be increased to cover the solution cell or thick films.
3) Since the spectrum contains a peak in the violet region, it is necessary that the examination cuvette cells are quartz.
4) The distilled water used should be double ionization water.

5.3 Future Works

Many future works are suggested, including:

1) Using the methyl blue, the methyl red, mixed dyes or one of the laser medium dyes instead of the methyl orange.
2) Study the effect of varying different laser parameters in addition to the irradiation time such as, wavelength and power.
3) Study the effect of different polymer, such as using high density polymer and conductive polymer.
4) Study the electrical and mechanical properties of the prepared films.
5) Using different deposition techniques and investigating the thin films instead of thick films.

[1] N. Khajehzadeh, 'Analytical Techniques for Online Mineral Identification', no. February, pp. 1–93, 2018, doi: 10.13140/RG.2.2.27721.19043.

[2] Robert O. Ebewele, *Polymer science and technology*, vol. 16, no. 3. New York, 1995. doi: 10.1016/0261-3069(95)90127-2.

[3] W. S. · JyotirmoyMazumder and LaserMaterial, *Laser Material Processing , 4th ed*. Springer, 2008. Available: http://medcontent.metapress.com/index/A65RM03P4874243N.pdf

[4] F. O. Prof and W. Jan, 'laser : Principle and Applications', pp. 1–133, 2009.

[5] J. Sólyom, *Fundamentals of the Physics of Solids, Volume 1 Structure and Dynamics*. New York This: Springer, 2007.

[6] A. Rockett, *The materials science of semiconductors*. USA: Springer, 2008. doi: 10.1007/978-0-387-68650-9.

[7] D. K. Ferry, 'Introduction', in *Semiconductors (2nd Edition)*, 2019. doi: 10.1088/978-0-7503-2480-9ch1.

[8] A. H. Al-Aarajiy, 'Preparation and Characterization of NiPc / Si Organic Solar Cell', University of Baghdad, 2014.

[9] K. Takimiya, S. Shinamura, I. Osaka, and E. Miyazaki, 'Thienoacene-based organic semiconductors', *Adv. Mater.*, vol. 23, no. 38, pp. 4347–4370, 2011, doi: 10.1002/adma.201102007.

[10] W. Brütting, *Physics of Organic Semiconductors*. 2006. doi: 10.1002/3527606637.

[11] M. Hasan and N. Khaleel, 'Study the Linear and Nonlinear Optical Properties for Methylene Blue Dye Doped SiO 2 Nanoparticles', University of Babylon, 2022.

[12] S. Moulay, 'Review: Poly(vinyl alcohol) Functionalizations and Applications', *Polym. - Plast. Technol. Eng.*, vol. 54, no. 12, pp. 1289–1319, 2015, doi: 10.1080/03602559.2015.1021487.

[13] R. Nagarkar and J. Patel, 'Acta Scientific Pharmaceutical Sciences (ISSN: 2581-5423) Polyvinyl Alcohol: A Comprehensive Study', vol. 3, no. 4, pp. 34–44, 2019.

[14] A. F. Saleh, A. M. Jaffar, N. A. Samoom, and M. W. Mahmmod, 'Effect Adding PVA Polymer on Structural and Optical Properties of TiO_2 Thin Films', *J. Al-Nahrain Univ. Sci.*, vol. 17, no. 2, pp. 116–121, 2017, doi: 10.22401/jnus.17.2.15.

[15] C. C. Demerlis and D. R. Schoneker, 'Review of the oral toxicity of polyvinyl alcohol (PVA) - PDF Free Download', *Food Chem. Toxicol.*, vol. 41, no. 3, pp. 319–326, 2003, Available: https://kundoc.com/pdf-review-of-the-oral-toxicity-of-polyvinyl-alcohol-pva-.html

[16] M. F. B. A. Aziz, 'Polyvinyl alcohol (PVA) based gel electrolytes : characterisation and applications in dye-sensitized solar cells faculty of science', university of malaya original, 2017.

[17] C. Baiocchi, M. C. Brussino, E. Pramauro, A. B. Prevot, L. Palmisano, and G. Marcí, 'Characterization of methyl orange and its photocatalytic degradation products by HPLC/UV-VIS diode array and atmospheric pressure ionization quadrupole ion trap mass spectrometry', *Int. J. Mass Spectrom.*, vol. 214, no. 2, pp. 247–256, 2002, doi: 10.1016/S1387-3806(01)00590-5.

[18] K. O. Iwuozor, J. O. Ighalo, E. C. Emenike, L. A. Ogunfowora, and C. A. Igwegbe, 'Adsorption of methyl orange: A review on adsorbent performance', *Curr. Res. Green Sustain. Chem.*, vol. 4, no. July, p. 100179, 2021, doi: 10.1016/j.crgsc.2021.100179.

[19] H. S. Mohammed, 'Study the Effect of Immobilization on Electrostatic Potential for Methyl Orange Dye', *MJPS*, vol. 5, no. 1, 2018, doi: 10.52113/2/05.01.2018.

[20] N. Mohammadi, H. Khani, V. K. Gupta, E. Amereh, and S. Agarwal, 'Adsorption process of methyl orange dye onto mesoporous carbon material-kinetic and thermodynamic studies', *J. Colloid Interface Sci.*, vol. 362, no. 2, pp. 457–462, 2011, doi: 10.1016/j.jcis.2011.06.067.

[21] K. K. Chawla, *Composite materials*. New York: Springer, 2012. doi: 10.1007/978-0-38774365-3.

[22] R. Hsissou, R. Seghiri, Z. Benzekri, M. Hilali, M. Rafik, and A. Elharfi, 'Polymer composite materials: A comprehensive review', *Compos. Struct.*, vol. 262, no. November 2020, pp. 0–3, 2021, doi: 10.1016/j.compstruct.2021.113640.

[23] S. S. Chiad, N. F. Habubi, S. F. Oboudi, and M. H. Abdul-allah, 'Effect of Thickness on The Optical Parameters of PVA : Ag', *Diyala J. Pure Sci.*, no. July, pp. 153–161, 2011.

[24] N. A. B. Sabah A. Salman, Muhammad H. Abdu-allah, 'Optical Characterization of Red Methyl Doped Poly (Vinyl Alcohol) Films', *SOP Trans. Phys. Chem.*, vol. 2, no. 3, pp. 1–9, 2014, doi: 10.15764/pche.2014.02001.

[25] M. F. Hadi Al-kadhemy, A. AbdulMunem Saeed, F. J. Kadhum, S. A. Mazloum, and H. K. Aied, 'The effect of (He–Ne) laser irradiation on the optical properties of methyl orange doped PVA films', *J. Radiat. Res. Appl. Sci.*, vol. 7, no. 3, pp. 371–375, 2014, doi: 10.1016/j.jrras.2014.05.006.

[26] E. M. Antar, 'Effect of γ-ray on optical characteristics of dyed PVA films', *J. Radiat. Res. Appl. Sci.*, vol. 7, no. 1, pp. 129–134, 2014, doi: 10.1016/j.jrras.2014.01.002.

[27] K. Haneen, N. N. Jandow, and N. F. Habubi, 'Thickness Effect on Urbach Energy and Dispersion Parameters of Co 3 O 4 Thin Films Prepared by Chemical Spray Pyrolysis', no. September, 2017.

[28] N. F. Habubi, K. H. Abass, S. Chiad, D. M. A. Latif, J. N. Nidhal, and A. I. Al Baidhany, 'Dispersion Parameters of Polyvinyl Alcohol Films doped with Fe', *J. Phys. Conf. Ser.*, vol. 1003, no. 1, 2018, doi: 10.1088/1742-6596/1003/1/012094.

[29] D. Jyoti and B. A. T. T. Mostako, 'Investigation on dispersion parameters of Molybdenum Oxide thin films via Wemple – DiDomenico (WDD) single oscillator model', *Appl. Phys. A*, pp. 1–13, 2020, doi: 10.1007/s00339-020-03996-3.

[30] S. Kumari Nisha, S. Sivakumar, and S. Achutha, 'Polyvinyl alcohol/methyl orange flexible film as reusable pH indicator', *Mater. Today Proc.*, vol. 42, pp. 1008–1011, 2021, doi: 10.1016/j.matpr.2020.12.003.

[31] A. K. Maini, *Lasers and optoelectronics : fundamentals, devices, and applications*. United Kingdom: Wiley, 2013.

[32] A. Ali and J. Mohammed, 'Influence of the Laser Radiation on the Structural and Optical Properties of an Organic Pigment', Babylon / College of Science, 2022.

[33] K. a Nowakowski, 'Laser beam interaction with materials for microscale applications', 2005.

[34] J. Tang, 'Unlocking potentials of microwaves for food Safety and quality', *J. Food Sci.*, vol. 80, no. 8, pp. E1776–E1793, 2015, doi: 10.1111/1750-3841.12959.

[35] S. Mkata, 'Uv vis spectroscopy practical.', *Phys. Prakt. I*, pp. 1–11, 2017, Available: https://www.coursehero.com/file/76918963/UVVis-HS17pdf/

[36] Agilent, 'The Basics of UV-Vis Spectrophotometry', *The basics of UV-Vis Spectrophotometry*, p. 36, 2021.

[37] A. C. E, O. N. N, and I. G. O, 'Basic Calibration of UV/ Visible Spectrophotometer', *Int. J. Sci. Technol.*, vol. 2, no. 3, pp. 247–251, 2013.

[38] P. Justin Tom, 'UV-Vis Spectroscopy: Principle, Strengths and Limitations and Applications', *Technology Networks*, pp. 1–10, 2021 Available: https://www.technologynetworks.com/analysis/articles/uv-vis-spectroscopy-principle-strengths-and-limitations-and-applications-349865

[39] D. Neamen, 'Semiconductors Physics and Devices', 2003.

[40] G. Burns, *Solid State Physics*. New York, 1985.

[41] L. K. and A. H. Clark, *Polycrystalline and Amorphouse Thin Films and Device*, Lawrence A. New York, 1980.

[42] D. A. E. J. Ones, 'Fourier Transform Infrared Spectra', *Fourier Transform Infrared Spectra*, 1978, doi: 10.1016/c2009-0-22072-1.

[43] A. M. Hussein *et al.*, 'Steps toward the band gap identification in polystyrene based solid polymer nanocomposites integrated with tin titanate nanoparticles', *Polymers (Basel).*, vol. 12, no. 10, pp. 1–21, 2020, doi: 10.3390/polym12102320.

[44] Z. A. Hasan, 'Effect Magneto – Optic on Ferromagnetic Nanoparticle Polymer Composite Films', *NeuroQuantology*, vol. 19, no. 6, pp. 25–29, Jul. 2021, doi: 10.14704/nq.2021.19.6.NQ21063.

[45] saif hasan, 'Effect of Ultraviolet Irradiation on Linear and Nonlinear Optical Properties of Metal-Phthalocyanine', no. 2006, 2020.

[46] M. S. A. Mohsen, 'Effect of Laser Irradiation on the Structural and the Optical Properties of (PVA-CoCl2) Composite', University of Kerbala, 2022.

[47] E. M. Nasir, M. T. Hussein, and A. H. Al-Aarajiy, 'Investigation of Nickel Phthalocyanine Thin Films for Solar Cell Applications', *Adv. Mater. Phys. Chem.*, vol. 9, no. 8, pp. 158–173, 2019, doi: 10.4236/ampc.2019.98013.

[48] R. Marjan and A. H. Al-aarajiy, 'Effect of Irradiating Energy on Optical Energy Band Gap of Copper Phthalocyanine Solutions', *Optoelectron. LASER*, vol. 41, no. 6, pp. 31–40, 2022, doi: 10050086.2022.06.04.

[49] A. A. Ejam and N. A. A. Wahhab, 'Concentration effect on the optical properties of laser irradiation copper phthalocyanine (CuPc blue) solution', *NeuroQuantology*, vol. 20, no. 3, pp. 1–15, 2022, doi: Laser Physics Letters https://doi.org/10.1088/1612-202X/ac979b.

[50] N. A. AbdulWahhab, 'Optical properties of SnO2 thin films prepared by pulsed laser deposition technique', *J. Opt.*, vol. 49, no. 1, pp. 41–47, 2020, doi: 10.1007/s12596-020-00587-6.

[51] M. H. Noory and Z. A. Hasan, 'Influence the Addition (SiO2) Nanoparticles on Optical Properties for Methylene Blue Dye', *NeuroQuantology*, vol. 20, no. 1, pp. 143–149, 2022, doi: 10.14704/nq.2022.20.1.nq22068.

[52] E. W. Aslaksen, 'Optical Dispersion and the Structure of Solids', *Phys. Rev. Lett.*, vol. 24, no. 14, pp. 767–768, 1970, doi: 10.1103/PhysRevLett.24.767.

[53] M. DiDomenico and S. H. Wemple, 'Oxygen-octahedra ferroelectrics. I. Theory of electro-optical and nonlinear optical effects', *J. Appl. Phys.*, vol. 40, no. 2, pp. 720–734, 1969, doi: 10.1063/1.1657458.

[54] S. H. Wemple and M. DiDomenico, 'Behavior of the electronic dielectric constant in covalent and ionic materials', *Phys. Rev. B*, vol. 3, no. 4, pp. 1338–1351, 1971, doi: 10.1103/PhysRevB.3.1338.

[55] F. Yakuphanoglu, A. Cukurovali, and I. Yilmaz, 'Single-oscillator model and determination of optical constants of some optical thin film materials', *Phys. B Condens. Matter*, vol. 353, no. 3–4, pp. 210–216, 2004, doi: 10.1016/j.physb.2004.09.097.

[56] A. S. Alkelaby, K. H. Abass, T. H. Mubarak, N. F. Habubi, S. S. Chiad, and I. Al-Baidhany, 'Effect of MnCl2 additive on optical and dispersion parameters of poly methyl methacrylate films', *J. Glob. Pharma Technol.*, vol. 11, no. 4, pp. 347–352, 2019.

[57] A. K. Walton and T. S. Moss, 'Determination of refractive index and

correction to effective electron mass in PbTe and PbSe', *Proc. Phys. Soc.*, vol. 81, no. 3, pp. 509–513, 1963, doi: 10.1088/0370-1328/81/3/319.

[58] L. D. Whittig and W. R. Allardice, 'X-ray diffraction techniques', *Methods Soil Anal. Part 1 Phys. Mineral. Methods*, vol. 9, no. 9, pp. 331–362, 2018, doi: 10.2136/sssabookser5.1.2ed.c12.

[59] H. H. W. Stanjek, 'Basics of X-Ray Diffraction', pp. 107–119, 2004.

[60] F. S. Ruggeri, T. Šneideris, M. Vendruscolo, and T. P. J. Knowles, 'Atomic force microscopy for single molecule characterisation of protein aggregation', *Archives of Biochemistry and Biophysics*, vol. 664. Academic Press Inc., pp. 134–148, Mar. 2019. doi: 10.1016/j.abb.2019.02.001.

[61] B. C. Smith, *Fundamentals of fourier transform infrared spectroscopy, second edition*. 2011.

[62] J. R. Ferraro, 'History of Fourier transform-infrared spectroscopy', *Spectrosc. (Santa Monica)*, vol. 14, no. 2, pp. 28–40, 1999.

[63] N. Jaggi, *Handbook of Applied Solid State Spectroscopy*, no. February 2007. 2006. doi: 10.1007/0-387-37590-2.

[64] P. C. Braga and D. Ricci, 'Methods in Molecular Biology TM Methods in Molecular Biology TM Edited by Atomic Force Microscopy Biomedical Methods and Applications Atomic Force Microscopy Biomedical Methods and Applications How the Atomic Force Microscope Works', vol. 242.

[65] I. D. Ivanov *et al.*, 'Atomic force microscopy visualization and measurement of the activity and physicochemical properties of single monomeric and oligomeric enzymes].', *Biofizika*, vol. 56, no. 5, pp. 939–944, 2011.

[66] D. M. Jameson, 'Introduction to fluorescence', *Introd. to Fluoresc.*, pp. 1–286, 2014, doi: 10.1201/b16502.

[67] L. Brand and M. L. Johnson, 'An Introduction to Fluorescence Spectroscopy', p. 15, 2011, Available:

http://books.google.com/books?id=GgFXweh0hmQC&pgis=1

[68] Y. Chen *et al.*, 'The impact of crystal cut error on the measured impurity profiles resulting from ion implantation', *IEEE Trans. Semicond. Manuf.*, vol. 13, no. 2, pp. 243–248, 2000, doi: 10.1109/66.843640.

[69] M. E. Azim-Araghi and A. Krier, 'Optical characterization of chloroaluminium phthalocyanine (ClAlPc) thin films', *Pure Appl. Opt. (Print Ed. (United Kingdom)*, vol. 6, no. 4, pp. 443–453, 1997, doi: 10.1088/0963-9659/6/4/007.

[70] B. D. Arya and N. Malik, 'FTIR Spectroscopic Analysis of Various Pharmatheutically Important Organic Dyes', vol. 1, no. 5, pp. 48–52, 2015.

[71] S. Gupta *et al.*, 'Composition dependent structural modulations in transparent poly(vinyl alcohol) hydrogels', *Colloids Surfaces B Biointerfaces*, vol. 74, no. 1, pp. 186–190, 2009, doi: 10.1016/j.colsurfb.2009.07.015.

[72] M. Yahia, I. S.Ganesh, V.Shkir, H. Y. Alfaify, S.Zahran, and A. M. Algarni, H.Abutalib, M. M.Al-Ghamdi, Attieh A.El-Naggar, A. M.Albassam, 'An investigation on linear and non-linear optical constants of nano-spherical CuPc thin films for optoelectronic applications', *Phys. B Condens. Matter*, vol. 496, 2016, doi: 10.1016/j.physb.2016.05.020.

[73] A. W. Hanson, 'The crystal structure of methyl orange monohydrate monoethanolate', *Acta Crystallogr. Sect. B Struct. Crystallogr. Cryst. Chem. Chem.*, vol. 29, no. 3, pp. 454–460, Mar. 1973, doi: 10.1107/S0567740873002748.

الخلاصة

تتناول هذه الدراسة تأثير التشعيع بالليزر البنفسجي على الخصائص البصرية و التشتت على المحاليل و اغشية بولي فينيل الكحول PVA و صبغة المثيل البرتقالي MO و متراكبهما PVA/MO و المحضرة بطريقة الصب. شععت العينات بأزمان مختلفة ١٠و ٢٠و ٣٠و ٤٠ دقيقة. تم اخذ القياسات البصرية للمحاليل و خواص التشتت للاغشية ويتم مقارنة هذه القياسات مع قياسات العينات غير المشععة. كما درست الخواص التركيبية المتضمنة فحص XRD, FTIR المعاملات التركيبية التي يتم دراستها مثل الحجم الحبيبي و الخشونة بواسطة AFM.

حضر محلول PVA بتركيز ١٠ غرام لكل لتر و تركيز MO ٠,٠١ غرام لكل لتر و يتم خلط المحلولين للحصول على المتراكب. بعد ذلك تم تحضير الاغشية السميكة بأسماك مختلفة حوالي ٢٠٠٠ و ٣٠٠٠ نانومتر لكل من PVA و MO و بحدود ٢٠٠٠ و ٤٠٠٠ و ٦٠٠٠ نانومتر لمتراكب PVA/MO. شععت المحاليل و الاغشية السميكة بالليزر البنفسجي ذو الطول الموجي ٤٠٥ نانومتر و لأوقات ١٠ و ٢٠ و ٣٠ و ٤٠ دقيقة.

تظهر الخواص البصرية للمحاليل و الاغشية نقصان في طيف الامتصاصية والانعكاسية مع زيادة زمن التشعيع بسبب تكسر الاواصر بينما تزداد النفاذية. فجوة الطاقة (المباشرة و الغير مباشرة) تزداد مع زيادة زمن التشعيع. ان الثوابت البصرية الاخرى مثلا (الامتصاصية، معامل الامتصاص، معامل الانكسار، معامل الخمود، ثوابت العزل الحقيقية والخيالية و التوصيلية البصرية) تقل بزيادة زمن التشعيع بالليزر.

تم دراسة معاملات التشتت للأغشية السميكة قبل وبعد التشعيع بالليزر حيث ان طاقة المذبذب الفردي وطاقة التشتت وفجوة الطاقة المباشرة ومتوسط قوة المذبذب تزداد مع زمن التشعيع، في حين أن طاقة أورباخ والطول الموجي للمذبذب يتناقصان مع زيادة زمن التشعيع.

جمهورية العراق
وزارة التعليم العالي و البحث العلمي
جامعة بابل / كلية العلوم
قسم الفيزياء

تأثير التشعيع بالليزر على الخواص التركيبية و البصرية و التشتت للأغشية السميكة لمتراكب المثيل البرتقالي / بولي فينيل الكحول

رسالة مقدمة الى قسم الفيزياء كلية العلوم جامعة بابل وهي جزء من متطلبات نيل شهادة الماجستير في علوم الفيزياء

من قبل

ساره ميسم طارق علي

بأشراف

أ.م.د نهال عبد الله عبد الوهاب **م.د. عدنان حمود محمد**

١٤٤٥هـ **٢٠٢٣م**